Fall 2018

Controls on Speleogenesis in the Upper-Mississippian Pennington Formation on the Western Cumberland Plateau Escarpment

Hali Steinmann
Western Kentucky University, halisteinmann@gmail.com

CONTROLS ON SPELEOGENESIS IN THE UPPER-MISSISSIPPIAN PENNINGTON
FORMATION ON THE WESTERN CUMBERLAND PLATEAU ESCARPMENT

A Thesis
Presented to
The Faculty of the Department of Geography and Geology
Western Kentucky University
Bowling Green, Kentucky

In Partial Fulfillment
Of the Requirements for the Degree
Master of Science

By
Hali June Steinmann

December 2018

CONTROLS ON SPELEOGENESIS IN THE UPPER-MISSISSIPPIAN PENNINGTON
FORMATION ON THE WESTERN CUMBERLAND PLATEAU ESCARPMENT

Date Recommended _11/1/18_

Patricia Kambesis
Dr. Patricia Kambesis, Director of Thesis

Fred D. Siewers
Dr. Fred Siewers

Nicholas Crawford
Dr. Nicholas Crawford

Cheryl D. Davis   _11/19/18_
Dean of Graduate Studies and Research   Date

This thesis is dedicated to my sisters, Lindsay, Connie, and Jennilee.

CONTENTS

LIST OF FIGURES

LIST OF TABLES

CONTROLS ON SPELEOGENESIS IN THE LATE-MISSISSIPPIAN PENNINGTON
FORMATION ON THE WESTERN CUMBERLAND PLATEAU ESCARPMENT

Hali Steinmann   December 2018   124 pages

Directed by: Pat Kambesis, Fred Siewers, and Nicholas Crawford

Department of Geography and Geology   Western Kentucky University

Much of the pioneering work on caves of the Cumberland Plateau (province spanning Tennessee, Kentucky, Alabama, and Georgia) has been stratigraphically located within the Mississippian Bangor and Monteagle Limestones, wherein some of the region's largest and most spectacular caves occur. Of interest to the understanding of this karst landscape, but severely underrepresented in the literature thereof, are caves and karst features in a heterogeneous sequence of clastics and carbonates known collectively as the Pennington Formation (Upper Mississippian). This work consisted of a regional study of Pennington caves on the western Cumberland Plateau escarpment (Alabama and Tennessee), and a case study of Pennington caves in Savage Gulf State Natural Area (Grundy County, Tennessee). The objective of this research was to determine controls on speleogenesis in the Pennington Formation, using cave geomorphology, dye tracing, and GIS to explore lithologic, hydrologic, and structural influences on karst processes. This resulted in a conceptual model for speleogenesis in the Pennington Formation, with the major controls being: 1) direct and diffuse recharge from the caprock, undersaturated with respect to calcite; 2) thin, horizontally bedded limestones sandwiched by shales and other insoluble rocks; and 3) networks of stress release fractures oriented parallel to major stream valleys. Our present understanding of the Cumberland Plateau could be advanced by further study of karst dynamics in the Pennington Formation.

CHAPTER 1: INTRODUCTION

Situated near the crown of the Cumberland Plateau's stratigraphic sequence is the

Pennington Formation, a heterogeneous geologic unit that contains intermittent soluble

rock layers such as limestone, along with varying amounts of shale, siltstone, and

sandstone. This research takes a mixed method approach with the goal of understanding

structural, lithologic, and hydrologic controls on karst processes in the Pennington

Formation, with emphasis on speleogenesis on the western escarpment of the

Cumberland Plateau (Tennessee and Alabama) and in Savage Gulf State Natural Area

(Grundy County, Tennessee). The research question is: what are the controls on

speleogenesis in the Pennington Formation and how are those controls reflected in the

morphology of caves? Karstification of the Pennington Formation has implications not

only for the geomorphology of the Cumberland Plateau, but also for local ecology,

biodiversity, water quality, and land management.

Few studies concerning Cumberland Plateau caves have delved into the variable

limestones and relatively small caves of the late-Mississippian Pennington Formation.

Cave survey and exploration are often biased towards large cave systems that have

"going leads" (areas yet to be explored or surveyed) or the potential to connect to other

cave systems. However, much of the plumbing in karst systems consists of thin cracks

and flooded conduits that remain inaccessible to even the smallest and bravest of cavers.

The Pennington Formation's thin limestone members contain hundreds of caves (defined

in Tennessee and Alabama as a natural cavity traversable for at least 50 ft/15 m), and host

karst conduit networks at scales below this threshold but significant to local hydrology.

The purpose of this research is to identify the major controls on speleogenesis in the

Pennington Formation in order to clarify its place within the greater context of Cumberland Plateau hydrology and landscape evolution.

This study utilized information from state cave surveys in conjunction with other digital geographic data to interpret cave morphologies in the context of regional and local geology and hydrology. The methodology includes data mining from state cave surveys, morphometric analysis of 60 digital cave models based on analog cave maps, cave survey, cartography, and dye tracing of karst features in Savage Gulf State Natural Area, and spatial analysis using Geographic Information Systems. The manuscript is organized into six chapters. The literature review (Chapter 2) introduces cave and karst topics pertinent to this study. Chapter 3 details the study area (western escarpment of the Cumberland Plateau) from a regional and local perspective. Chapter 4 presents the methodology used to investigate caves and karst features in the Pennington Formation, followed by the results of this work in Chapter 5. The discussion, implications, and suggestions for future work are given in Chapter 6.

CHAPTER 2: LITERATURE REVIEW

Karst is a term describing landscapes that are developed in soluble rocks such as carbonates or evaporites and contain features such as caves, disappearing streams, and dolines or sinkholes (Figure 1) (Ford and Williams 2007). This chapter first introduces the conditions necessary for karst processes to occur, broken down into four major components: lithology (2.1.1), aqueous geochemistry and hydrology (2.1.2), geologic structure and relief (2.1.3), and time (2.1.4). Speleogenesis, i.e. the formation of caves, and patterns of cave morphology are covered in Section 2.2. Section 2.3 covers conceptual and physical modeling of the karst landscape and karst features, including cave survey and cartography (2.3.2), geomorphometry of caves (2.3.3), the use of fluorescent dye in karst aquifer studies (2.3.4), and Geographic Information Systems (2.3.5). Finally, the Pennington Formation is introduced in Section 2.4.

2.1 Introduction to Karst
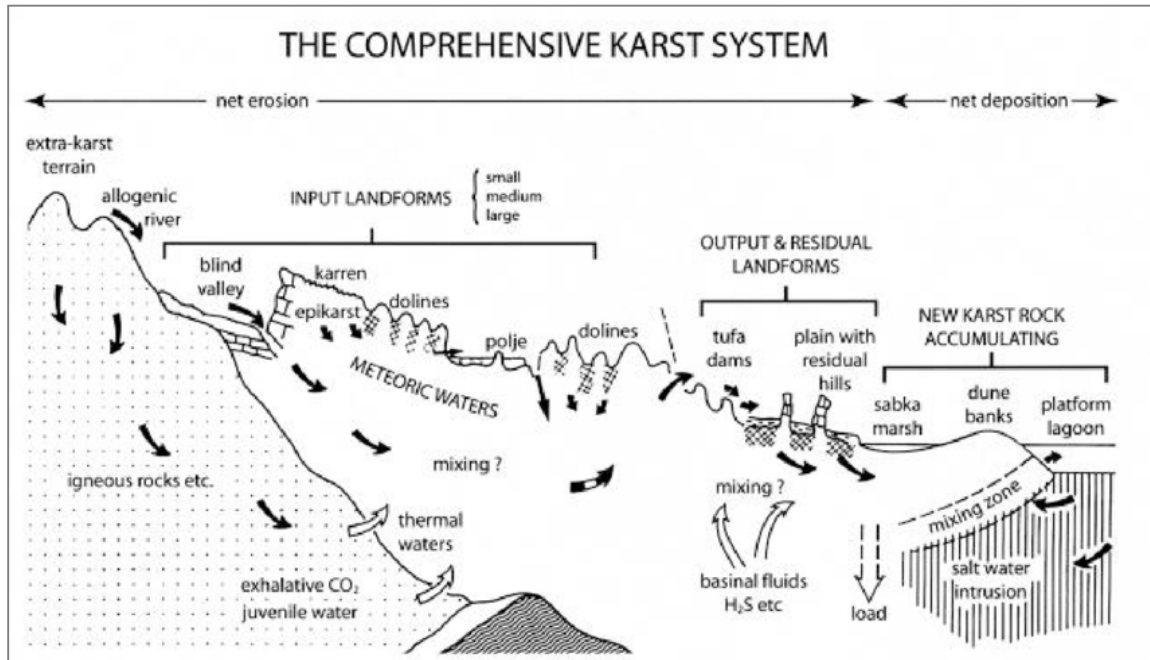
Figure 1. A comprehensive karst conceptual model (Ford 2006).

2.1.1 Lithology of Carbonate Rocks

Carbonate rocks are formed from sediments, unconsolidated materials, which include the shell fragments and other parts of aquatic plants and animals that use calcium carbonate in their bodily structures. These sediments accumulate in shallow marine environments, and may be cemented in place by calcite precipitated directly from seawater. Cementation is also possible through the process of recrystallization after exposure to fresh water, which may be accomplished either by crustal uplift or sea level decline. Telogenetic carbonate rocks are those in which compaction and recrystallization of minerals within pore spaces severely reduces the original matrix porosity and permeability of the sediment. In telogenetic karst, bedding plane partings and other discontinuities in the otherwise massive rock may be hugely significant as inception horizons for early karst conduit development (Palmer 2001; Filipponi et al. 2009).

Periods of sediment accumulation may be noticeable as individual beds in the stratigraphic record, with bedding plane partings representing a disruption or change in the rate of sedimentation. A sequence of beds with similar character is known as a formation. Unconformities are breaks in a sedimentary sequence that represent an interruption of deposition, and possibly erosion of beds underlying the unconformable surface (Driese et al. 1994; Palmer 2007a). Where soluble rocks have been subaerially exposed at or below an unconformity, paleokarst features (e.g. ancient dolines, karren, and collapsed caves) may be preserved, and modern karst features may develop above or below the unconformity (Driese et al. 1994; Klimchouk et al. 2000).

A disconformity is an unconformity within sedimentary rocks with little to no difference in inclination between beds; that is, younger beds are deposited roughly

parallel to older beds (Driese et al. 1994; Humbert 2001). In marine and near-shore sedimentary deposits, the transgression and regression of sea level control the genetic environment affecting composition of lithologic sequences (Van Wagoner et al. 1988). Since marine environments are highly variable over time and space, carbonate rocks are often interbedded with other less-soluble rocks like siltstone, shale, and sandstone (Ford and Williams 2007).

The thickness and stratigraphic position of soluble units is important in defining the shape and size of caves and karst aquifers (Ford and Ewers 1978; Powell 1969; White 1969). The rock types present above and below a soluble unit, especially impermeable or less soluble rocks, ultimately constrain recharge and discharge. Impermeable strata at the base of karst aquifers cause water to be expelled as springs, while impermeable or otherwise resistant strata atop karst rocks can retard exposure and dissolution of soluble rock (Crawford 1978; Sasowsky 1999). Presence of a caprock, as it is often called in the karst literature, helps maintain the relief and thus hydraulic gradient necessary for karst development (Crawford 1978; Kastning 1999).

Another indirect lithological consideration of importance to karst geomorphology is the genesis of soils from various parent materials (Palmer 2007a). Sandstone weathering products produce sandy soils that are less effective at retaining carbon dioxide as clay-rich soils derived from finer-grained rock types like siltstone or carbonates (Klimchouk et al. 2000). However, sandy soils are relatively inert and typically maintain the low pH of rainwater as it passes through; therefore, water draining from sandy soils may be more chemically aggressive than water whose pH has been mitigated by more alkaline soils (Palmer 2007a). For this reason, the lithologic transition from relatively

insoluble, impermeable rock like sandstone to soluble rock such as limestone is optimal for the development of karst features because recharge originating from sandstone caprock is chemically aggressive toward limestone (White 1969; Davis and Brook 1993; Palmer 2001).

2.1.2 Aqueous Geochemistry and Hydrology

This research is concerned with the dissolution of carbonate rocks in meteoric water, therefore a brief explanation of the aqueous geochemistry of this system is at hand. The reader is directed to the plethora of available texts (White 1988; Klimchouk et al. 2000; Ford and Williams 2007; Palmer 2007a) for more information on this topic as well as detailed descriptions of dissolution in non-carbonate rocks, dissolution involving non-meteoric or deep-seated water, and dissolution by sulfuric acid or biochemical reactions.

At its most fundamental, the weathering of carbonate bedrock is a function of the geochemical gradient between water and rock being in disequilibrium. Dissolution occurs when water is undersaturated with respect to calcite, especially in water that is slightly acidified by carbonic acid originating from soil-water interactions (Ford et al. 1985). Precipitation (i.e. deposition) of mineral solids occurs when water is oversaturated with respect to calcite, resulting in features such as flowstone, stalactites and stalagmites at a range of scales (Ford et al. 1985; Klimchouk et al. 2000). Saturation index is a measure of water's potential to either dissolve or deposit rock. Denudation is a term that describes the rock mass that has been removed from a karst landscape via dissolution over time (Ford et al. 1985).

Climate is a major factor determining the rates of karst development because climatic processes dictate mean annual temperature and the spatial and temporal

distribution of precipitation. Increases in mean annual temperature and precipitation generally result in higher rates of karst development. This is not only because more fluid is available to react with calcite, but also because warm, wet climates host greater levels of plant and microbial productivity, and thus greater levels of soil carbon dioxide production (dissolution is enhanced when water reacts with soil carbon dioxide to form carbonic acid) (Palmer 2007a). Fluviokarst describes a type of karst landscape in which the chemical and erosive power of major rivers and streams leads to features like large trunk cave passages, ponors, blind valleys, and sinkholes at the heads of tributaries (Gunn 2004; Anthony and Granger 2006; White 2009).

Aquifers are geologic formations that contain and/or conduct groundwater (Palmer 2007a, Worthington and Ford 2009). Karst aquifers are unique in that flow is heterogeneous and anisotropic, making aquifer behavior difficult to predict (Field and Nash 1997; Worthington 2009). Depending on conditions, parts of the aquifer may be vadose, above the water table, or phreatic, below the water table. Pathways of high hydraulic conductivity in karst aquifers are enlarged by dissolution; therefore the shape and size of the aquifer can evolve relatively rapidly (Ford and Williams 2007; Worthington 2009).

In karst hydrologic systems, the dissolution of rock enhances permeability of the channel network over time (Palmer 1990; Worthington 2009; Worthington and Ford 2009). Mature karst aquifers are characterized by tertiary porosity, in which turbulent flow affects further evolution and enlargement of the channel (Ford and Williams 2007; Worthington 2009). Unlike a sandstone aquifer where water occupies intergranular pore spaces, water in telogenetic carbonate rocks rarely enters matrix porosity (Palmer 1991;

LaFleur 1999). Rather, discontinuities such as joints, bedding planes, and fractures

transmit water through the aquifer, resulting in positive feedback between areas of

increased hydraulic conductivity and chemical weathering of preferred conduits (Siemers

and Dreybrodt 1998; Kaufmann and Braun 1999). Highly developed karst landscapes

may have little or no surface flow components, with subsurface conduits carrying the

majority of the drainage (Palmer 1990; Kaufmann and Braun 1999; LaFleur 1999). The

hydraulic capacity of karst aquifers is largely dependent on the amount of fluid available

to dissolve rock; therefore, climate, catchment size, and mode of recharge are important

factors controlling the scale of karstification (Powell 1969; LaFleur 1999; Groves and

Meiman 2005).

Recharge to an aquifer depends on the amount of precipitation and the

fluctuations in base level over a given time period (Powell 1969, LaFleur 1999). Water's

point of entry into karst rocks may be obvious, e.g. a surface stream disappears into a

cave, or subtle and quite difficult to observe, as in the case of hypogene caves formed by

deep groundwater. Epigenic recharge refers to relatively shallow circulation of meteoric

water, which interacts with surface components such as soil and vegetation (Palmer

2011). Autogenic recharge refers to meteoric water falling directly on areas of carbonate

bedrock. Allogenic recharge describes water entering karst systems after flowing across

or through insoluble rocks. Often, autogenic recharge becomes saturated with calcite as it

percolates through the epikarst, contributing to the formation of stalactites and

stalagmites in caves. Allogenic recharge is more likely to be undersaturated with respect

to calcite and readily dissolve carbonate rock (Palmer 2001). In either regime, sinking

streams or other point sources are referred to as discrete or concentrated recharge, and

percolation distributed over a large area is described as diffuse (White 1969; Palmer 2001). Most karst systems are characterized to some degree by both allogenic/autogenic and discrete/diffuse modes of recharge (Kastning 1999).

The majority of dissolution, as well as stream downcutting via transport of clastic sediments, occurs during extreme but short-lived hydraulic events, i.e. floods (White 2009, Groves and Meiman 2005). The greatest dissolutional and erosional power is exerted on the system during high magnitude, low frequency storm events with short duration of above-average discharge (Field and Nash 1997; Vesper and White 2004; Groves and Meiman 2005). In thin, confined limestone units the effect is commonly anastomotic mazes (Palmer 2001; Palmer 2011).

The residence time of water in unconfined karst aquifers is often short-lived (White 1969; Groves and Howard 1994); water can flow miles per day as opposed to feet per year in other aquifer types (Mull et al. 1988). Karst aquifers are particularly vulnerable to contamination because of the relatively rapid transport of runoff and contaminants from surface to groundwater (Mull et al. 1988; Veni 1998). This is especially true where topographic relief creates a steep hydraulic gradient (Ford and Williams 2007). Certain parts of a karst aquifer may act as "annexes" that store and later release water (Palmer 2001; Palmer 2011). A well-developed epikarst, the zone of soil and regolith between karst bedrock and the surface, may play host to a suspended aquifer that is slowly drained from below (Williams 2008).

2.1.3 Geologic Structure and Topographic Relief

Geologic structure exerts a great deal of control over the pattern and distribution of karst features (Palmer 1991; Sasowsky 1999), therefore, an understanding of regional

tectonic and geomorphic history is necessary to assess karst landscapes. The exposure of

carbonate rocks at the surface, and the relief necessary for karst development, both

depend on structural uplift and/or erosion (Ford and Williams 2007). The nature and

orientation of structural discontinuities like bedding planes, joints, and faults strongly

influence the inception of karst conduits and the behavior of recharge and discharge

through karst rocks (Moser and Ricci 1974; Sasowsky 1999; Ford and Williams 2007). It

is crucial to understand geologic structure and gradient in karst aquifers because the

topographic relief that is apparent on the surficial landscape is often misrepresentative of

the true flow direction of karstic groundwater; there may be cutarounds, distributary flow

paths, and unknown inputs that confound the interpretation of aquifer parameters

(Varnedoe 1973; Mull et al. 1988).

Fractured bedrock gives rise to pathways of increased hydraulic conductivity that

become preferential flow routes for recharge (Ford and Ewers 1978; Sasowsky 1999;

Palmer 1991; Palmer 2001). In telogenetic carbonates, discontinuities are crucial in

establishing the framework for dissolutional cavity enlargement in otherwise low-

porosity/low-permeability limestone and dolomite (White 1969; Palmer 1991; Kastning

1999; Sasowsky 1999). Groves and Howard (1994) modeled the minimum aperture width

of joints for formation of cave passages, finding that fractures with an initial width of 50

μ m or larger are optimal for speleogenesis. A fracture flow model created by Siemers

and Dreybrodt (1998) illustrated that the condition of the rock prior to initiation of

conduit development strongly influences the resultant conduit pattern, since there is

positive feedback between widening fractures and flow. Most fractures occur as sets of

parallel and conjugate joints (Kastning 1999) and are typically more closely spaced in

thinly bedded rocks than in thick strata (Powell 1969; Palmer 2007). Where dissolution is uniform through sets of joints in a soluble rock, particularly beneath resistant caprock, network maze caves can form (Palmer 1991).

Joints and fractures are not only a structural consequence of tension and compression (Wilson and Stearns 1958), but also can be the result of isostatic rebound following erosion (Crawford 1978; Sasowsky and White 1994; Simpson and Florea 2009). As rock mass is removed or "unloaded" from valleys by streams, inward and upward stresses affect the remaining rock mass. Unloading stress, the result of isostatic rebound, causes bedding planes in the valley bottom to break apart and fractures to open up along the valley walls parallel to the master stream (Sasowsky and White 1994; Simpson and Florea 2009). Stress release fractures are young features resulting from recent events, i.e. erosion and crustal rebound. In karst landscapes, stress release fractures create pathways of increased hydraulic conductivity that may evolve into caves. In this situation, solutional and mechanical processes are acting as integrated components of the denudational system (Sasowsky and White 1994; Simpson and Florea 2009).

Another structural consideration concerning cave development is the dip of bedding planes (Crawford 1978; Crawford 1992; Palmer 2007a). Bedding plane partings, which originate from a change in the type or amount of sediment during deposition, often serve as inception horizons for karst feature development (Ford and Williams 2007). Tectonism and isostasy can cause differential uplift of strata, such that horizontally oriented beds and bedding plane partings become inclined, affecting the passage of water over and through strata (Palmer 2007a). Crawford (1965; 1992) recognized trends in karstification in relation to the dip of bedding planes on the Cumberland Plateau, in

11

particular the formation of blind karst valleys where beds are inclined inward, towards the plateau top. Others (Sasowsky and White 1994; Palmer 2007a; Simpson and Florea 2009) have noted that passages forming in the vadose zone are often oriented down-dip, while phreatic passages have no systematic relation to the dip direction and may extend along strike. This distinction may be useful in determining the hydrologic origins of cave passages in dipping strata.

2.1.4 Evolution of the Karst Landscape over Time

Caves may survive for millions of years in the landscape (Anthony and Granger 2004; 2006; Sasowsky et al. 1995); however, the same processes that engender their formation eventually aid in their demise. Rates of dissolution and erosion control the exposure and denudation of soluble rocks from the landscape (Simms 2004; White 2006). In cases where soluble rocks are protected by relatively impermeable, insoluble rocks, topographic highs can be maintained despite the relatively rapid removal of carbonates (Crawford 1992; Smart and Campbell 2003; Worthington 2009). In the Cumberland Plateau karst region, multi-level caves and their sediments are evidence of the lowering of regional base level over time (Crawford 1978; Anthony and Granger 2004). As streams continue to erode the sandstone caprock, limestone is subsequently exposed and removed (Davis and Brook 1993; Knoll et al. 2015).

Anthony and Granger (2004; 2006) used cosmogenic nuclide dating to determine the age of sediment deposits from caves in the Bangor and Monteagle limestones, finding a relationship between age and landscape position (higher elevation caves preserve younger sediments as a result of base level lowering over time). Other dating methods include but are not limited to stable isotope dating in cave speleothems (Harmon et al.

12

1978) and calculations of denudation rate by observing mass lost in buried rock tablets (Davis and Brook 1993). Davis and Brook (1993) estimated the denudation rate on the Cumberland Plateau to be 56 mm/1000 years.

2.2 Speleogenesis and Patterns of Cave Geomorphology

Speleogenesis is a term describing the formation of caves and caverns (Klimchouk et al. 2000; Palmer 2007a). Caves are defined by arbitrary size designations that vary depending on specifications set forth by individuals or groups (Curl 1986; Klimchouk et al. 2004; Piccini 2011). The size of a void that constitutes a "proper cave" is necessarily anthropocentric, and voids too small for human exploration are usually disregarded in studies of speleogenesis (Curl 1986; Palmer 2007a; Piccini 2011). This is not to say that tiny or inaccessible voids and fissures are unimportant to cave development, only that their morphology is cryptic and must be studied indirectly. In addition to this, cave exploration effort is generally biased towards large cave systems with the potential for new discovery, meaning many small caves go unsurveyed.

Solutional caves can form in vadose, phreatic, or epiphreatic conditions, with existing discontinuities in rock (e.g. fractures, bedding plane partings) being the primary zones of cave inception (Ford and Ewers 1978; Palmer 1991; LaFleur 1999). White (2007) defines three phases of cave formation: initiation, where fractures are widened by laminar flow, enlargement, where conduits grow through dissolution and clastic transport under turbulent flow, and decay, where passages are hydrologically abandoned and may fill with sediment or flowstone. These phases provide a general framework for the geomorphic history of caves; however, progression through the developmental stages is not always linear (Ford 1999, Palmer 2007b).

13

Dissolution occurs whenever undersaturated water is in contact with rock (Siemers and Dreybrodt 1998; Simms 2004) and increases significantly in turbulent flow conditions (Palmer 1991; Kaufmann and Braun; White 2007b). However, if the saturation of calcite reaches a certain threshold, karst processes can act in retrograde, adding material through the precipitation of calcite rather than removing rock through dissolution (White 1969; Palmer 2007a; Palmer 2007b). Competing rate processes of isostacy and erosion further complicate the progression of karst and cave development as material is removed from the system (Simms 2004; White 2009). Overprinting describes complex morphologies that arise when caves undergo periods of stagnation or deposition followed by renewal of incision/dissolution (Jacoby et al. 2013).

Palmer (1991; 2007a) proposed a widely accepted classification scheme for cave morphologies as they relate to the mode and source of recharge and the structural properties of the surrounding rock (Figure 2). Discrete stream flow into an aquifer from sinking streams or sinkholes tends to create branching or dendritic passages resembling surface drainages, while diffuse flow through joints gives rise to network mazes with many intersecting passages (White 1969; Palmer 2007a; Palmer 2011). Tube shaped passages indicate phreatic conditions, while canyon shaped passages are more commonly associated with vadose conditions (Palmer 2001; Worthington 2004). Speleogenetic processes in epigenetic karst are ultimately a function of the mode, amount, and chemistry of surface recharge.

STRUCTURAL CHARACTER OF ROCK
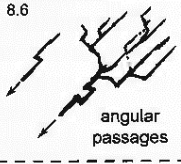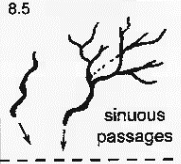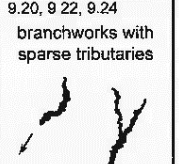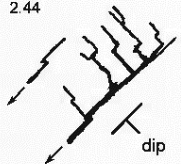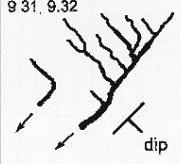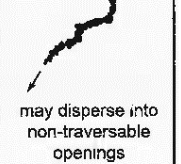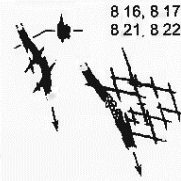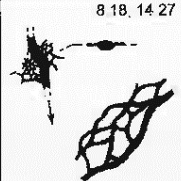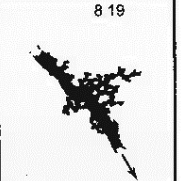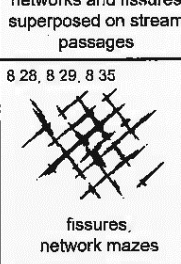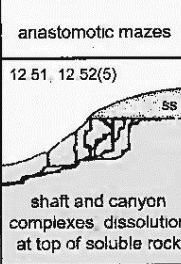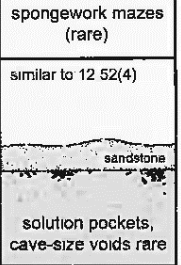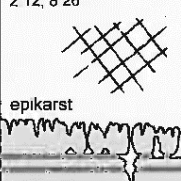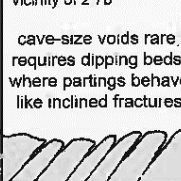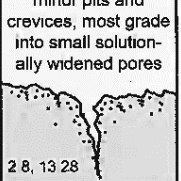
		GENERAL CAVE PATTERN	STRUCTURAL CHARACTER OF ROCK		
			fractures	bedding-plane partings	intergranular pores
KARST DEPRESSIONS	sinkholes (small discharge fluctuation)	Branchwork stream passages, usually in multiple tiers. Also single-passage stream caves. Vadose passages trend mainly down the dip. Passages are sinuous in bedded rocks, angular in highly fractured rocks.	*gentle dip* — 8.6 angular passages; *steep dip* — 2.44 dip	*gentle dip* — 8.5 sinuous passages; *steep dip* — 9.31, 9.32 dip	9.20, 9.22, 9.24 branchworks with sparse tributaries; may disperse into non-traversable openings
	sinking streams (great discharge fluctuation)	Crude branchworks and single-passage stream caves, with network or anastomotic diversions and flood-water injection features. Some are formed along stream banks, swamps, or lakes	8.16, 8.17 8.21, 8.22 networks and fissures superposed on stream passages	8.18, 14.27 anastomotic mazes	8.19 spongework mazes (rare)
RECHARGE TYPE — DIFFUSE	through overlying or underlying insoluble rock	Extensive networks, shaft-canyon systems, or porosity zones, according to rock structure. Caves concentrate just below the base of the insoluble rock	8.28, 8.29, 8.35 fissures, network mazes	12.51, 12.52(5) shaft and canyon complexes, dissolution at top of soluble rock	similar to 12.52(4) solution pockets, cave-size voids rare
	into porous or fractured soluble rock	Epikarst and shallow networks in fractured rock, formed by dispersed recharge to all fissures. Rudimentary spongework in porous rock.	2.12, 8.26 epikarst	vicinity of 2.7b cave-size voids rare, requires dipping beds, where partings behave like inclined fractures	minor pits and crevices, most grade into small solutionally widened pores; 2.8, 13.28

Figure 2. Characteristic patterns of cave morphology, classified based on type of recharge and structural properties of parent rock (from Palmer 2007a).

Branchwork passages are the underground analog of surface streams and rivers, and consist of passages that join each other as tributaries (Palmer 2001, Simpson and Florea 2009). They are recharged by sinkholes and other point sources. In horizontally bedded or gently dipping rocks, branchwork caves may exhibit meanders akin to those found in surface streams (Palmer 2001). Branchwork caves can form in bedding plane partings or fractures, and account for roughly sixty percent of known caves (Palmer

15

2007a). On the Cumberland Plateau, caves most often consist of branching stream passages (Simpson and Florea 2009).

Sinking streams and vertical shafts are features associated with direct allogenic recharge (Brucker et al. 1972; Klimchouk et al. 2000; Ford and Williams 2007). Shafts and domes are vadose features commonly formed where vertical fissures or joints intersect to form areas of high hydraulic conductivity (Brucker et al. 1972; Klimchouk et al. 2000). The location of vertical shafts within a "capped" karst landscape can be correlated with the edge of the caprock; as erosional retreat of the caprock progresses, new areas of soluble rock are exposed and shaft formation retreats much like the knickpoint in a stream (Brucker et al. 1972; Klimchouk et al. 2000). Shafts in the Appalachian low plateaus are geologically young features that often intersect underlying cave systems that may pre-date shafts (Brucker et al. 1972).

Maze caves can be formed in a number of different ways, but in general are comprised of intersecting passages with multiple closed loops (Palmer 2001; Palmer 2007a). Flooding may contribute to maze formation where high discharge is injected into many alternate routes (Palmer 2009; Palmer 2011). If the major features constraining flow are bedding planes, anastomotic mazes form, while if intersecting fractures or joints are the controlling features, the result is a network maze. In a thin limestone layer bounded by relatively impermeable/insoluble rocks, the effect of floodwater injection may be intensified (White 1969). Continuous diffuse flow through fractures can also result in network maze caves if recharge is uniform to all major conduits (Sasowsky and White 1994; Palmer 2007a). This situation is exemplified where thin, fractured caprock layers overlie soluble units. The small amount of water permeating into the system is

highly solutionally aggressive, and fractures are gradually widened. Conduits are then subject to further modification by flooding of major streams or rivers, which expedites the enlargement of passages (White 1969; Palmer 2007a; Palmer 2009).

Aside from passages themselves, smaller-scale solutional features like rills and scallops, as well as depositional features like sediments and speleothems, are indicative of the conditions at the time of their formation. Scallops, which can be carved during phreatic situations and are sometimes preserved in dry, hydrologically abandoned caves, signify the velocity and direction of water movement (Lauritzen et al. 1985). Flowstone, also known as travertine, is re-precipitated calcite that can take a wide range of forms, from "frozen" waterfalls and rimstone dams to stalactites, stalagmites, columns, and so on. (Palmer 2007a). These features may prove important in the interpretation of a cave's history as they are indicative of different physical and geochemical regimes.

Sediments in caves may originate from the surficial landscape or from within the cave itself. Levenson and Emmanuel (2017) found that in addition to dissolution, the detachment of individual grains by electrostatic repulsion contributes significantly to the weathering of carbonate rocks, and may contribute minor sedimentary deposits to cave passages. Breakdown refers to deposits derived from gravitational movement of rock within the cave (i.e. rock falls), and is related to the thickness and competence of ceiling bedding (Palmer 2007a). The presence of colluvium and sediment in cave passages influences the manner in which passages are enlarged by dissolution (Dogwiler and Wicks 2004; Ford 2006). Sediment carried in by streams in fluviokarst systems can "shield" the cave floor, decreasing its reactivity with water, while dissolution proceeds laterally and upwards over exposed rock. This phenomenon is known as paragenesis

(Farrant and Smart 2011). In this sense, cave streams have two beds or channels: the floor and the ceiling, both subject to different corrosive-erosive processes (Klimchouk et al 2000).

One problem with using cave morphology to construe geomorphologic history is that caves rarely conform to one type, and often contain evidence of multiple phases of development (Klimchouk et al. 2000; Ford 2006). Overprinting is a term used to describe cave passages in which complex genetic histories cause passage morphology to reflect a number of different possible modes of development, which can be difficult to verify (Jacoby et al. 2013). Another concern is that processes of cave development in many instances are construed from fossil passages rather than active phreatic conduits; Lauritzen (1985) likens this to studying a corpse rather than the physiology of a living organism. Regardless of these limitations, studies of cave morphology can significantly increase our understanding of the ways water, sediments, organic materials, and biota might move through underground voids and play a role in overall landscape and ecosystem development.

2.3 Karst Modeling

Karst models, whether conceptual or physical, attempt to aid in the understanding of many different aspects of karst geologic systems and processes. Physical models of karst systems may include things like cave maps superimposed on satellite imagery (Moravec and Moore 1974) or dye tracing experiments (David and Brook 1993), as well as digital quantification and statistical characterization of the physical aspects of caves (Kambesis et al. 2015). Conceptual models rely heavily on existing physical models, taking a step further into the realm of interpretation usually on a landscape scale. These

18

include the karst conceptual models proposed by Worthington (2009), White (2009), Crawford (1965), Palmer (1991), and others. This section describes various methods of modeling caves and karst features that have proven useful in the overall discernment of karst landscape evolution.

2.3.1 Survey and Cartography

A cave map is valuable not only to those wishing to navigate caves, but also to scientists and environmental managers of karst landscapes (Dasher 1999). However, there are limitations to cave survey, not least of which is the difficulty of representing a complex, three-dimensional void with a two dimensional map. Line plots give the distance and direction between survey points (stations), while pictorial illustrations in plan view, profile view, and cross-sectional views of the cave give information about the nature of cave passages and features therein (Dasher 1999). There are also human limitations to cave survey, including time, bodily dimensions, energy, and so on.

Cave survey and cartography generally involves three phases or steps: first, collecting the in-cave data (exploration and survey), then, reducing the field data into a usable digital or graphical format, and lastly, drafting the final map or diagram (Dasher 1999). The traditional method of in-cave data collection uses a measuring tape, compass, and inclinometer. Increasing pressure to make surveys more detailed and accurate has led to the use of technologies such as the total station, Leica DistoX2 laser distance meter, and digital still camera photogrammetry (Redovniković et al. 2016). The DistoX2 is a popular tool that makes it possible to survey parts of the cave unreachable by other methods; the fact that it is handheld, portable, lightweight, and suitable for carrying into tight, wet, and muddy places has led to its use in cave surveys around the globe.

2.3.2 Use of Fluorescent Dye in Karst Aquifers

Karst aquifer studies often include a water-tracing component, in order to delineate hydrologic boundaries and determine flow routes and velocities (Crawford 1978; Davis and Brook 1993; Taylor and Nelson 2008). Many caves are humanly traversable only to a point, beyond which direct observations of conduits cannot be made. One indirect approach commonly used in karst hydrology is the injection of fluorescent dye as a tracer (Veni 1999; Taylor and Greene 2008). Dye is injected into the aquifer at a discrete recharge point such as the throat of a sinkhole or sinking stream. Possible discharge points are then monitored for the resurgence of the tracer chemical. Properly conducted dye traces yield valuable information about point-to-point hydrologic connectivity between recharge areas and discharge points (e.g. springs, wells) as well as travel time between points. Repeating tracer tests of the same system in different flow regimes can shed light on changes in aquifer behavior during high and low stage. In karst aquifers this is particularly useful since flow routes are susceptible to change depending on the hydraulic capacity of karst conduits (Mull et al. 1988).

Qualitative dye tracer studies can be done relatively inexpensively using passive detectors (made with activated charcoal) to capture resurging dye (Davis and Brook 1993; Taylor and Greene 2008). With a qualitative sampling design, a rough estimate of flow velocity through the aquifer can be made, and it is possible to reveal the general nature of flow systems (i.e. convergent to one spring versus divergent to many springs) (Mull et al. 1988). With any tracer test, is important to first test for background levels of fluorescence (which in natural waters may be derived from organic acids or human

inputs) and to avoid contamination of samples, since dyes are detected in minute amounts during analysis (Taylor and Greene 2008).

Quantitative dye tracer studies use the same basic methods as qualitative dye tracing, but with increased frequency of sampling that generally requires more time and expense. By continuously measuring discharge and concentration of dye at a resurgence point in the aquifer, one can approximate the mean residence time, mean flow velocity, storage, and other hydrologic parameters (Taylor and Greene 2008).

Analysis of dye tracer tests is subject to certain limitations, a major one being that results are only representative of the conditions at the time of the test (Taylor and Greene 2008). Typically, aquifers are tested in moderate flow regimes, and separate tests run during flood stage may provide additional information as needed. As with any scientific endeavor, the best dye trace results are those that can be repeated. This is especially true in karst terranes where aquifer behavior is subject to change as a result of stage (Taylor and Greene 2008).

2.3.3 Geomorphometry of Caves

Morphometry, the measurement and analysis of form or shape, is used in geomorphology as a quantitative approach to landform analysis (LaFleur 1999; Klimchouk 2003; Klimchouk et al. 2004). When assemblages of landforms, such as caves, are considered from a morphometric standpoint, patterns may emerge that highlight likenesses or differences in specific groups (Piccini 2011; Kambesis 2014). Morphologic patterns can indicate how cave systems developed and what the hydrologic conditions were at the time (Gallay et al. 2016).

In many studies, cave survey data are reduced to obtain morphometric parameters related to their Euclidean geometry, i.e. length, depth, area, volume, and ratios drawn from these, as well as non-linear dimensional characteristics derived from fractal analysis (Piccini et al. 2011; Kambesis 2014). Selected morphometric parameters are described below, and methods for calculating specific indices are discussed in Chapter 4 (Table 3).

Cave field is the two-dimensional area taken up by cave passages (Klimchouk 2003; Piccini 2011). The simplest method of calculating the area of the cave field is to measure the area of the smallest rectangle enclosing the plan view map. Similarly, the cave block is the volume enclosing the entirety of cave passages, and can be calculated by multiplying the cave field by the vertical extent of the cave (Klimchouk 2003; Piccini 2011). These parameters are useful in defining other parameters that are indicative of the extent of karst development (Piccini 2011). For example, areal coverage, which describes the percentage of space occupied by cave passages, can be calculated by dividing the cave passage area by the area of the cave field. Cave porosity, also expressed as a percentage, can be derived from the cave volume and the cave block volume.

Specific volume describes the average dimension of cave passages, based on volume and total cave length. Passage network density gives an indication of the distribution of passages in relation to one another; simple tube-like caves have a low passage network density, while complex maze-like caves have high passage network density. Horizontality index (H_i) and verticality index (V_i) theoretically range from 0 to 1, with high values representing strong horizontal or vertical control, respectively. Vertical shafts have a V_i approaching 1 with a low H_i, while caves confined to horizontal bedding

planes with limited vertical development have a low V_i with H_i approaching 1 (Piccini 2011).

The two-dimensional orientation of cave passages can be described using rose diagrams, circular histograms displaying the frequency of directional data (Piccini 2011). Trends in passage directionality might indicate the effects of structural discontinuities on the hydrologic system and cave development. The frequency distribution of survey shot directions may point to the importance of vertical discontinuities, and when compared with the mean direction of major tectonic structures, may resolve the question of their influence (Piccini 2011).

Typically, morphometric analysis of caves is most successful in small to medium sized caves with limited vertical complexity (Piccini 2011; Kambesis 2014). If a representative population of caves is available, the data can be subjected to statistical analyses to determine the relationships of indices. Comparison of indices derived from cave survey data can help distinguish different "populations" or "families" of caves with similar morphologies, which may result from similar modes of development (Frumpkin and Fischhendler 2005; Piccini 2011; Kambesis 2014). The utility of cave morphometric analysis can be extended to other fields as well; Christman and Culver (2001) note that the quantification of available habitat, an important ecological parameter, requires estimations of cave length, area, volume, and fractal dimension.

The benefit of using morphometry in geomorphic studies is that it is less subjective than interpretations based solely on observation. However, a good understanding of the geologic and hydrologic context is necessary and therefore field observations can and should contribute greatly to the understanding of morphometric

phenomena, which are inherently descriptive (Klimchouk et al. 2004). Morphometry does not determine specific processes, but it can help identify patterns and define categories of karst features (Kambesis 2014). By correlation with other parameters like hydraulic behavior and landscape position, there is potential in morphometric studies to extrapolate the characteristics of a known network to areas that have not yet been explored (Pardo-Iguzquiza et al. 2011).

2.3.4 Geographic Information Systems (GIS)

GIS provides a framework for scientific analysis of the natural world, and is a tool for storing, processing, retrieving, and representing data, using tables, graphs, data transformation tools, statistical and spatial analysis tools, data filters, and viewing platforms for 2D and 3D data (Albert 2017). The basic assumption of spatial analysis in GIS is that visualizations of spatial data (maps) have the ability to show patterns, and patterns can be related to processes or phenomena of interest. The ability to integrate many types of data from a variety of sources gives GIS users an advantage when it comes to visualizing and contextualizing spatial data, and has been used successfully in cave and karst studies to identify patterns in the landscape (Jacoby et al 2013). Geographic Information Systems like the example presented herein are crucial for the management and protection of public lands, especially where karst processes enhance the vulnerability of water as a natural resource (Veni 1999).

2.4 The Pennington Formation (Cumberland Plateau)

The Cumberland Plateau's stratigraphic sequence is comprised of sedimentary rocks deposited first in shallow marine environments during regional transgression in the Mississippian, and then in fluvial-deltaic environments during a major regression in the

Pennsylvanian. In the Cumberland Plateau physiographic province, the two major

sequences are separated by a regional disconformity atop the Pennington Formation

which is the uppermost Mississippian unit. The lithologic composition of the Pennington

Formation reflects the highly variable environments of deposition, with both carbonate

and clastic rock types. This research is concerned with the formation of karstic caves in

the unnamed limestone members of the Pennington Formation where it crops out on the

western escarpment of the Cumberland Plateau.
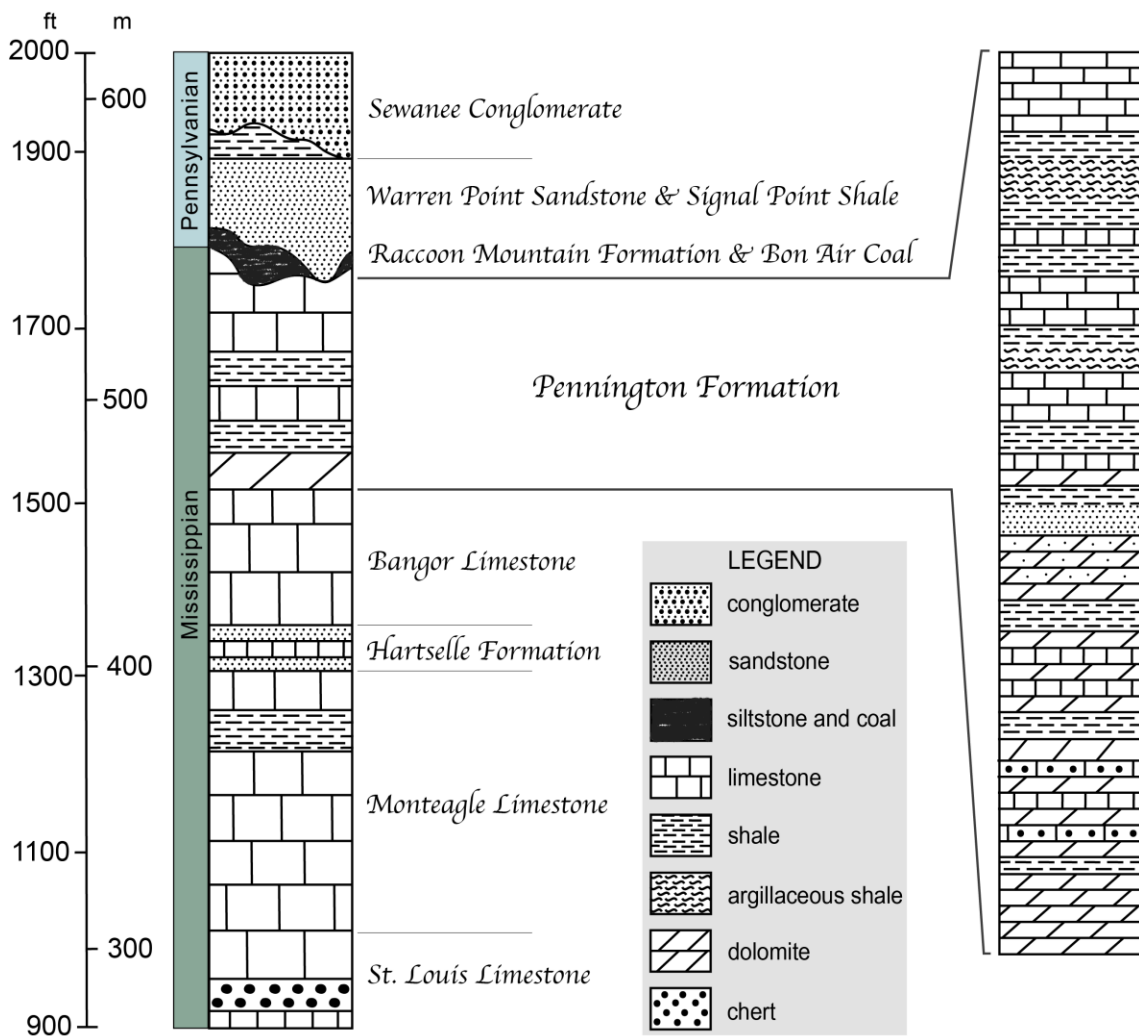
Figure 3. (Left) Generalized stratigraphic section of Mississippian and Pennsylvanian rocks on the western escarpment of the Cumberland Plateau; (Right) detailed lithology of the Pennington Formation (based on Jones and Moore 1982; Shaver et al. 2006).

25

2.4.1 Lithology and Depositional Environments

The upper Mississippian Pennington Formation lies roughly between 300 and 550 meters above sea level (m.a.s.l.) on the Cumberland Plateau (Figure 3). It consists of red and green shale and siltstone, fine-grained dolomite, dark grey limestone, calcareous sandstone, and other mixtures of clastic and carbonate rocks (Rodgers 1953; Milici 1974; Milici et al 1979). Inconsistency in thickness of the formation (0 to 150 m) is the result of an undulating erosional surface (Rodgers 1953), which is discussed in Section 2.4.2. The Pennington Formation rests atop the massive and highly karstified Bangor limestone and is overlain disconformably by relatively impermeable and insoluble Pennsylvanian-aged clastic rocks (Figure 3) (Rodgers 1953; Crawford 1978, Knoll et al. 2015). In eastern Tennessee, the Pennington Formation is thicker and is primarily composed of terrigenous clastic deposits, while on the western escarpment of the Cumberland Plateau in Tennessee and Alabama it is thinner and more calcareous (Thomas 1972; Milici 1974; Milici et al. 1979). Thickness of the unit also diminishes westward as a result of synsedimentary uplift of the Cincinnati Arch (Peterson 1962).

Pennington rocks were deposited in tidal flat, tidal channel, levee, and intertidal environments (Milici 1974; Ettensohn and Chesnut 1984; Bergenback 1993). A paleogeographic reconstruction of the region in Late-Mississippian time (Figure 4) shows a shallow sea and shoreline with drainages carrying clastic sediment from the continental Canadian shield southward (Peterson 1962). Facies changes to the north, at the edge of the Appalachian Basin, confound the measure of the total extent of the Pennington Formation as it grades into other rocks (Ettensohn and Chesnut 1984). The Cincinnati Arch was emergent during the middle to late Missisippian, such that the thickness of

26

formations diminishes in the direction of the arch axis in the Pennington and younger

sequences (Peterson 1962). Units underlying the Pennington Formation, i.e. the Bangor

and Monteagle limestones, tend to be more consistent in lithology and thickness over the

extent of the Cumberland Plateau (Brahana and Bradley 1989).
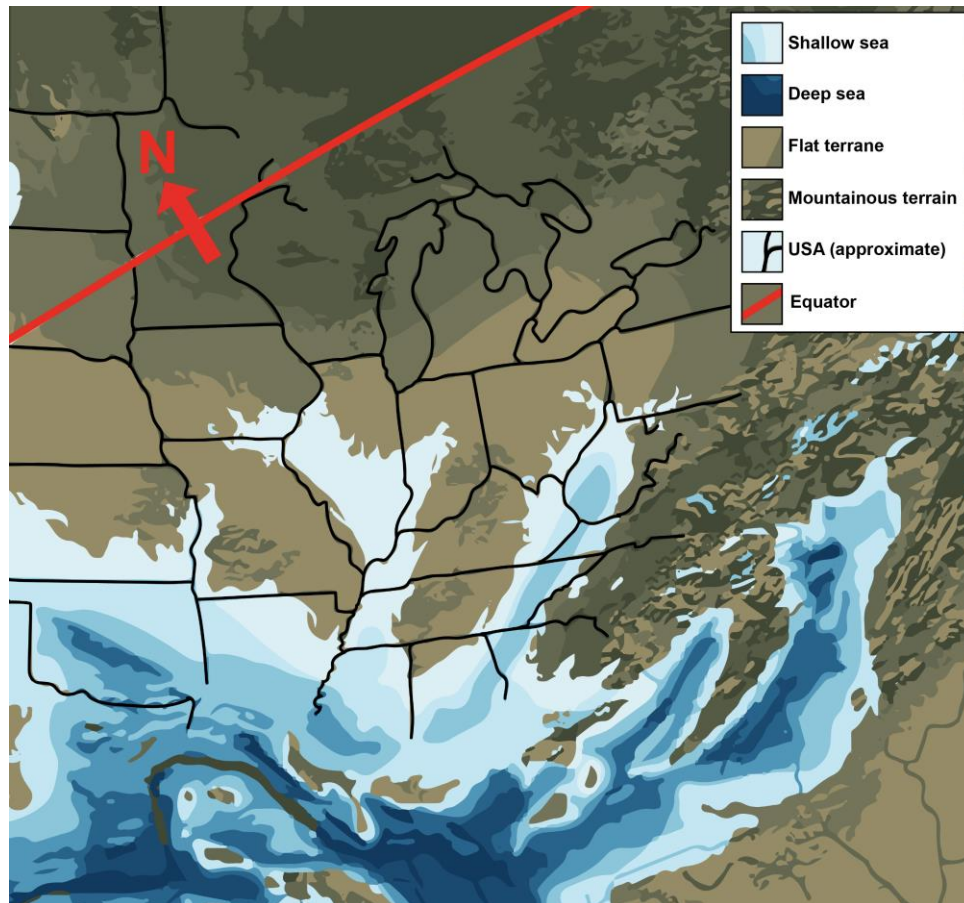
Figure 4. Paleogeography in Late Mississippian time (based on Blakey and Wong 2003).

Brahana and Bradley (1989) describe the Pennington as "an effective confining

layer separating the Pennsylvanian sandstone aquifer from the Mississippian aquifer,"

and Crawford (1965) identified it as an aquiclude; however, facies changes throughout

the extent of the unit complicate this relationship. It is difficult to make assumptions

about karst development where carbonate and clastic rock are interbedded in the

Pennington Formation; it is expected that where the frequency of shale increases in the

formation, so does the likelihood that intervening limestones will be argillaceous and non-karstic (Klimchouk et al. 2000), but this does not always hold true. Small, poorly connected solution conduit systems may develop in sandwiched limestones, as well as dolines and collapse features (Klimchouk et al. 2000).

Cross sections across the state of Tennessee by Milici et al. (1979) show the variation in lithology of the Pennington Formation (Figure 5). The western escarpment of the plateau has appreciable limestone units, while to the north and east the Pennington consists of primarily shale with very thin interbedded limestones (Milici et al. 1979). These lithologic differences have strong implications for aquifer behavior in the Pennington Formation; the nature of the hydrologic system where the unit is dominated by shale is markedly different from where it is karstic in nature.
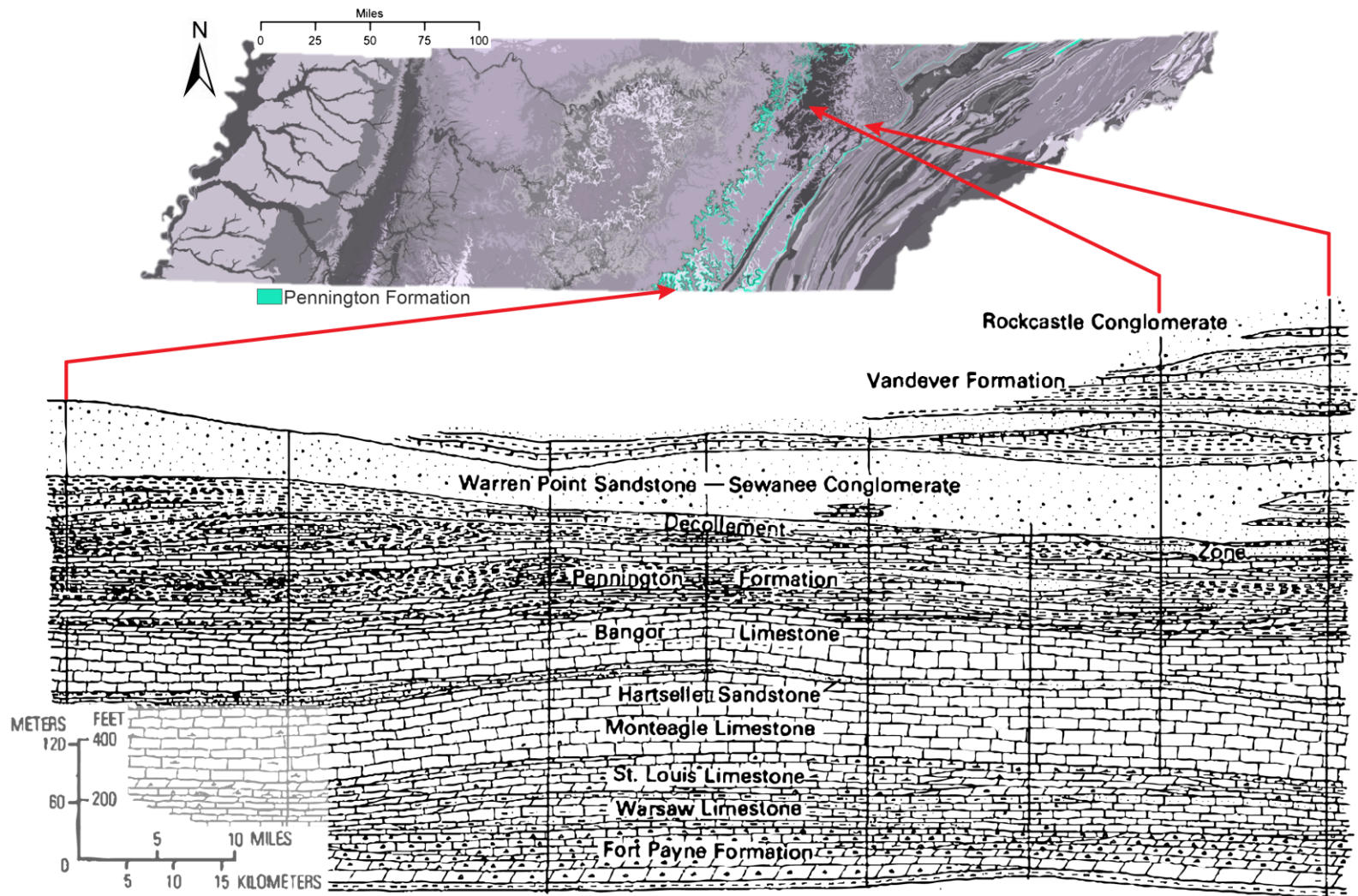
Figure 5. Outcrop area of the Pennington Formation in Tennessee (USGS 2016b) and stratigraphic cross section from south to north along the western Cumberland Plateau (Milici et al. 1979).

2.4.2 Mississippian-Pennsylvanian Disconformity

An unconformable surface atop the Pennington Formation marks a period of intense erosion prior to deposition of Pennsylvanian aged rocks. Field, petrographic, and stable isotope evidence supports the assumption that the upper surface of Mississippian rocks was eroded to a gently undulating surface (relief up to 12 m locally) with paleokarst and paleosols preserved in several outcrops of the Pennington Formation (Driese et al 1998). The contact records a change from primarily marine to definitively non-marine depositional environments, separated by a period of significant karst landscape development (Rodgers 1953; Milici et al. 1979).

The disconformity at the contact between upper Mississippian and basal Pennsylvanian beds is characterized by a gently undulating paleotopography, vertic paleosols, breccias containing Mississippian and Pennsylvanian aged rocks, and paleokarst consisting of dolines, solution pans, collapse features, and solutionally enlarged joints (Driese et al. 1994; Humbert 2001; Knoll et al. 2015). The presence of rhizocretions and microrhizoliths in Pennington mudstones indicates colonization of this surface by plants (Caudill et al. 1996), while vertic paleosols suggest a tropical to subtropical climatic environment with seasonal precipitation (Driese et al. 1998).

2.4.3 Caves and Karst Features

Hundreds of caves have been recorded where the Pennington formation crops out on the Cumberland Plateau escarpment in Tennessee and Alabama (Figure 6), most with an average length of 170 meters but some with lengths over 5,000 meters (Alabama Cave Survey 2018; Tennessee Cave Survey 2017). Of caves where the geologic unit was reported, 328 caves in Tennessee's database were reported in the Pennington Formation,

while 326 Pennington caves were reported in Alabama (Table 1). Studies focusing on the local and regional karst geology of the plateau have often overlooked caves within the Pennington Formation (Anthony and Granger 2004; White 2007) or grouped this unit with the clastic caprock sequence (Crawford 1978; Sasowsky 1992; Palmer 2007).

Table 1. Nature of Pennington cave entrances in Tennessee and Alabama (TCS 2017).

Field Indication	(n = 328) Tennessee Caves	(n = 326) Alabama Caves
In bluff/outcrop	152	68
Sink/Inflowing Stream	58	76
Spring	48	34
In hillside	37	94
Wet-weather streambed	25	18
Roadcut/Quarry	6	0
Obscure/level ground	1	36

Caves and karst features of the Pennington formation are notable in that they are confined between clastic caprock and impermeable shale. The fact that the Pennington Formation directly underlies the caprock is significant for karst development, since Pennington limestones are the first soluble rock encountered by solutionally aggressive streams draining the plateau top (Davis and Brook 1993). The implications of karstification in the Pennington Formation on karst features in these underlying, generally more pure and massive limestones are unknown. In a case study in Sinking Cove, Tennessee (western Cumberland Plateau escarpment), Pennington caves acted as the uppermost level of a stair-stepped, predominantly vadose karst aquifer system draining several blind valleys (Davis and Brook 1993).
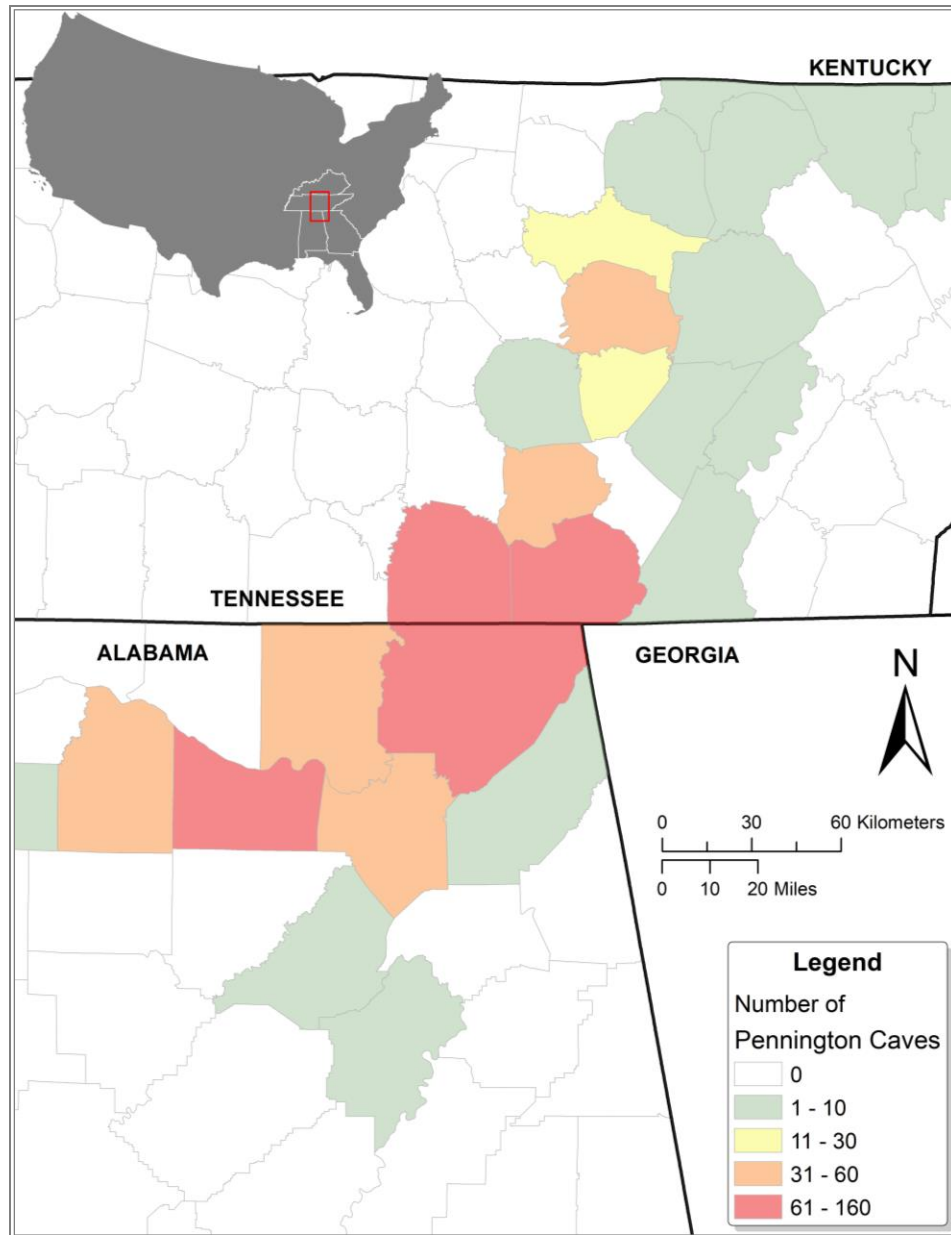
Figure 6. Number of Pennington caves per county in Tennessee and Alabama (Tennessee Cave Survey 2017; Alabama Cave Survey 2018). *NB* the Pennington Formation crops out in Georgia and Kentucky but no cave data were obtained for those states.

2.5 Summary

Karst landscapes exhibit unique hydrologic characteristics and cryptic features which make them difficult to study and understand. However, studies of cave morphology and hydrology can help elucidate patterns of karst development and groundwater flow. Since karst terrane underlies roughly 20 percent of the United States

(Klimchouk et al. 2000), it is essential for land users and managers to understand the implications that caves and the unique geology of karst terrane have for water quantity and quality, ecosystem functioning, land management, and human development. Karst features in the Pennington Formation have often been overlooked in scientific research on Cumberland Plateau caves, leaving a considerable gap in the understanding of this complex karst region.

CHAPTER 3: STUDY AREA

This research is concerned with Pennington caves on the western escarpment of the Cumberland Plateau in Tennessee and Alabama. Savage Gulf State Natural Area was selected as a representative case study based on existing geologic information (Hardeman et al. 1966; Jones and Moore 1982) about the Pennington Formation and reports of 18 Pennington caves within the park boundary (Tennessee Cave Survey 2017).

3.1 The Cumberland Plateau Province

The Cumberland Plateau is a sedimentary layer cake of carbonate and clastic rock types spanning from northern Alabama and Georgia in the south through Tennessee into Kentucky to the north (Figure 7). Its stratigraphy reflects a geologic history of regional transgression in the Mississippian, dominated by carbonate deposition, and a major regional regression in the Pennsylvanian, dominated by clastic deposits originating from the eroding Appalachian highlands (Ettensohn 1980). Burial, uplift, and erosion of this surface resulted in a modern day rolling upland of resistant, cliff-forming sandstones, dissected by steep valleys cut into solution-prone limestone and dolomite. The entire physiographic province dips slightly to the east-southeast off the crest of the Cincinnati Arch, a continental bulge (Rodgers 1953; Wilson and Stearns 1958; Milici et al. 1979). The succession of units and fossils is not complete across the plateau due to tectonically related erosion and nondeposition, yet the majority of rocks adhere to basic chronologic and superpositional relationships (Ettensohn 1980).

The eastern Cumberland Plateau province has been structurally deformed numerous times by Alleghenian thrust-faulting with tectonic transport direction primarily to the northwest (Wilson and Stearns 1958; Knoll et al. 2015). The Pine Mountain

overthrust, the Cumberland overthrust, and the Sequatchie Valley Anticline are features

significant to the regional geomorphology on the eastern Cumberland Plateau

escarpment; structural discontinuities like folds, low angle faults, and systematic vertical

joints in the caprock exert strong control on topography and hydrology (Wilson and

Stearns 1958; Knoll et al. 2015). This study focused on the western plateau escarpment,

where structural deformation is subtler.
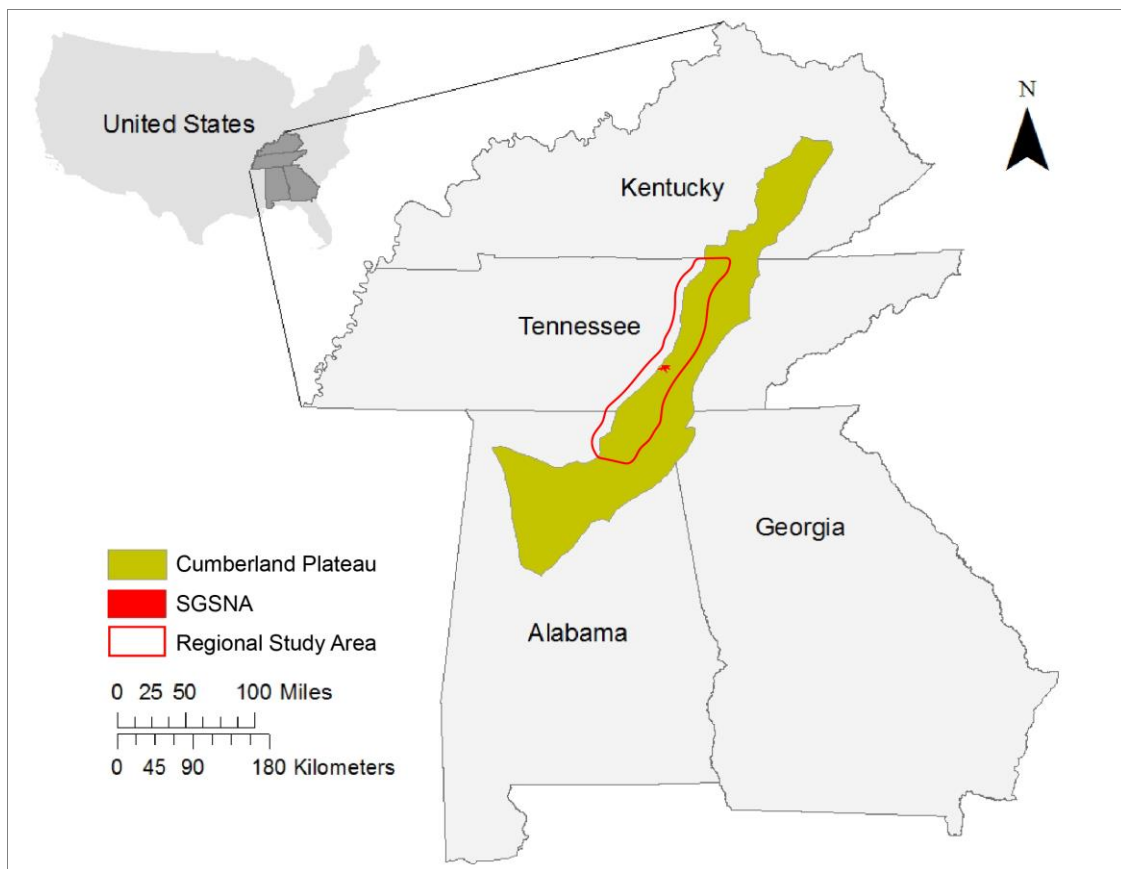
Figure 7. Map showing the extent of the Cumberland Plateau physiographic province (USGS)
with the regional study area outlined and Savage Gulf State Natural Area highlighted in red.

In comparison to the eastern escarpment of the Cumberland Plateau, the western

escarpment has been subject to only minor structural deformation. Rock units have

maintained a near-horizontal orientation with beds dipping one to two degrees east-

southeast (May 1983), about 25 feet per mile (Wilson and Stearns 1958), depending on

locality. The north half of the study area is disturbed only by the Cincinnati Arch, while bedding thrusts in Pennsylvanian strata in the southern half of the study area (the Cumberland overthrust sheet) cause some superficial folding and faulting (Wilson and Stearns 1958; Knoll et al. 2015). At the border of the Cumberland Plateau overthrust sheet with the undisturbed area (near Spencer, Tennessee), echelon thrusts and vertical cross faults are present, but these typically do not penetrate deep beneath the caprock (Wilson and Stearns 1958).

On the escarpment, resistant bluffs with thin regolith give way to gentler hillslopes with deep regolith coating carbonate bedrock (Rodgers 1953; Crawford 1992; Simms 2004). Near-vertical joints in the sandstone caprock, related to compressive stress in the Appalachian province, allow the bluffs along the upper escarpment to maintain a vertical aspect (Simms 2004; Knoll et al. 2015). As the caprock is undermined and collapses, the release of confining pressure causes stress release fractures to open parallel to valley walls. These mechanical apertures are important in that they often host and guide underground solution conduit networks (Sasowsky and White 1994).

The Cumberland Plateau escarpment is a fluviokarst-dominated landform (White and White 1983; Crawford 1992; Granger et al. 2001; White 2007b; White 2009). Cave systems comprising multiple levels of trunk passage are the sum of the chemical weathering of limestone and the lowering of regional base level by mechanical erosion of major rivers (Hack 1966; Powell 1969; Smart and Campbell 2003; Anthony and Granger 2004). Two categories of caves have been described in this system: plateau margin caves, which actively interact with modern drainages (Crawford 1992), and Cumberland-style caves, which are abandoned fossil conduits related to past stable base levels (Sasowsky

1992; Anthony and Granger 2004). Later hydrologic activity may cause Cumberland-style caves to be overprinted with the effects of multiple base levels. Both cave types play a role in landscape evolution on the Cumberland Plateau, as the chemical and mechanical weathering of carbonates is the driver of overall areal shrinkage of the plateau surface (Crawford 1992).

Karst and non-karst aquifer systems, varying in their ability to maintain flow to surface streams, drive the removal of material from the system. In Pennsylvanian rocks, fractures in rocks with low intergranular permeability (shale, sandstone, and conglomerate) host an aquifer perched above basal shales, often resulting in small, perennial springs or seeps at the base of the Pennsylvanian strata (May 1983; Knoll et al. 2015). The karstic Mississippian aquifer system is generally unconfined, though intermittent shales host perched components that resurge as springs at multiple levels on the escarpment (Crawford 1992; Davis and Brook 1993). Streams draining the plateau are often short-lived on the surface, as carbonate bedrock promotes water movement almost exclusively through conduits or solutionally widened openings that pirate surface streams (May 1984, Crawford 1992). However, some water may be retained in the epikarst, where a sponge-like network of pore spaces in soil and weathered bedrock hold water that slowly drains into karst conduits. Crawford's (1992) work stresses the importance of subterranean stream invasion, conduit cavern development, and slope retreat in the evolution of the Cumberland Plateau karst landscape (Figure 8).

The climate in the study area is classified as humid mesothermal (Hart et al. 2012). Precipitation is distributed fairly evenly throughout the year, with long, hot summers and short, mild winters. Snowfall is fairly minimal. Short periods of water

surplus or deficit are experienced often. The complex topography and geology of SGSNA

support a range of edaphic conditions (Hammer et al. 1987; Kruckeberg 1986; Hart et al.

2012). Lithologic diversity enhances soil diversity, which in turn enriches biological

diversity (Kruckeberg et al. 1986). In general, soils are relatively nutrient-poor and acidic

atop the sandstone caprock and increase in organic content and pH in valleys where

carbonates are exposed at the soil rock interface (Hammer et al. 1987).
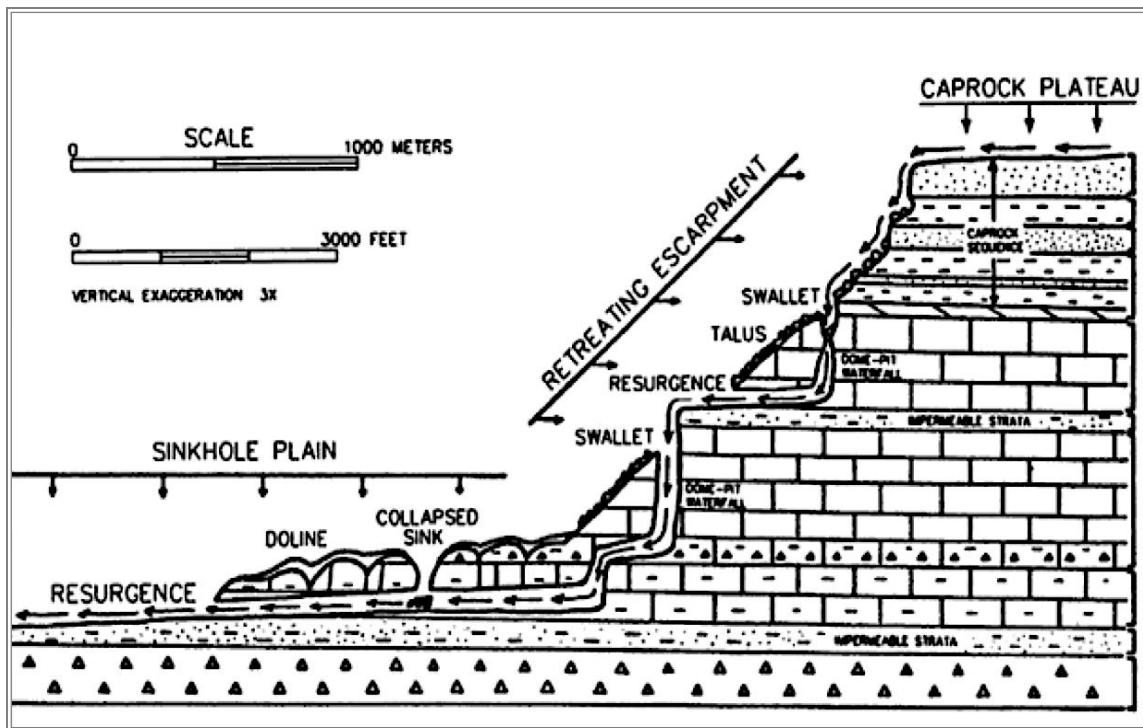
Figure 8. Profile view (simplified) of the karst hydrologic system and multi-level cave
development on the Cumberland Plateau escarpment (Crawford 1978).

Caves on the Cumberland Plateau form beneath valleys or within valley walls

(Crawford 1978; White 2007), serving as preferential paths for flow in accordance with

local base level (Powell 1969; Smart and Campbell 2003). Caves in Tennessee and

Alabama have been recognized in the scientific literature as chronological proxies for

major erosional and depositional events related to episodic incision of major rivers,

evidence of which is rare on the surficial landscape (Sasowsky et al. 1995; Anthony and

Granger 2004; Anthony and Granger 2006; White 2007; White 2009).

The Cumberland Plateau is recognized as an area of globally significant

salamander diversity (Kirchberg et al. 2016), and is considered one of the most diverse

aquatic ecoregions in the country (Duncan and Lockwood 2001). Tennessee karst

terranes are rich in cave biota and endemic troglobites (Culver and Pipan 2009;

Christman and Culver 2001), with notable diversity of crustaceans, beetles, salamanders,

and small aquatic invertebrates (Barr 1967). Of the great diversity of habitats and taxa

found on the Cumberland Plateau (Clements and Wofford 1991; Evans at al. 2016), caves

support perhaps the most sensitive ecological communities (Culver and Pipan 2007; Veni

2013). Being that karst terranes are among the most sensitive environmental systems on

the planet (Veni 1999), their management should be prioritized if groundwater protection

is the end game (TDEC 2003).

3.2 Case Study: Savage Gulf State Natural Area

Savage Gulf State Natural Area (SGSNA) is a 15,590-acre (6309 hectares) tract

owned by the state of Tennessee and managed as a Class II natural area by the Tennessee

Department of Environment and Conservation (TDEC). It is a part of the South

Cumberland Recreation Area (Hart et al. 2012). SGSNA is located entirely in Grundy

County, southeast Tennessee, on the western edge of the Cumberland Plateau escarpment

(Figure 9).
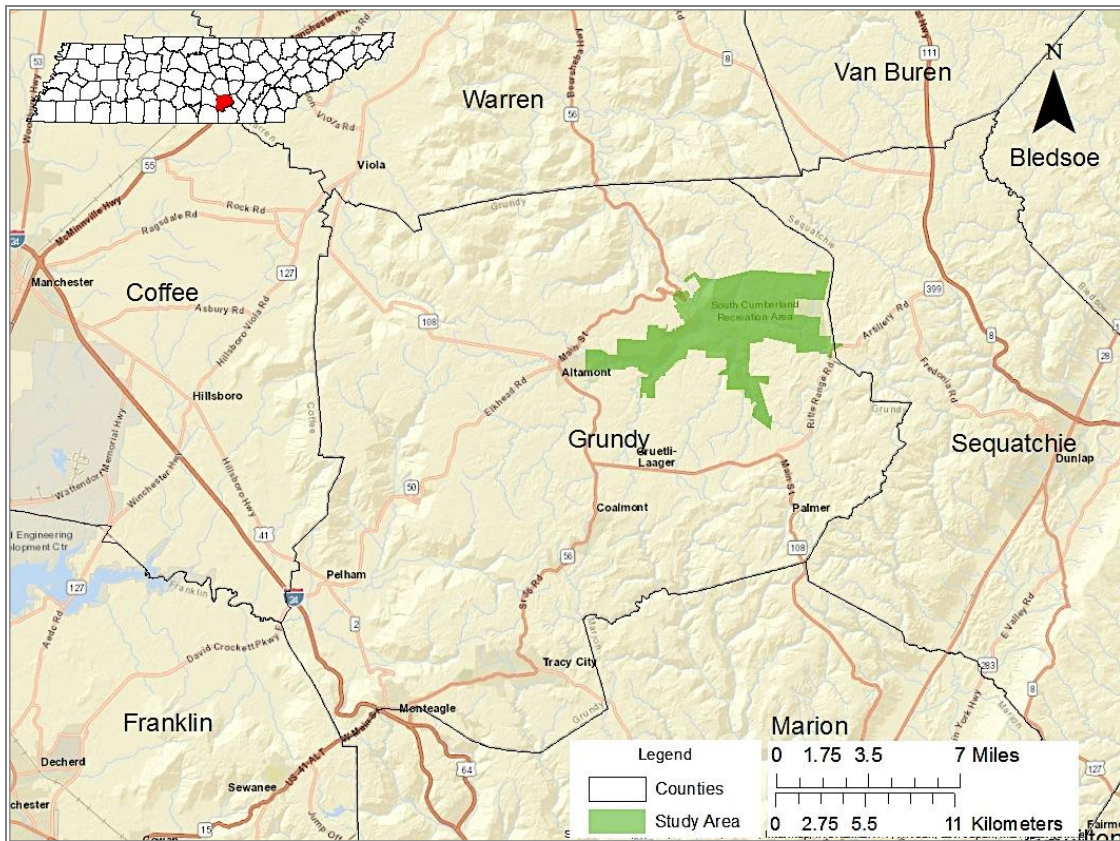
Figure 9. Map showing the location of Savage Gulf State Natural Area and major towns within Grundy County and surrounding counties.

In the mid-1800s, construction, dairy farming, coal extraction, and logging operations began atop the plateau in Grundy County, in what are now the towns of Coalmont, Altamont, Greutli-Laager, and Palmer. Later modifications included impoundments for drinking water, fire suppression, and recreation (Kirchberg et al. 2016). Designated in 1975, SGSNA protects a vast expanse of rich forest and is a listed as a National Natural Landmark (United States Department of the Interior) for its biodiversity (DeSelm and Sherman 1982) and 'unique geologic features' (Hart et al. 1984). Use of the reserve is now restricted to recreation and research (Hart et al. 2012).
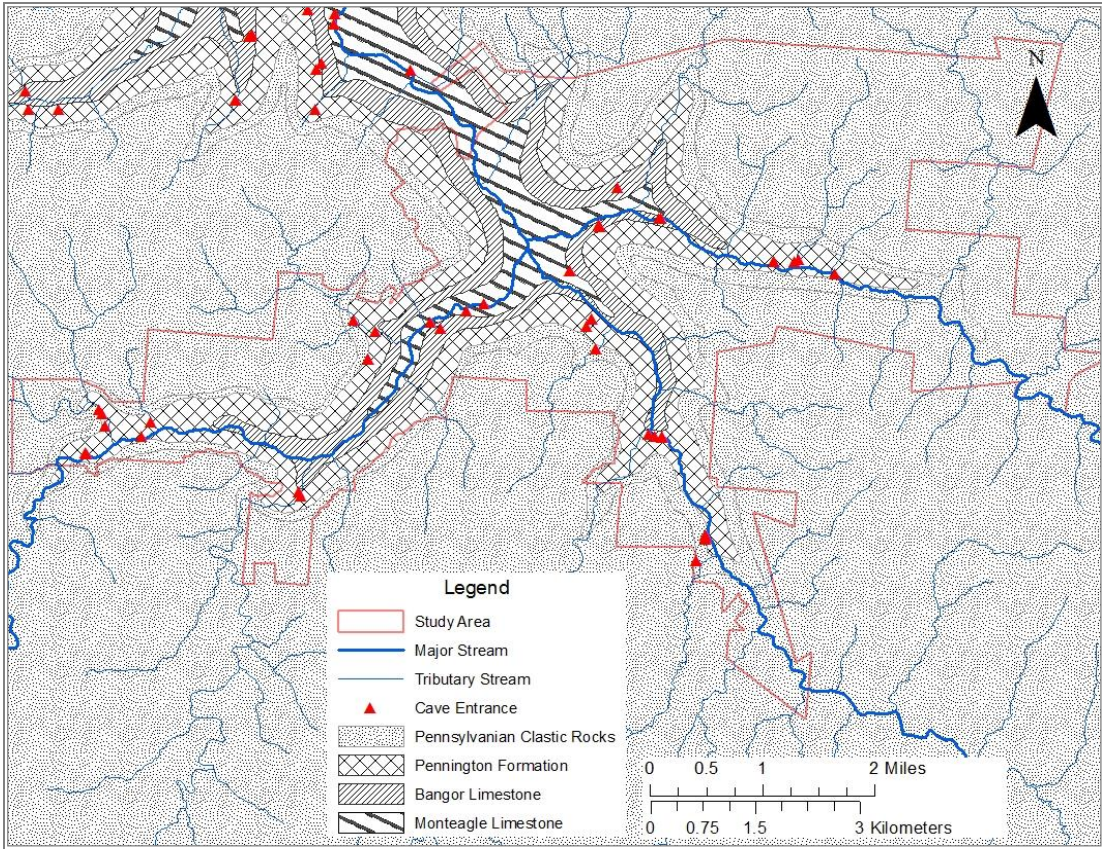
Figure 10. Generalized geologic map of Savage Gulf State Natural Area (from Hardeman et al. 1966) showing major streams and cave entrances (Nicholson et al. 2005; Tennessee Cave Survey 2017; USGS 2016a; USGS 2016b).

SGSNA bounds three major tributary valleys at the head of the Collins River watershed: Big Creek, Collins Creek, and Savage Creek (Figure 10). All are tributaries to the Collins River, which has a drainage area of 2042 km^2 or 811 mi^2 (TDEC 2003). The Collins is a tributary to the Caney Fork River, which joins the Cumberland River before entering the Ohio and Mississippi Rivers. The Collins River watershed supports a variety of land uses and land covers. In SGSNA, the watershed is heavily forested. Land cover changes associated with human activities such as mining, logging, quarrying, and development outside the park boundaries are potential threats to the quality of water entering SGSNA (McGrath et al. 2004; Dale et al. 2009).

41

CHAPTER 4: METHODOLOGY

This research took a mixed-methods approach to defining controls on speleogenesis in the Pennington Formation. Queries were conducted on exist**ing cave information databases.** Spatial cave data were generated and manipulated using specialized cave mapping software. Primary and secondary spatial data were manipulated and analyzed in ESRI's software suite (e.g. ArcMap, ArcCatalog, ArcScene), which is used for geographic overlay, visualization, contextualization, comparison, and analysis of data. Cave models were imported in 2 and 3 dimensions and overlaid with LiDAR (light detection and ranging) derived digital elevation models. The goal was to better understand the hydrology and geomorphology of caves, cave entrance locations, karst conduits, springs, swallets, and dolines in the Pennington Formation. The data available for visualization in the GIS are an amalgam of primary and secondary datasets acquired by the author from October 2016 through April 2018. Data sources are listed in Table 5.

A regional assessment and synthesis of data available via state cave surveys was conducted (Section 4.1). Sixty analog cave maps from the Pennington Formation were digitized (4.2) and their morphometric parameters calculated (4.3). Structural trends in cave passages and valleys were analyzed using the digital cave models (4.4). Stratigraphic relationships within the Pennington formation were analyzed using regional stratigraphic data (4.4). Then, a localized assessment of Pennington caves and karst aquifer characteristics was conducted in Savage Gulf State Natural Area (4.5). This included cave and karst feature inventory (4.5.1), survey and cartography (4.5.2), and dye tracing (4.5.3). Finally, GIS was used to integrate, visualize, and analyze these data (Table 2).

Table 2. Map layers and data sources used in GIS.

Layer	Data Source
Elevation	USGS DEMs and LIDAR (available online at https://catalog.data.gov/dataset/lidar-point-cloud-usgs-national-map)
Contour Lines	Derived from USGS DEM or USGS 1:24,000-scale topo maps
Karst Feature Inventory	Collected with Garmin handheld GPS (Feb-Dec 2017)
Geologic Maps	National Geologic Map Database: Available online at https://ngmdb.usgs.gov/
Caves	Primary survey data collected by the author and digitized in COMPASS Cave Mapping Software; OR; digital model created from analog maps available in the Alabama Cave Survey (2018) and Tennessee Cave Survey (2017)
Stream, Lake, Watershed	US Hydrography dataset (available online at https://nhd.usgs.gov/index.html)
Fluorescent Dye Tracer Test	Primary data collected by the author (July 2017; November 2017)
State Natural Area Boundary	Available online at http://tn-tnmap.opendata.arcgis.com/

4.1 Data Mining and Sample Selection

The Tennessee Cave Survey (TCS 2017) and Alabama Cave Survey (ACS 2017) are proprietary cave information databases run by member-elected officials in each state. These invaluable datasets include cave information (e.g. directions, gear requirements, geology), geographic coordinates of cave entrances, and cave maps, submitted primarily by citizen surveyors and scientists. Both the TCS and ACS are actively growing as new caves are discovered and known caves are mapped. Data mined from the TCS and ACS are indicated below and discussed in depth later in this manuscript.

The TCS and ACS databases were queried for caves that were reported as being formed on the Cumberland Plateau and within the Pennington Formation. There are several problems with this, one being that cave geologic formations are not always accurately reported (or reported at all). Therefore, geologic maps, cave narratives (descriptions) and maps, and other available data were used to select caves that are

formed fully within the Pennington. Caves located at or near the Pennington contact, but with the majority of navigable passage formed within either the Pennsylvanian caprock or the Bangor Limestone, were excluded from the subsample of caves used in morphometric analysis since their morphology is not considered representative of karst processes occurring within the Pennington Formation. Caves located within or to the east of the Sequatchie Valley were also excluded from this analysis, which is focused on the Western Cumberland Plateau escarpment. Ultimately, 60 Pennington cave maps (of the approximately 75 maps available) were selected for conversion to digital three-dimensional models and use in morphometric analyses (Figure 11). A list of selected caves can be found in Appendix B.

4.2 Digitization of Analog Cave Maps

Creating digital cave models for the Pennington Formation first involved compiling all the published maps for confirmed Pennington caves on the Cumberland Plateau escarpment in Tennessee and Alabama. Only maps of sufficient grade (grade 4 or 5) with sufficient detail were used. The selection process resulted in 60 cave maps (26 from Tennessee and 34 from Alabama) which were subjected to digital modeling and further analysis.
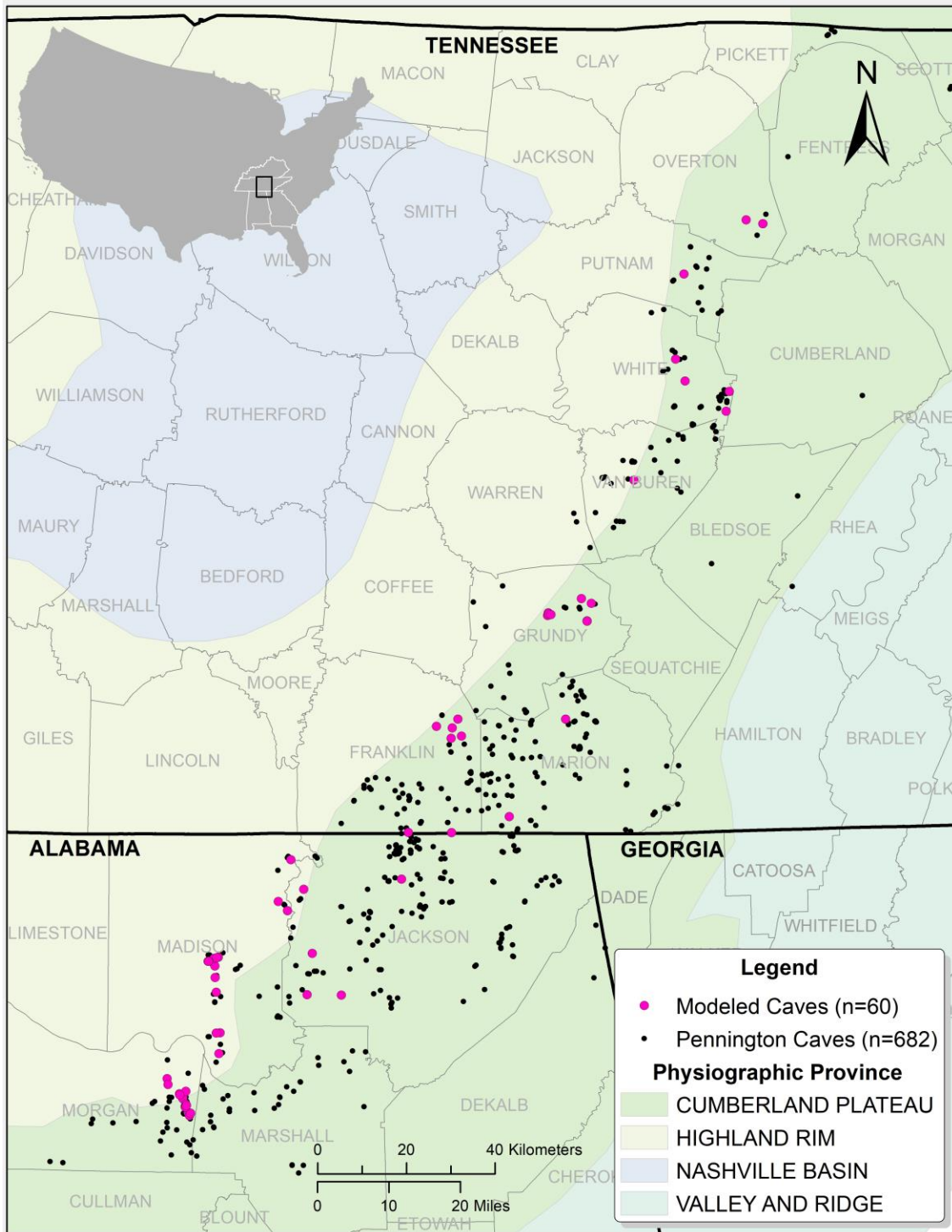
Figure 11. Map showing the distribution of all known cave entrances in the Pennington Formation of Tennessee and Alabama (n=682), with modeled caves (n=60) in pink.

Compass Cave Mapping Software suite (Project Manager, SVG Exporter, CaveXO, and Map to Dat) is shareware available online (Fish 2018) and can be used to manage survey data and export files into a variety of formats for drafting maps and creating GIS-ready layers (Figure 12). Pennington cave morphologies lend themselves to this type of analysis because they are generally limited in vertical extent and complexity, making it possible to construe cave dimensions relatively easily from plan-view maps. Survey data (azimuth, inclination, and distance) was recreated for each cave using the Compass "Map to Dat" software and the scale, declination, and visual indications available on the map (e.g. distance above/below datum, ceiling height, pit depth). If no declination was indicated, the end date of the survey or the year the map was published was used to calculate declination. The resultant ".dat" file was imported to Compass Project Manager and georeferenced using the "Geocalculator," which uses the cave entrance coordinates and datum to spatially reference the cave model in the Universal Transverse Mercator system.

Passage dimensions (distance left, right, up, and down from each survey station) were added to the line plot data (distance, azimuth, and inclination) using the Cave Editor. Estimation of passage dimension was dependent on information available on the map, which in some cases was extremely limited. Passage dimensions were used to create three dimensional digital models of each cave in the Compass CaveXO software. 3D shapefiles for each cave were then imported into a GIS.
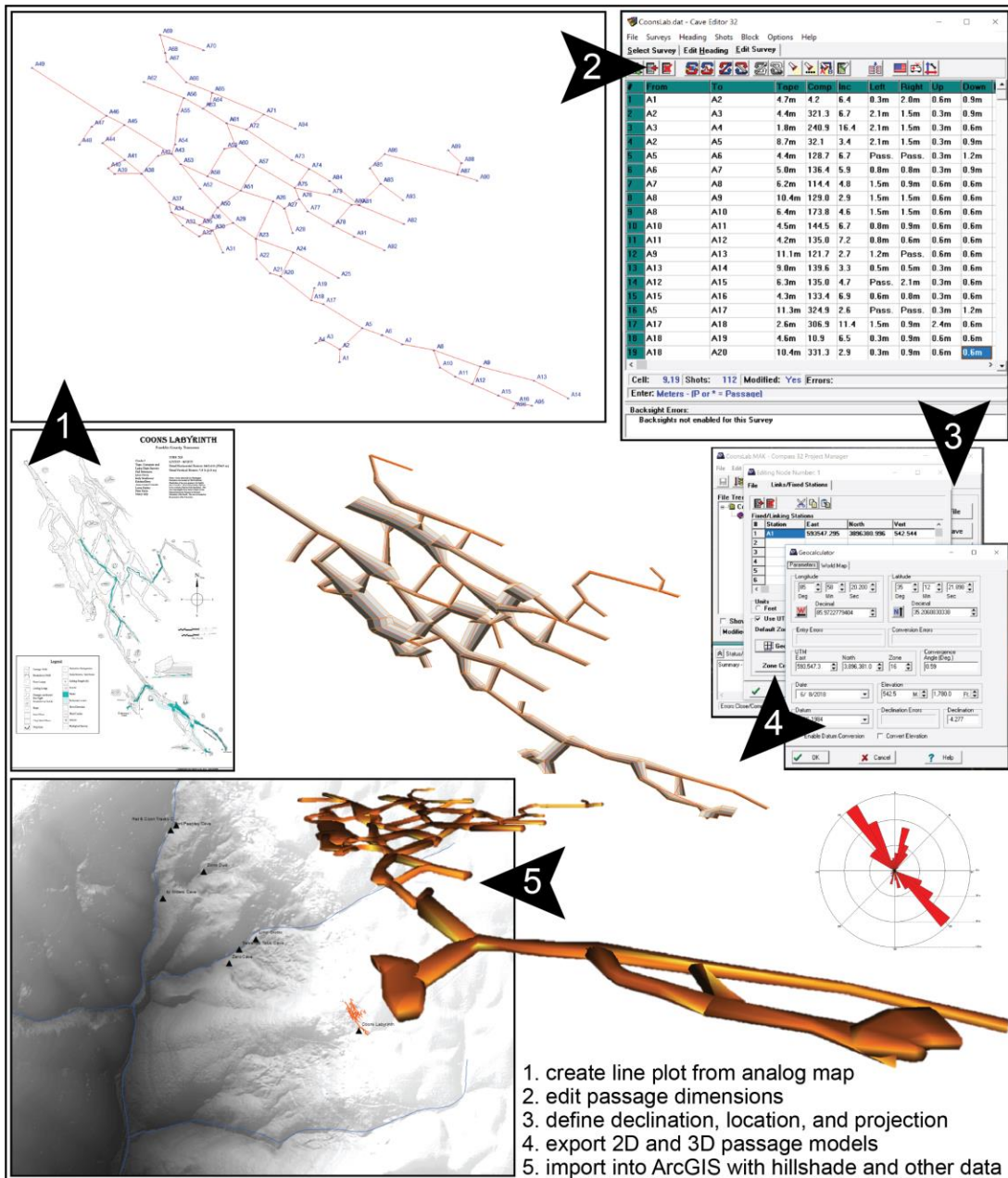
Figure 12. Work flow diagram showing steps taken to digitize analog cave maps and make rose diagrams in Compass Cave Mapping Software (with Coons Labyrinth Cave as an example).

4.3 Cave Morphometric Analysis

Morphometric characteristics of 60 modeled Pennington Caves were used to

quantify attributes of cave morphology and study patterns of cave development (Table 3).

Parameters were determined using the calculations given by Klimchouk et al (2004).

Survey data were processed in Compass Cave Mapping software, which allows for the reduction of data and extraction of certain parameters via the "Cave Statistics" window. Cave survey length, plan or horizontal length, vertical extent, floor area, surface length, surface width, and volume were extracted in this manner. This information was recorded in an excel spreadsheet, which was used to derive morphometric indices (areal coverage, specific volume, passage network density, porosity, horizontality index, and verticality index). Cave field was defined as the area of the smallest rectangle enclosing the plan view of the map (surface length by surface width), and cave block was defined as the volume of a rectangular prism enclosing the entire cave (cave field multiplied by vertical extent).

Table 3. Morphometric indices derived from cave survey data and their methods of calculation (after Klimchouk et al. 2004; Piccini 2011)

Parameter	Method of Calculation	Significance
Areal coverage	Cave area ÷ area of the cave field, expressed as %	Describes the manner in which a cave occupies 2-dimensional space
Specific volume	Cave volume ÷ cave length	Characterizes the average dimensions of cave passages
Passage network density	Cave length ÷ area of the cave field	Describes how densely packed passages are
Cave porosity	Cave volume ÷ volume of the cave block, expressed as %	Describes the manner in which a cave occupies 3-dimensional space
Verticality index (V_i)	Vertical range ÷ cave length	High V_i may signify influence of vertical structural features
Horizontality index (H_i)	Plan length ÷ total cave length	High H_i may signify strong bedding plane control

4.4 Stratigraphic and Structural Analyses

An existing web-based GIS, the National Geologic Map Database (Ngmdb.usgs.gov 2018), was used to study the stratigraphy of the Pennington Formation

throughout the Cumberland Plateau region via 1:24,000-scale geologic quadrangle maps. Cross sections, thicknesses, and elevation of the Pennington Formation were taken from geologic quadrangle maps in Alabama, Tennessee, and Kentucky and used to create regional cross-sectional diagrams (Figures 19A and 19B). These, along with elevation data for Pennington cave entrances, were used to indicate the presence and stratigraphic position of soluble rocks and thus favorable zones for speleogenesis in the Pennington Formation.

Rose diagrams were used to study the influence of fracture permeability (e.g. faults, stress release fractures) on cave genesis by comparing the mean angle of cave passages with the mean angle of stream valleys in which caves are formed. Rose diagrams representing the frequency of survey shot directions were created for each of the 60 modeled caves using the Compass toolset. The number of "bins" around a 360-degree compass rose was set at 36, and the azimuth data from cave digital models were analyzed based on frequency of occurrence. The prominent passage direction for each cave was determined from rose diagrams, and valley direction was measured in the stream nearest each cave using a protractor and topographic maps. Angles were converted to a 0 to 180-degree scale to avoid issues of bimodality in the analysis.

To calculate the mean angle of cave passages and valleys, directional data (azimuth of cave passages and valleys) were transformed into rectangular polar coordinates in Excel by finding the intersection of each angle with a unit circle of radius 1 (Hintze 2007). The sine and cosine functions were used to place this location in standard Cartesian space. Mean angles were then calculated using the following equations (Equation 1), where X and Y are the coordinates of the mean angle, n is the

49

sample size, r is the mean vector, and Θ_r is used to calculate the mean angle (Hintze 2007).

$$Y = \frac{\sum_{i=1}^{n} \sin_a}{n} \qquad X = \frac{\sum_{i=1}^{n} \cos_a}{n}$$

$$r = \sqrt{X^2 + Y^2}$$

$$\cos \bar{a} = \frac{X}{r} \qquad \sin \bar{a} = \frac{Y}{r} \qquad \theta_r = \arctan\left(\frac{\sin \bar{a}}{\cos \bar{a}}\right) \qquad \textbf{(Equation 1)}$$

Simple statistics were used to determine the nature and strength of the relationship between cave and valley directional trends. The Rayleigh z test was used to test the null hypothesis that there is no sample mean direction. The Rayleigh z statistic (Appendix D1) was defined by the equation $z = nr^2$, where n is the sample size and r is the vector from the mean angle equation. This test is used under the assumption that data are unimodal (i.e. there is not more than one clustering of points around the circle) and not diametrically bidirectional (Hintze 2007). Critical values for the Rayleigh z test were taken from Zar (1984).

The Watson's U^2 test (Appendix D2) was used to test the null hypothesis that the two sets of azimuths (valley trend and cave trend) are not significantly different. This non-parametric test was used because the data are not normally distributed. First, the azimuth data were sorted smallest to largest and the entire dataset was ranked in order to calculate the expected frequency of each measurement. The following equation (Equation 2) was used to find the Watson U^2 statistic, where n_1 and n_2 are the respective sample sizes, N is the sum of n_1 and n_2, and d_k is the difference between the cumulative

frequencies for each measurement (Hintze 2007). Critical values for the Watson's U2 statistic were taken from Zar (1984).

$$U^2 = \frac{n_1 n_2}{N^2}\left[\sum d_k^2 - \frac{\left(\sum d_k\right)^2}{N}\right]$$

(Equation 2)

4.5 Case Study: Savage Gulf State Natural Area

In order to ground-truth the trends and patterns observed in the regional and morphometric analysis, Pennington caves and karst features in Tennessee's Savage Gulf State Natural Area were examined in greater detail via inventory, survey, cartography, and fluorescent dye tracer testing. SGSNA was chosen as a type section for studying Pennington caves because 18 Pennington caves were already recorded in the park boundaries, evidence that carbonate members present in this part of the formation (Jones and Moore 1982; Figure 3) allow for karstification at multiple levels within the section.

4.5.1 Karst Feature Inventory

A multipurpose reconnaissance of Pennington Formation karst features in Savage Gulf State Natural Area was conducted in the winter and spring of 2017 under a Scientific Research and Collecting Permit (No. 2017-019) from Tennessee Department of Environment and Conservation (TDEC). Cave entrance coordinates from the Tennessee Cave Survey database were field-checked and new coordinates were recorded as needed. Possible dye injection sites (swallets) and resurgences (springs) were identified and ultimately selected based on site accessibility and the amount of flow present at recharge/discharge points. Karst features were GPS marked with a Garmin GPSMAP® 64S® handheld GPS unit and categorized according to definitions given in Table 4. Since

51

cave entrances are often associated with other karst features (e.g. dolines, springs), there are instances where two features share the same geographic location.

Table 4. Karst Feature Dictionary.

Feature	Definition
Cave	A cavernous void space in soluble rock, enterable by a human being and greater than 50 feet (or 15 meters) in total length or depth
Conduit	A solutionally enlarged void space such as a fracture in soluble rock, not enterable by a human being, but showing evidence of some past or modern drainage
Doline	A closed topographic depression (sinkhole) arising from dissolution and/or collapse
Swallet	The point where a surface stream sinks partially or entirely belowground; a.k.a. "sinking stream"
Spring	The point where groundwater resurfaces

4.5.2 Cave Survey and Cartography

Cave maps are the basis for interpreting local hydrogeomorphology and karst conduit development (Dasher 1999; Veni 1999). Pennington caves selected for this research were surveyed and mapped according to the cartographic standards set forth by the Cave Research Foundation (2010). Maps and cave locations from the Tennessee Cave Survey and Alabama Cave Survey were accessed via paid membership to each of those organizations. Two Pennington cave maps were available for SGSNA (Bear Hole and Small Bluff Cave), and six of the remaining caves were surveyed for this research. These include Greeter Falls Cave, Greeter Gill Cave, Easter Rise Cave, Pinnacle Rock Cave, Fall Creek Saltpeter Cave, and Jezabel Cave.

Survey teams consisted of at least two persons, with three being the ideal number for one team. Teams conducted systematic surveys of Pennington caves using traditional methods of measuring tape, compass, and inclinometer, along with a laser distance/azimuth/inclination device, the Leica™ DistoX (modified to include a non-magnetic, rechargeable battery) (Redovniković et al. 2016). Despite the efficiency and

accuracy of the laser distometer, a fiberglass tape measure was needed for instances where the laser was deemed ineffective (e.g. areas where sunlight or reflections interfere with the laser beam) or less accurate (e.g. distances exceeding 100 feet). Plan view, cross sectional views, and a running profile view of each cave were drawn by hand in the field and later scanned in high resolution in order to draft digital maps using Adobe Illustrator drawing software.

4.5.3 Fluorescent Dye Tracer Testing

Dye tracing was used in this study to investigate the behavior of a karst conduit system associated with caves in the Penninngton Formation in SGSNA. Qualitative hydrologic tracer tests with fluorescent dyes were performed at high and low stage in order to establish hydrologic connectivity between major swallets in Big Creek and Firescald Creek, and several springs and cave streams on the northwest bank near the confluence of these two streams (Figure 13). These tests served to investigate the possibility of stream piracy of Firescald Creek by Big Creek through caves and karst springs in the Pennington Formation upstream of the apparent confluence. All fluorescent dye tracer tests were registered with the Tennessee Department of Environment and Conservation (Division of Water) prior to dye injection.

A karst feature inventory conducted in the study area identified two caves and seven springs which are the subjects of this dye trace (Table 4). Each site was georeferenced using a handheld GPS. Two separate rounds of testing were performed, one in July 2017 (dry season) and another in November 2017 (wet season).

Table 5. Description of fluorescent dye monitoring and injection sites shown in Figure 13.

Site	Description
1	Greeter Gill Cave (receptor in waterfall near survey station 10)
2	Spring, intermittent, on the west bank of Firescald Creek
3	Spring, intermittent, on the west bank of Firescald Creek
4	Spring, intermittent, on the west bank of Firescald Creek
5	Spring, intermittent, on the west bank of Firescald Creek
6	Spring, intermittent, on the west bank of Firescald Creek
7	Spring, intermittent, on west bank at confluence of Firescald Creek & Big Creek
8	Spring, perennial, on the north bank of Big Creek
9	Easter Rise Cave, a spring cave on the north bank of Big Creek
10	Downstream of the confluence of Firescald Creek and Big Creek
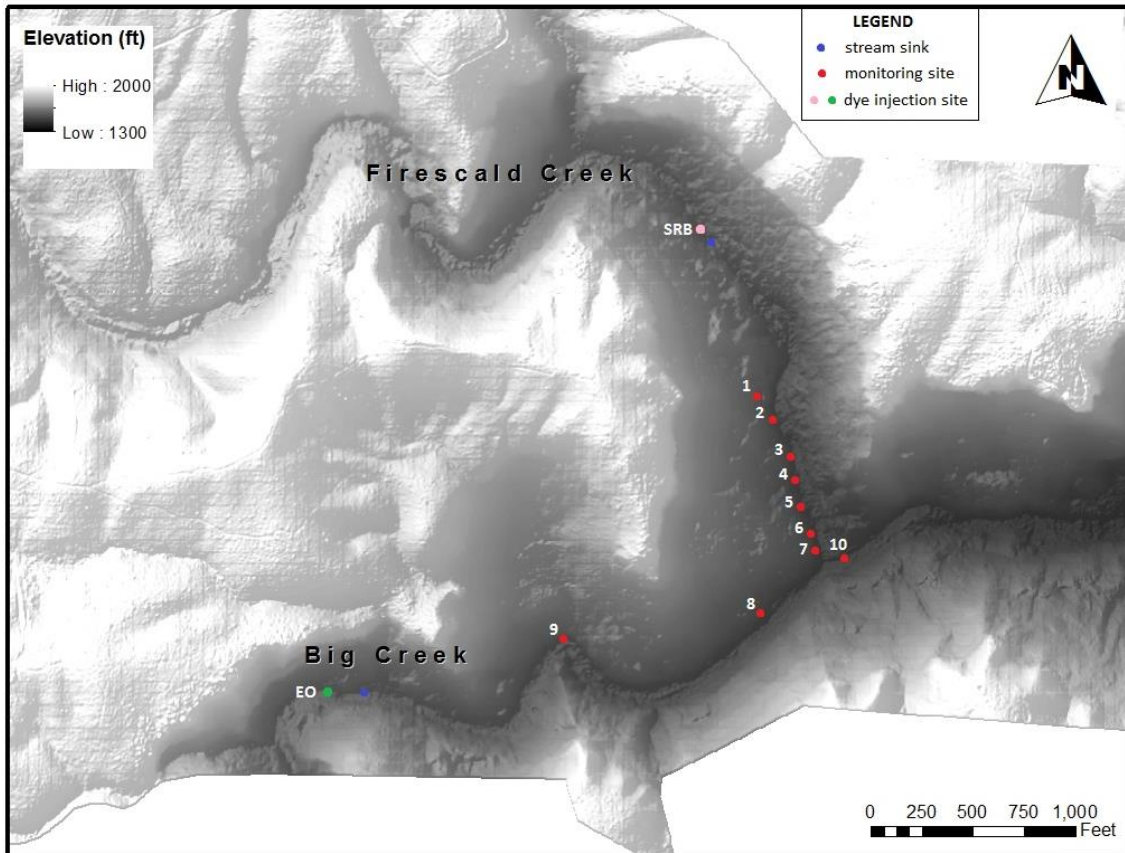
Figure 13. Digital elevation model of the study area showing dye injection locations (EO = Eosine, SRB = Sulphorhodamine-B, and monitoring sites (see Table 4).

Before conducting tracer tests, background levels of fluorescence were determined using activated charcoal receptors installed at each site for approximately one week. Receptors were anchored with cotton string and/or galvanized steel wire to trees, roots, or rocks in or near the water. The Crawford Hydrology Lab's Step-by-Step Field Procedures and Recommendations were followed when installing and changing dye receptors (CHL 2016b). A small cooler was used to transport dye receptors between the field and the lab, with careful attention not to expose the receptors to light.

For the first round of dye tracer testing, background receptors were installed on July 9 2017, then collected and replaced on July 15. On July 21, 500 mL of Eosine (EO) was injected upstream of the major stream sink in Big Creek, and 500 mL of Sulphorhodamine B (SRB) was injected upstream of the sink in Firescald Creek. Leakage of the EO into the main carrying pack was noted at the Big Creek injection point, and decontamination with bleach was implemented to avoid contamination of the other site. Results from this trace indicate these efforts were successful, i.e. contamination did not occur. Dye receptors were collected and replaced at each of the ten sites on July 29 and August 13, and collected for a final time on September 3 2017.

For the second round of dye tracer testing, background receptors were installed on November 12 2017, then collected and replaced on November 19. On November 19 (after installing new receptors), 3000 mL of EO was injected upstream of the major sink in Big Creek, and 3000 mL of SRB was injected upstream of the major sink in Firescald Creek. Dye receptors were collected and replaced at each site on November 22 and collected for a final time on November 26 2017.

Sample preparation and analysis was conducted in the Crawford Hydrology Laboratory at Western Kentucky University using the lab's standard operating procedures (CHL 2016a). In the laboratory, dye receptors were rinsed clean of dirt and debris with tap water, then placed on an aluminum foil-lined drying rack and dried in a 50°C drying oven for at least 12 hours. After drying, 1 gram of charcoal from each receptor was weighed into a labeled plastic sample cup, then eluted with smart solution for thirty minutes. The resulting solution was poured into labeled glass vials, which were capped and placed in a 6°C refrigerator to await analysis.

The Crawford Hydrology Laboratory's Shimadzu spectrofluorophotometer was used to determine presence or absence of dye in each sample. All samples were first run against low-concentration standards for each dye, then against high-concentration standards if dye was detected in high concentrations. Crawford Hydrology Lab's standards dictate that a dye must be positively detected more than once, on separate sampling dates, for a legally defensible "positive" to be indicated. However, singular positive "hits" are still discussed in this analysis, as the aim of this dye trace is scientific investigation and not legal dispute.

CHAPTER 5: RESULTS

The purpose of this study was to identify controls on speleogenesis in the Pennington Formation on the western Cumberland Plateau escarpment in Tennessee and Alabama by examining cave geomorphology, hydrology, and geology at regional and local scales. The results from the regional study and case study shed light on important aspects of Pennington cave development on the western Cumberland Plateau escarpment, including stratigraphic, structural, and hydrologic trends.

5.1 Morphology and Morphometry of Pennington Caves

Three general cave morphologies are identified here (Figure 14) to facilitate the discussion of these features in the context of their geologic and hydrologic origins in the Pennington Formation. The speleogenetic processes giving rise to each type of cave are unique, but not independent of one another, therefore a large number of caves have features indicative of more than one process (overprinting). A large number of caves fail to conform to only one category; in these cases, caves were classified by what was subjectively considered the dominant "type."

Branch or tube-like caves consisting of major conduits and their tributaries are the most common cave morphology in the Pennington Formation, making up 79% of the 660 caves in the sample, and 66% of the caves modeled (n=60). These passages are a hallmark of fluviokarst systems and often reflect the dendritic pattern of surface drainages. This cave type is abundant on the Cumberland Plateau where tributaries feed into large "trunk" cave conduits, known locally as "boreholes". Grapevine Cave (Figure 14, lower) is an example of a branch type cave in the Pennington Formation.

Shafts or pits are the second most common Pennington cave morphology, making up 16% of all (n = 660) Pennington caves and 16% of modeled (n=60) Pennington caves. Shafts are sometimes superimposed with passage morphologies, but in the Pennington Formation many pit type caves occur in isolation, as is the case with blind vertical shafts like Turtle Pit (Figure 14, upper right).

The least common cave morphology is the maze, making up 5% of all (n=660) Pennington caves and 16% of modeled (n=60) Pennington caves. Mazes consist of dense networks of passages containing many closed loops, often with near-perpendicular junctions. Mazes are associated with dissolution in vertical fractures in thin bedding planes, and can form beneath jointed caprock or as a result of floodwater injection into confined fracture networks (Palmer 1991). Humongous Maze Cave (Figure 14, upper left) is an example of a Pennington maze cave.

The average reported length of Pennington caves (n=660) was 170 meters. Modeled caves (n=60) had an average length of 459 meters. The distribution of cave lengths for all Pennington caves on the western plateau escarpment (n=660) and for modeled Pennington caves (n=60) reflects the power law. In both samples, the vast majority of caves are under 100 meters in length, and very few caves surpass 1000 meters in length. This is concordant with the assumption that cave lengths exhibit fractal geometry (Curl 1986). Maze type caves (n=30) are some of the longest Pennington caves, with average length of maze caves 821 meters (2693 feet).
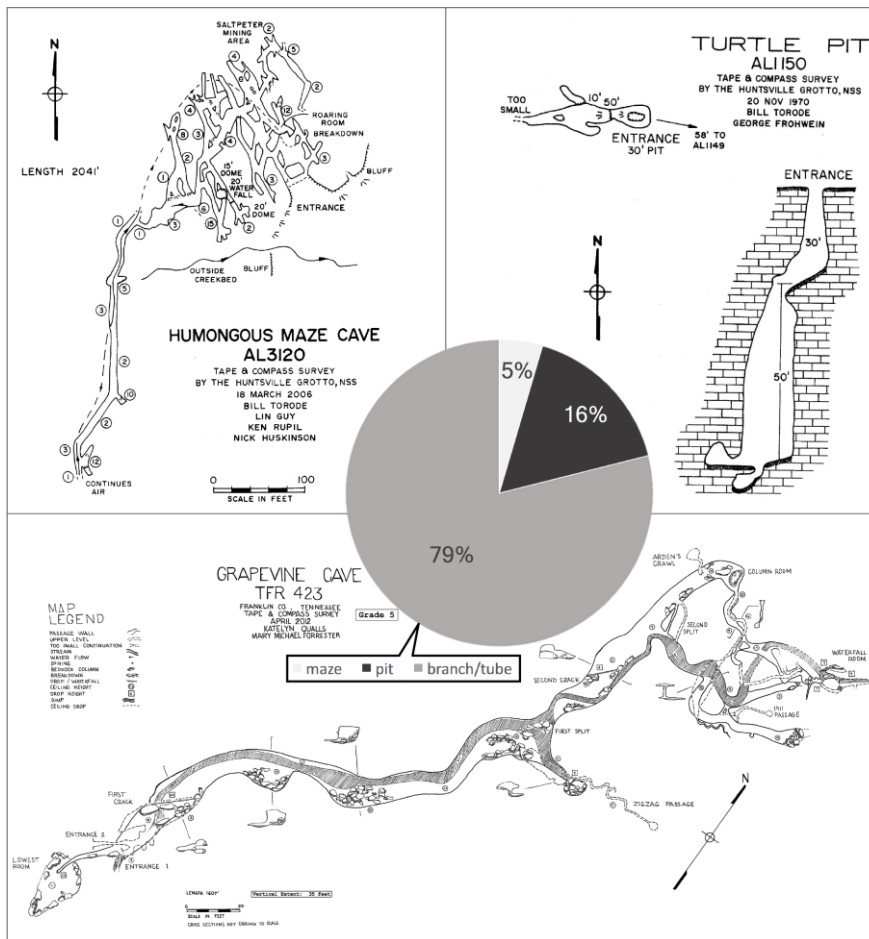
Figure 14. Examples of the three different cave types found in the Pennington Formation. Upper left: maze (5% of all Pennington caves, n=660), right: pit (16%), bottom: branch/tube (79%).
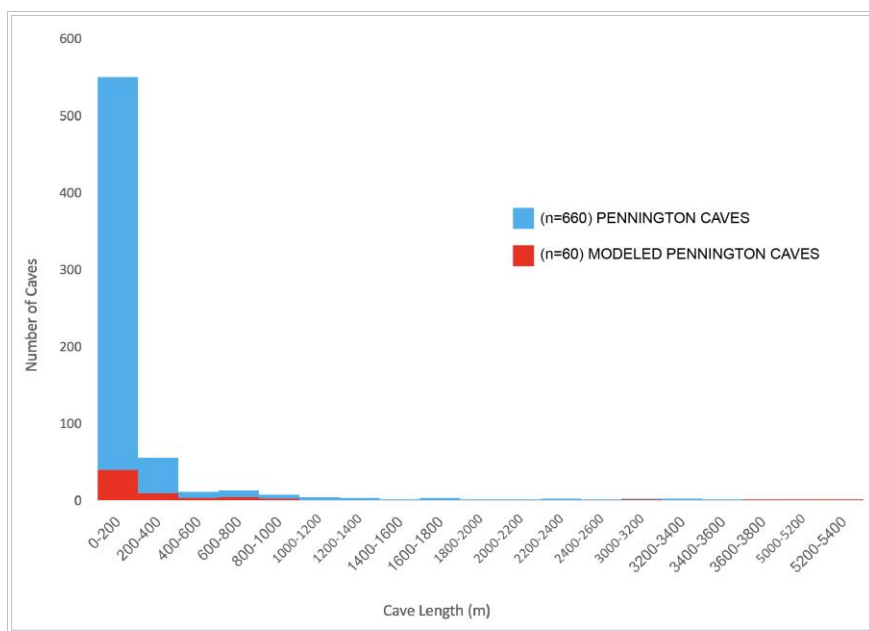
Figure 15. Histograms showing the distribution of Pennington cave lengths in Tennessee and Alabama (n=660) and the distribution of cave lengths in modeled Pennington caves (n=60).
The average reported vertical extent of Pennington caves in Tennessee and

Alabama is 7 to 12 meters, while modeled caves have an average vertical extent of 12.9

meters (Table 6). The average shaft depth is 11.7 meters. Again, the vast majority of

Pennington caves have extremely limited vertical extent, with only a handful of caves

surpassing the average. The average volume of modeled caves was 2957 cubic meters,

while the average specific volume (dimension of passages) was 12 square meters (Table

6). The horizontality index of caves in the model was 0.85 on average, suggesting strong

horizontal developmental controls, while the average verticality index of modeled caves

was 0.23, suggesting a limited amount of vertical development. The complete list of

modeled Pennington caves with all morphometric values is included in Appendix B.

Table 6. Parameters of modeled caves in the Pennington Formation compared with parameters calculable for all Tennessee Pennington Caves and all Alabama Pennington caves.

		Modeled (n=60)	Tennessee (n=328)	Alabama (n=332)
	Max	542.5	786.4	502.9
Elevation (m)	Mean	393.6	419.4	321
	Min	225.5	207.3	152.4
	Max	5381.8	5381.8	3355.8
Length (m)	Mean	459.4	169.9	172.9
	Min	8.9	2.4	5
	Max	55.5	47.5	91.4
Vertical Extent (m)	Mean	12.9	7.3	12.3
	Min	1.0	0.9	1.0
	Max	1.0		
Areal Coverage	Mean	0.35		
	Min	0.01		
	Max	68160.2		
Volume (m³)	Mean	2445.9		
	Min	28.0		
	Max	52.6		
Specific Volume (m²)	Mean	9.3		
	Min	1.2		
	Max	1.0		
Passage Network Density	Mean	0.17		
	Min	0.01		
	Max	1.0		
Horizontality Index	Mean	0.84		
	Min	0.25		
	Max	1.0		
Verticality Index	Mean	0.24		
	Min	0.01		

GIS was used to visualize morphometric data from cave models and look for patterns and trends. Figure 16 shows the spatial trends in horizontality index (left) and verticality index (right), using graduated symbols and colors to show the range of values. Horizontality index values were consistently high across the study area, while verticality index values tended to be low in the north and high in the south of the study area. No obvious spatial trends were identified for the other morphometric parameters (passage network density, areal coverage, specific volume, et cetera).
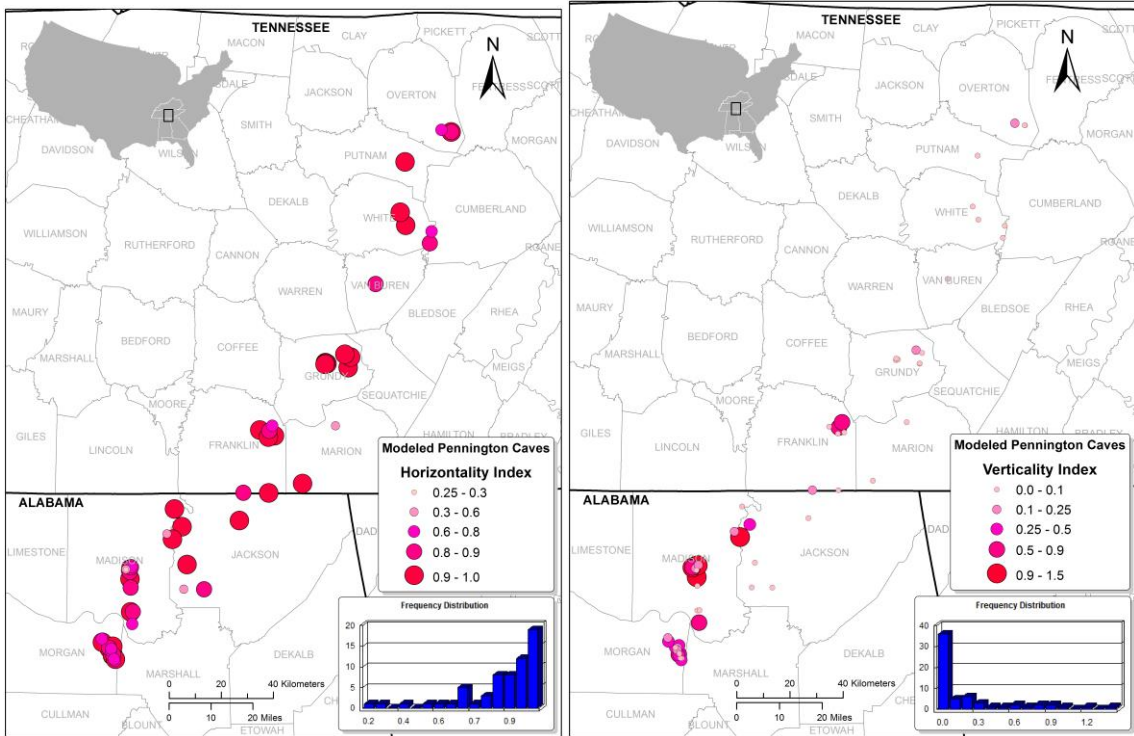
Figure 16. Maps showing modeled Pennington caves symbolized by horizontality index (left) and verticality index (right), and the distribution of values for each index (histograms).

5.2 Stratigraphic Analysis

The distribution of cave entrance elevation values and spatial trends in cave entrance elevation across all Pennington Caves on the western plateau escarpment in Tennessee and Alabama (n=660) is shown in Figure 17. Most cave entrances in the Pennington Formation occur between 350 and 450 m.a.s.l., though many Pennington caves in Alabama have entrances between 200 and 250 m.a.s.l. Modeled Pennington caves (n=60) had an average elevation of 394 m.a.s.l (Table 6). Pennington cave entrances in Tennessee tend to cluster at higher elevations (mean 420 m.a.s.l.) than in Alabama (mean 321 m.a.s.l.) (Table 6), which reflects the overall east-south-eastern dip of the plateau and the changing thickness and lithology of Pennington carbonates in the south of the study area.
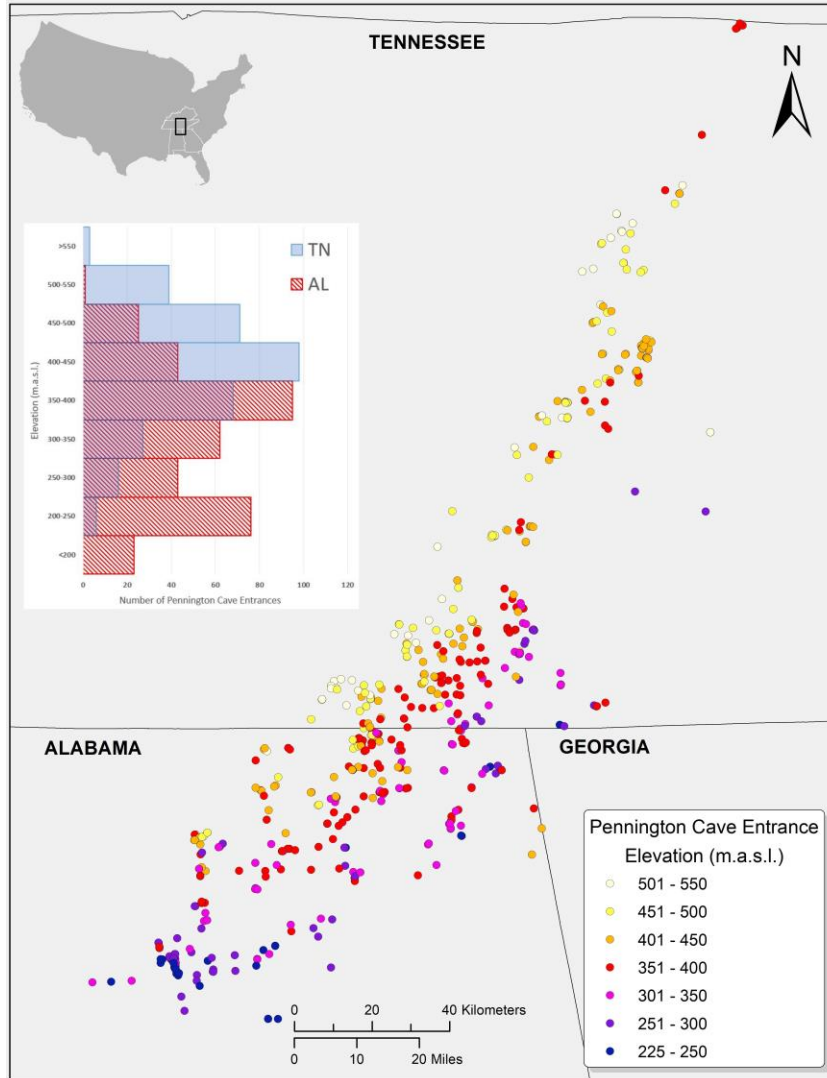
Figure 17. Pennington cave entrances (n=660) symbolized by elevation (m.a.s.l), with overlapping histograms (inset) showing the altimetric distribution of Pennington cave entrances in Tennessee (blue) and Alabama (red).

Stratigraphic cross sections through the study area (Figures 18, 19, and 20) show

the lithology and relative elevation of the Pennington Formation (based on 1:24,000-scale

geologic quadrangle maps), with Pennington cave entrance elevation data from each

quadrangle indicated symbolically. Since the thickness and lithology of the Pennington

Formation are subject to change at the scale of several kilometers, Figures 19 and 20

depict a vast generalization of the unit. However, the cross sections clearly show the

structural high of the Cincinnati Arch, which accounts for the diminishing elevation of

63

Pennington strata eastwards (Figure 20) and the doming upwards of strata in central Tennessee (Figure 19). The same trend can be observed in Pennington cave entrance elevation data (Figure 17). Cave entrance elevation data plotted on the cross-sectional diagrams (Figure 19 and 20) show how caves can be well-distributed throughout the Pennington Formation in some areas (Figure 20, B-B') and poorly distributed or not present in others (e.g. Bald Knob quadrangle, Brockdell quadrangle).
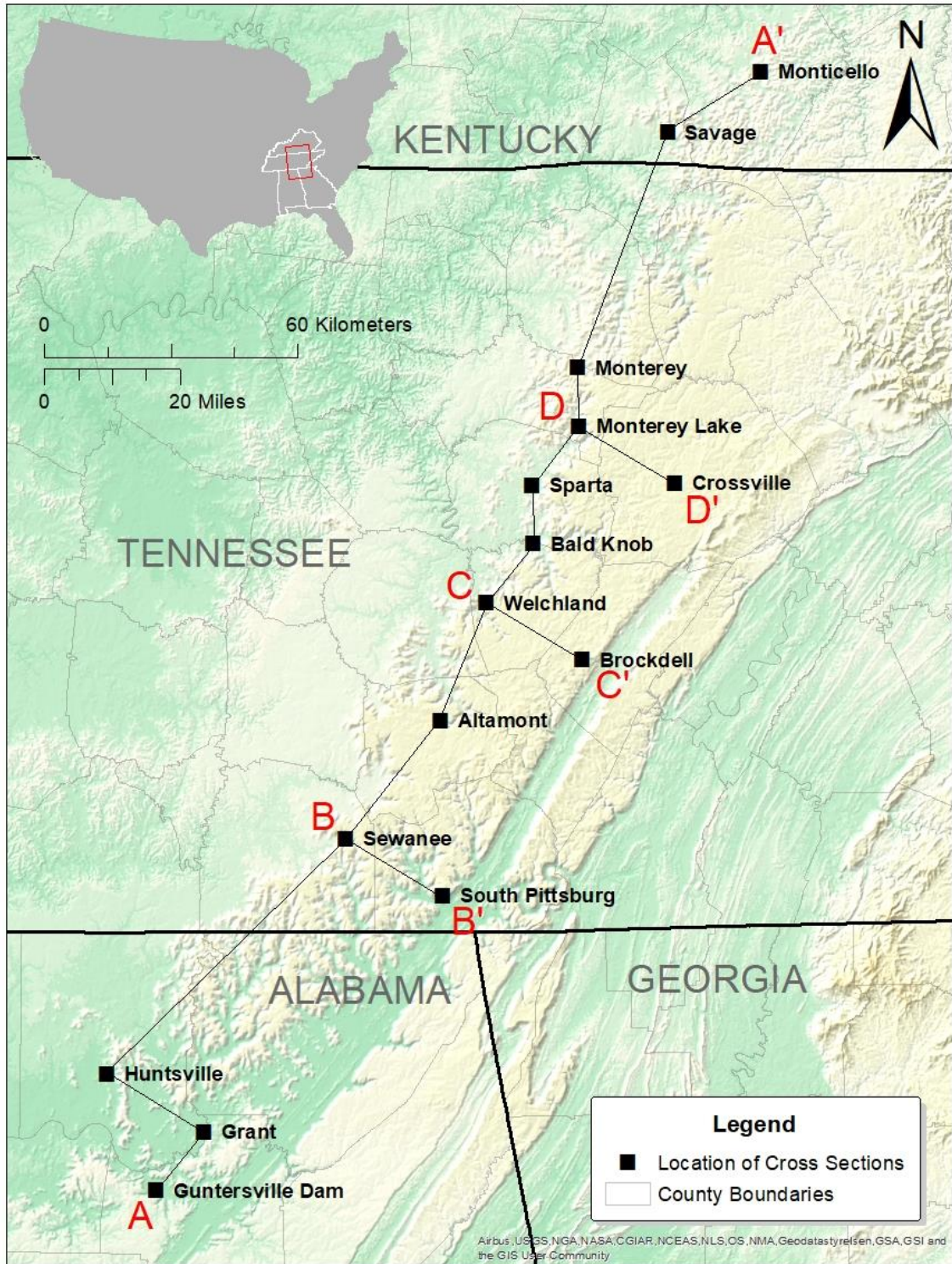
Figure 18. Location of geologic quadrangle maps (Ngmdb.usgs.gov 2018) used to construct stratigraphic cross sections shown in Figures 19 and 20.
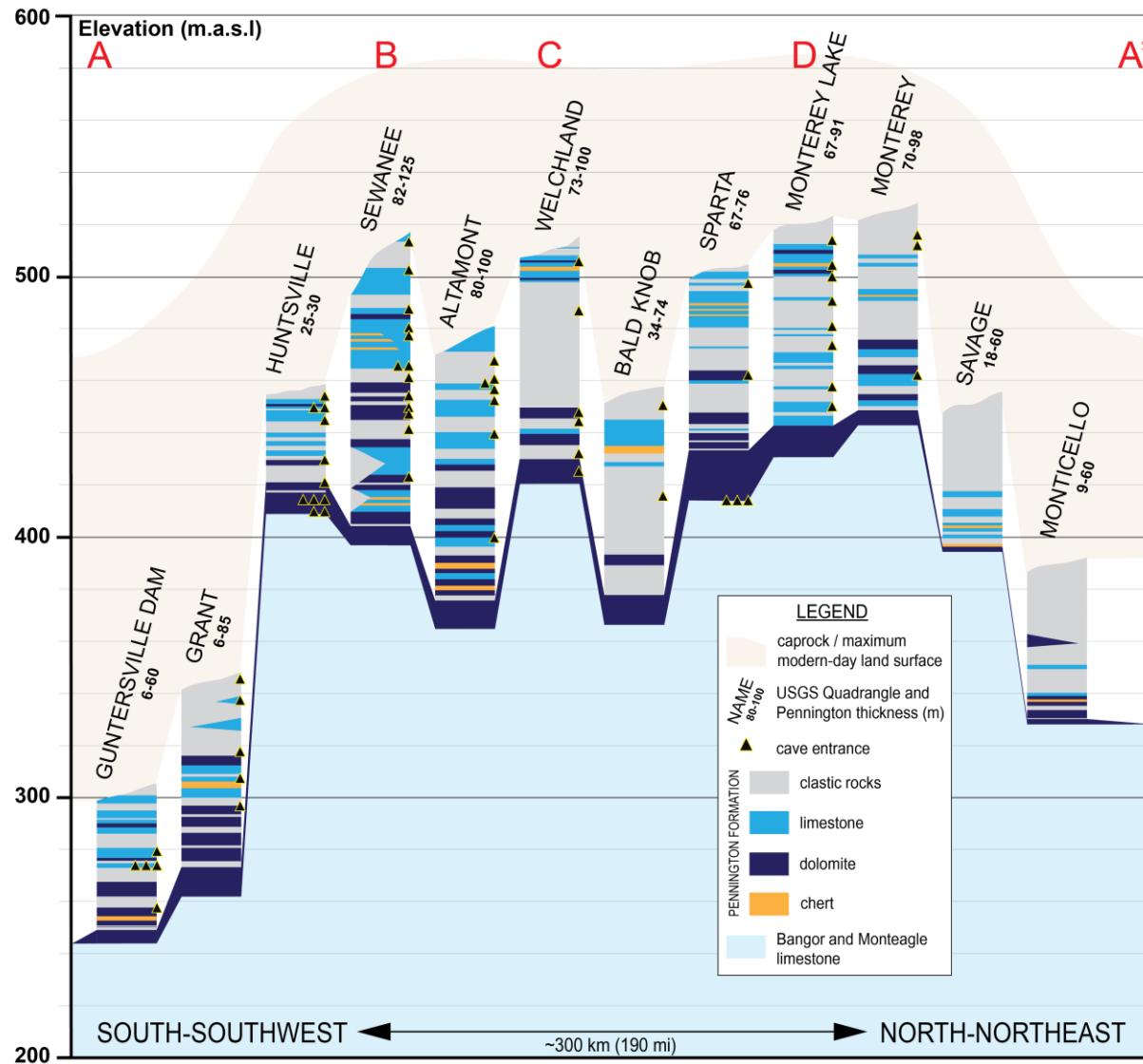
Figure 19. Stratigraphic cross section (A-A') of the Pennington Formation based on geologic quadrangle maps shown in Figure 18.
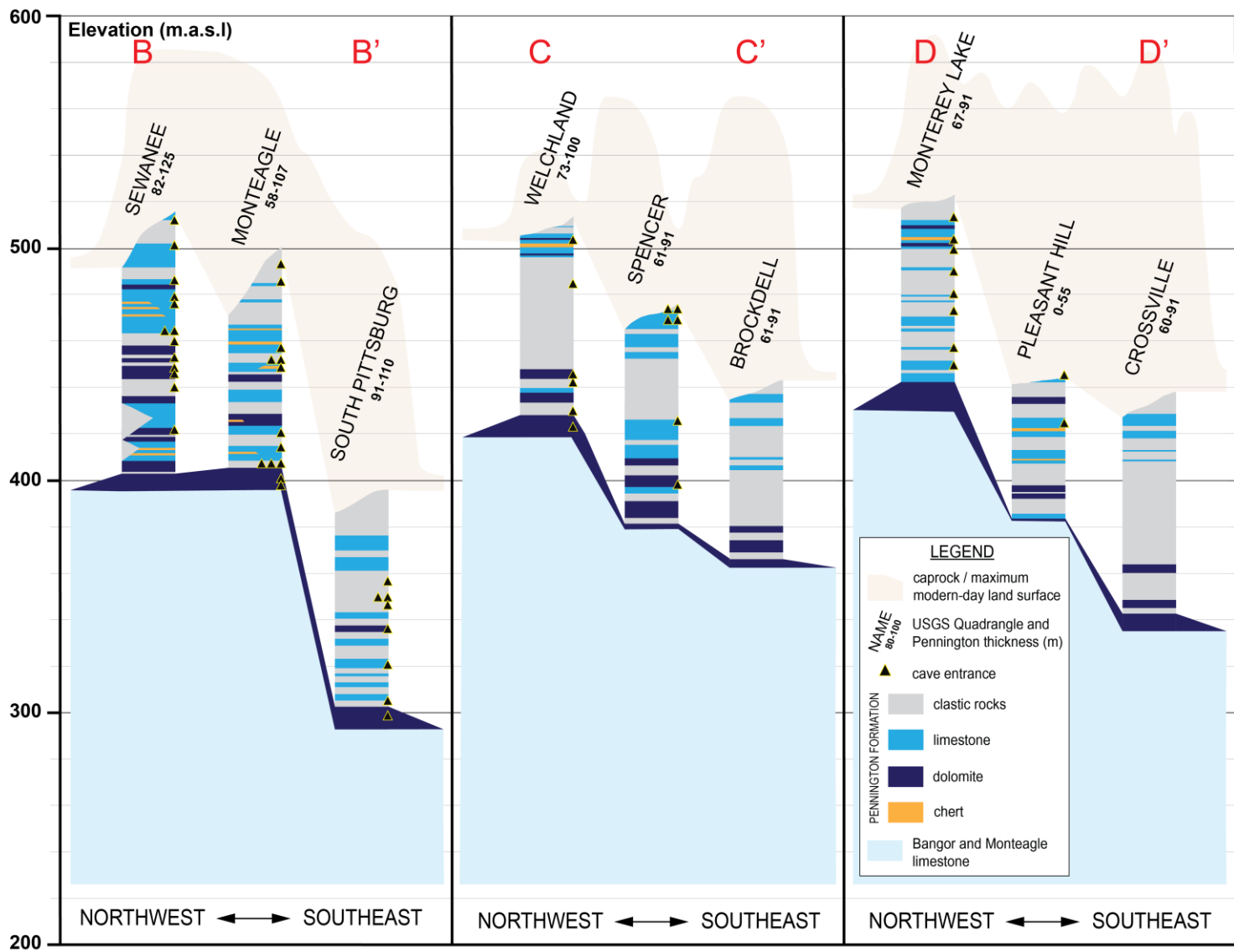
Figure 20. Stratigraphic cross sections (B, C, and D) of the Pennington Formation based on geologic quadrangle maps shown in Figure 18.

5.3 Structural Analysis

Rose diagrams from 60 Pennington cave models (Appendix C) show general agreement between the directionality of cave survey ties and the orientation of major stream valleys (Appendix D). Cave passages tend to develop parallel to the axis of the major stream valley in which they are formed. The mean angle of cave passages was 84.5 degrees (the null hypothesis that there was no mean direction was rejected with Rayleigh $z_{17.253}$, p<0.001). The mean angle of stream valleys was 98.3 degrees (the null hypothesis that there was no mean direction was rejected with Rayleigh $z_{20.051}$, p<0.001). Watson's U^2 test ($U^2_{0.0818}$, p>0.50) was used to accept the null hypothesis that the two groups of azimuths are not significantly different. Therefore, cave passage directionality in the Pennington Formation is related to valley directionality in a statistically significant way.

A prime example of this phenomenon is in Newsome Sinks karst area (Alabama). Twenty-six Pennington caves in this area have been surveyed and mapped, allowing a detailed look at speleogenesis locally. A geographic overlay of cave passages on a digital elevation model (Figure 21) shows passages trending parallel to the north-south oriented stream valleys. Rose diagrams constructed from the individual cave surveys, and from the compiled dataset of all cave survey in the Newsome Sinks area, show the high frequency of north-south passage directionality. Though cave passages are not as extensive, a similar pattern is observed in Savage Gulf State Natural Area, where passages trend in the direction of the valley in which they are formed (Figure 22).
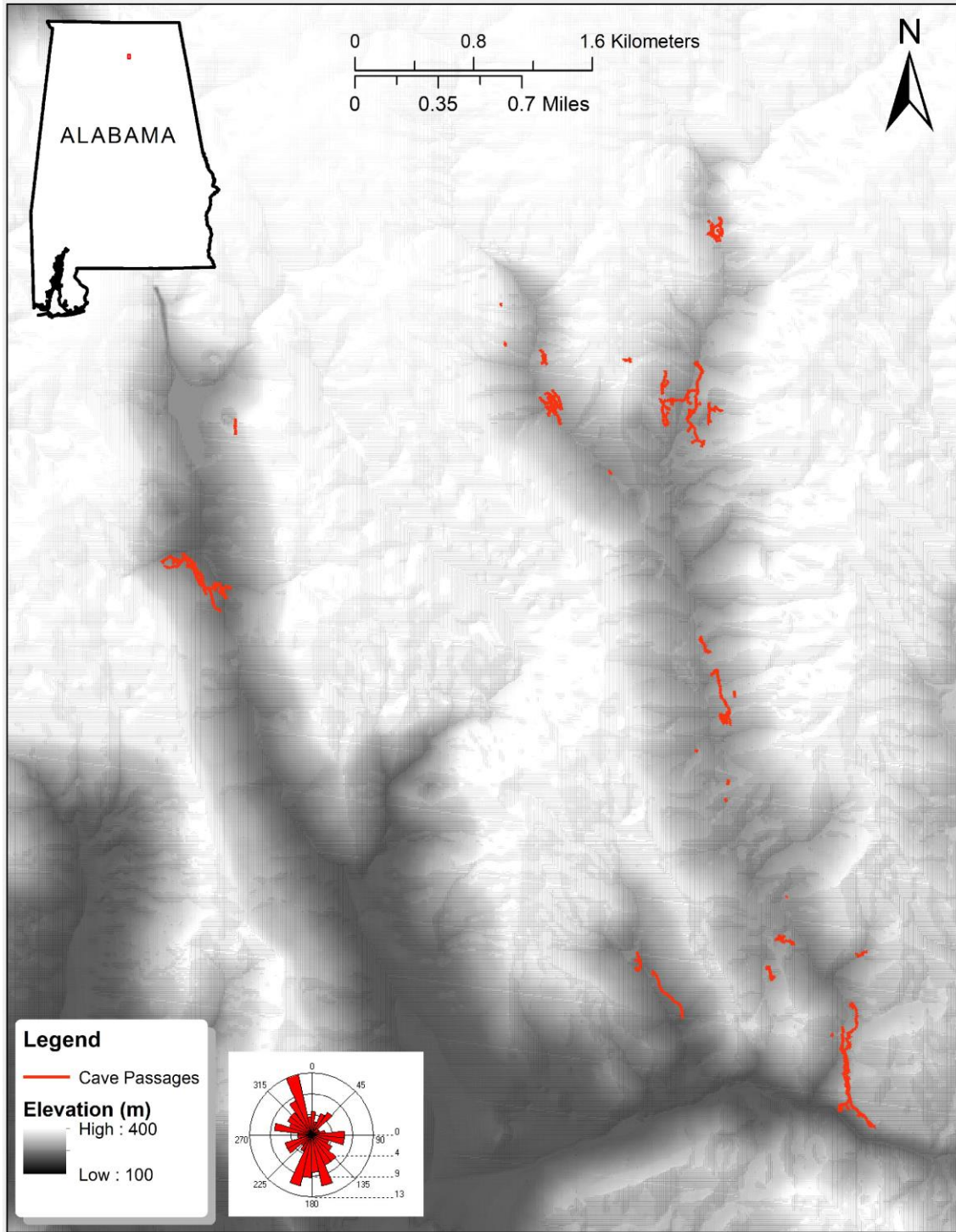
Figure 21. Mapped Pennington cave passages in Newsome Sinks karst area (Alabama), with a rose diagram showing the frequency of survey tie directions from digital passage models.
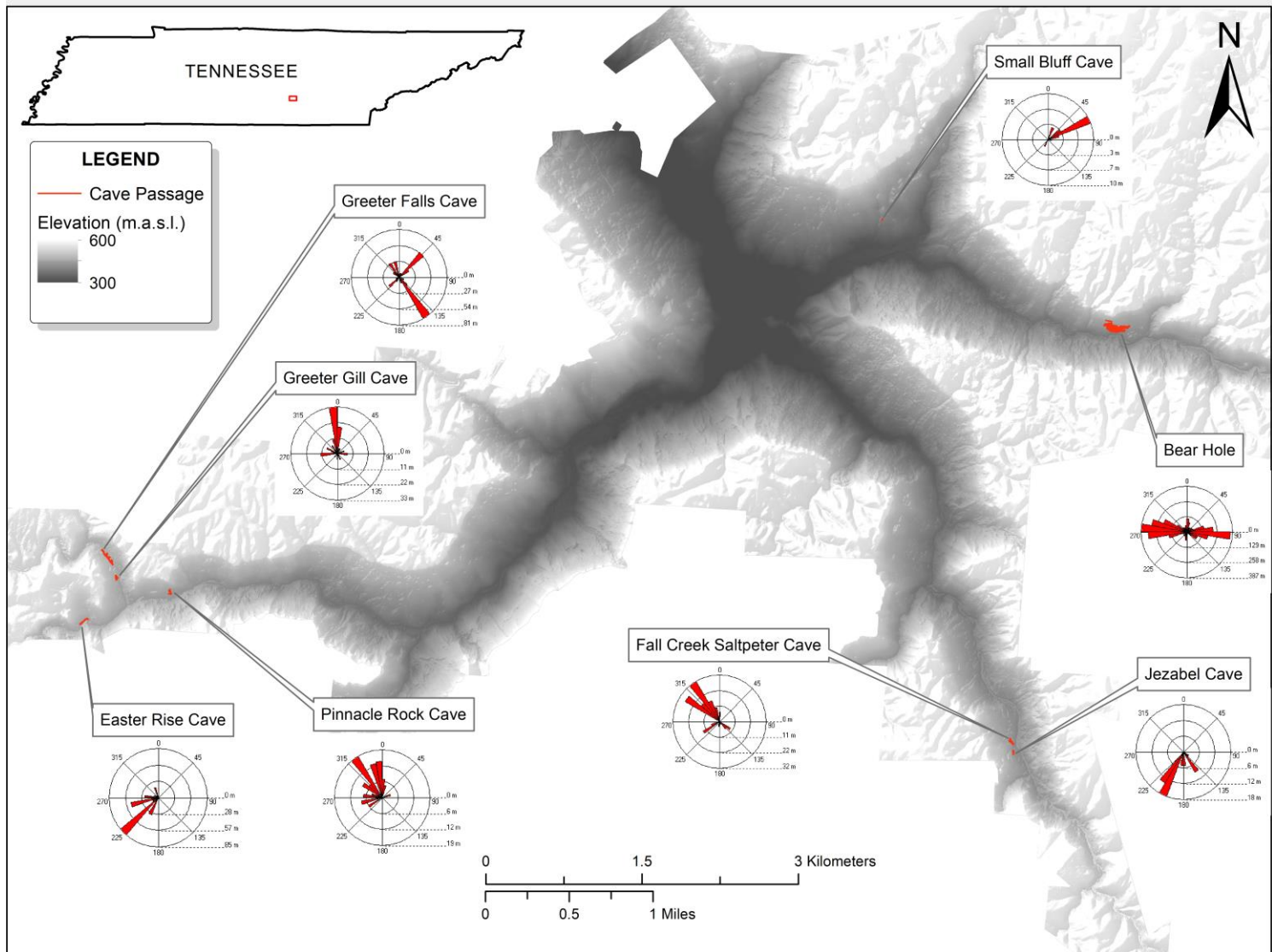
Figure 22. Mapped Pennington cave passages in Savage Gulf State Natural Area.

5.4 Results from Savage Gulf State Natural Area

The Tennessee Cave Survey listed eighteen caves entrances in the Pennington Formation in Savage Gulf State Natural Area; upon field inspection and overlay with geologic maps, it was determined that only 15 of these are true Pennington caves, the others occur in the Bangor limestone or at the Pennington-Bangor contact with only minor development in the Pennington Formation.

5.4.1 Inventory, Survey, and Cartography Results

The karst feature inventory covered parts of each of the three major drainages, and identified 15 caves, 14 karst conduits, 5 dolines, 4 swallets, and 23 springs. Six of these caves were surveyed and mapped over the course of the study. Cave maps are available in Appendix A and in the Tennessee Cave Survey. A short description of each cave follows:

Greeter Falls Cave (Appendix A2) and Greeter Gill Cave (Appendix A3) were subjects of the dye tracer tests (Section 5.4.2), which proved that they are hydrologically connected and thus different entrances to the same cave system. This cave system is formed in the uppermost limestone member of the Pennington Formation, which locally is sandwiched by shale. Greeter Falls Cave has four entrances on the banks of Firescald Creek. The main entrance is a swallet, upstream of a natural impoundment of the surface channel, where the entire flow of Firescald Creek can be observed disappearing underground in the wet season (Figure 23). In dry conditions, Firescald Creek is losing for several hundred meters upstream of the main entrance, and the cave becomes navigable. Some ponded water remains within the cave year-round, a result of the stream being perched on an impermeable layer. The other three entrances to Greeter Falls Cave

are in the valley floor downstream of the impoundment, and are flooded for most of the year. Each of the entry passageways is oriented perpendicular to the main passage, which parallels the surface valley of Firescald Creek. Scalloping on the walls and ceiling of the passages, shifting debris dams within the cave stream, and observations of the entrance at high stage all suggest turbulent flooding on a regular basis (Figure 23).

Greeter Gill Cave (Appendix A3) is a sinkhole entrance or "karst window" into the underground reaches of Firescald Creek. Though connected with dye, a physical connection with Greeter Falls Cave was not found. The passages in the Greeter Falls-Greeter Gill Cave system trend parallel to the surface valley of Firescald Creek and the cave stream discharges to a series of springs and seeps near the confluence with Big Creek. The system pirates flow from Firescald Creek to a spring on the north bank of Big Creek via a preferred hydrologic gradient through confined Pennington limestones, preempting by several hundred meters the apparent "blue-line" confluence shown on topographic maps.

Easter Rise Cave (Appendix A4) is formed in the same limestone member as the Greeter Falls system and is best described as a talus cave in a meander of Big Creek. Collapse of a 10-meter-high bluff has enclosed the stream behind a wall of breakdown with multiple entrances. The main entrance is a perennial spring issuing from the bluff and feeding into Big Creek. The remainder of the cave is a short. tubular stream passage ending in a constriction. Dye traces confirmed that this stream is fed by losing reaches of Big Creek upstream of the cave.

Figure 23. (Clockwise from upper left) Greeter Falls Cave (GFC) main entrance in the dry season; GFC main entrance in the wet season; view from above GFC main entrance of the impounded valley of Firescald Creek with all of the wet-season flow disappearing

underground; scallops on the ceiling and walls of GFC (passage is about 9 meters wide by 3 meters tall and scallops are 3 to 6 centimeters in diameter)

Pinnacle Rock Cave (Appendix A5) is a hydrologically active cave on the north side of the Big Creek valley, made up of solutionally enlarged joints trending north-south. Its wet-weather stream is fed by diffuse recharge through mixed clastic rocks overlying the cave. The stream sinks into breakdown at the cave entrance and reemerges as a small spring about 10 meters downhill of the entrance.

Fall Creek Saltpeter Cave (Appendix A6) is an upper, hydrologically abandoned portion of the cave system that also includes Jezabel Cave (Appendix A7). Both caves follow conjugate joints trending northwest-southeast and northeast-southwest. Fall Creek Saltpeter Cave is mostly dry and filled with coarse sandy sediment, while Jezabel Cave is hydrologically active year round. Jezabel Cave receives direct runoff into the cave mouth from a wet-weather surface stream and also likely interacts with the base level of the Upper Collins River. A small spring 6 meters downhill from the cave entrance flows directly into the Collins.

5.4.2 Dye Tracer Test Results

Complete dye analysis reports are included in Appendix F. Representative results from two separate rounds of tracing are discussed below.
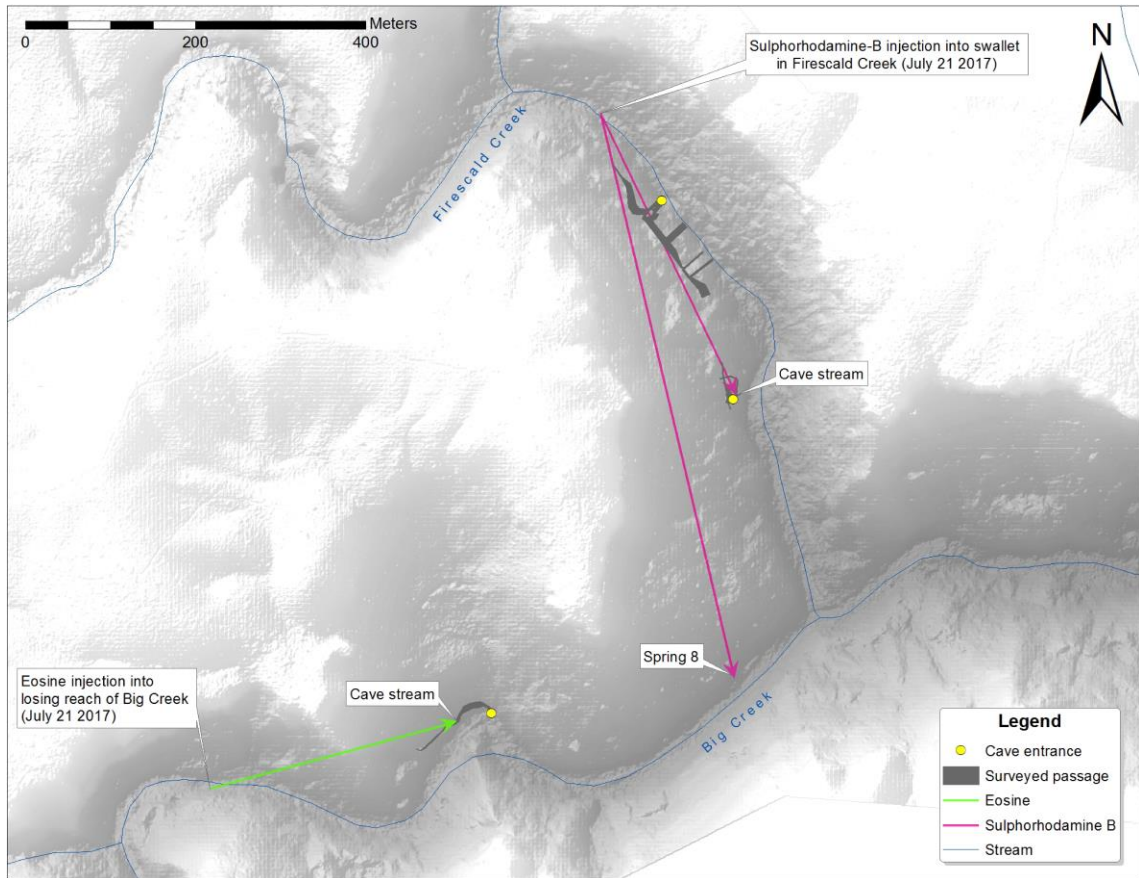
Figure 24. Results of a July 2017 dye tracer test of the Greeter Falls – Big Creek area.

In the first round of dye tracing (dry season; Figure 24), Eosine was positively identified by spectral analysis of two samples collected in Easter Rise Cave, a spring resurgence cave on the north bank of Big Creek. This confirms a hypothesized flow route from the sink in the upper reaches of Big Creek (Eosine injection site) to the cave stream.

Sulphorhodamine-B was positively identified in one sample collected in Greeter Gill cave, tentatively confirming the hypothesized flow route from the sink in Firescald Creek (SRB injection site) to the cave stream. Sulphorhodamine-B was also detected in one sample collected in a perennial spring located on the north bank of Big Creek, just upstream of the confluence with Firescald Creek. This tentative result suggests the possibility of underground stream piracy of Firescald Creek by Big Creek via karst conduits in the limestone of the upper Pennington Formation.

76

No dye was detected in the other seven monitoring sites (six of these sites were small, ephemeral springs/seeps located on the northern and western banks near the confluence of the two creeks, and the last site was located in Big Creek downstream of the confluence). Failure to detect dye in the ephemeral springs was attributed to dry weather conditions during the trace; these features were dry during all sample collection dates (yet flowing when background fluorescence data were collected). Failure to detect dye downstream of the confluence was attributed to dilution of dyes beyond the detectable limits.
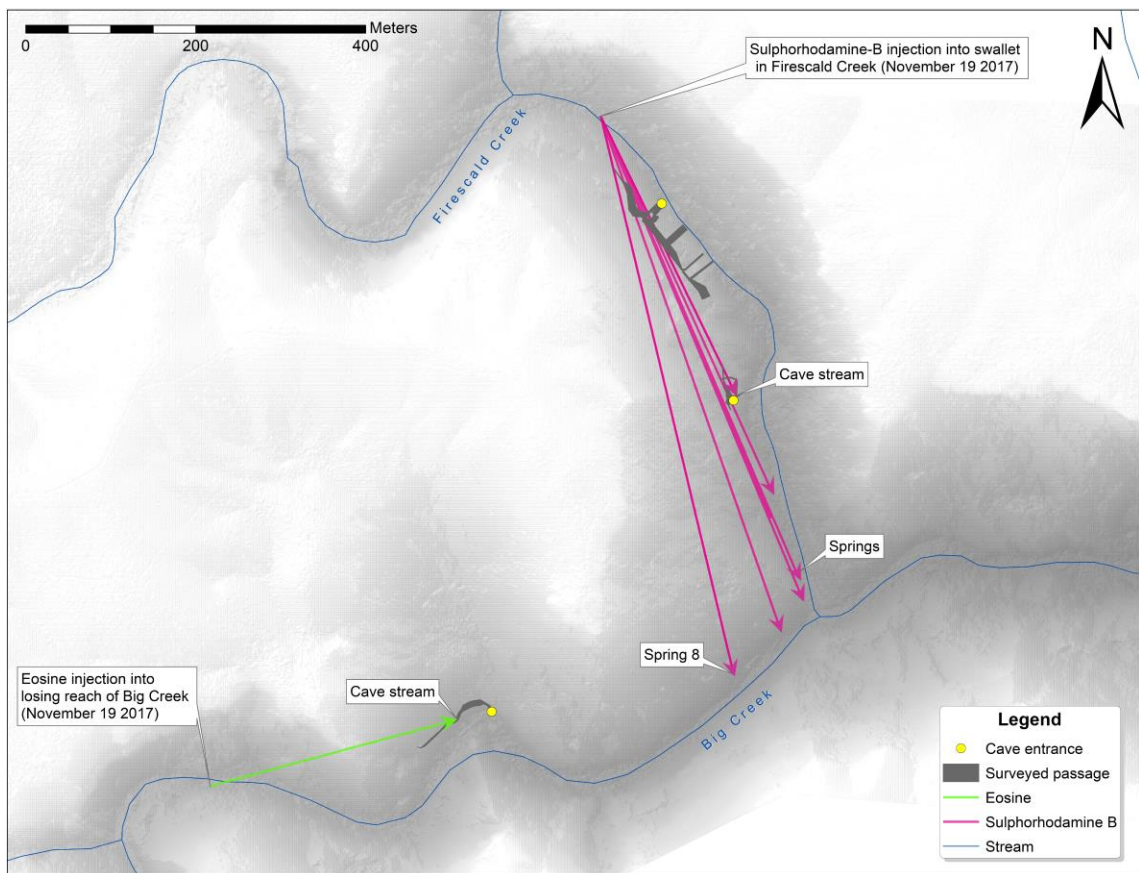
Figure 25. Results of a November 2017 dye tracer test of the Greeter Falls – Big Creek area.

In the second round of tracing (wet season; Figure 25), spectral analysis positively identified Eosine in Easter Rise Cave (Site 9). This result confirms an underground flow route from the swallet in Big Creek to the stream in Easter Rise Cave. This connection

was made in both August and November, suggesting that the perennial stream in Easter Rise Cave receives water from Big Creek even at low stage. Eosine was also identified in samples from downstream of the confluence of Firescald Creek and Big Creek; these were Big Creek (Site 10), Collins River Rise, and Grundy Big Spring. The latter two sites are about 14 kilometers down-valley from sites 1 through 10, and were sampled as fail-safes to ensure dye recovery if none of the primary monitoring sites was successful.

Analysis positively identified Sulphorhodamine-B in Greeter Gill Cave, six intermittent springs near the confluence of Firescald and Big Creeks, and in each of the failsafe locations. This result confirmed that there is hydrologic connectivity between Greeter Falls Cave (whose entrance is the major swallet in Firescald Creek) and Greeter Gill Cave (Site 1), as well as demonstrating a distributary flow path from the swallet in Firescald Creek to numerous springs down-valley. These results represent high stage, when springs were flowing continuously. It is worth noting that at low stage, the system behaved rather differently (see results of August 2017 trace of the same system). Behavior of a large spring on Big Creek (Site 8) is discussed in detail below.

Site 8 is a perennial spring on the north bank of Big Creek. During the August 2017 trace, Site 8 was the only spring with consistent flow. One positive hit for Sulphorhodamine-B during the first round of tracing suggested a potential route for stream piracy of Firescald Creek waters by Big Creek, a result later confirmed by multiple positive hits of Sulphorhodamine-B in Site 8 during the November 2017 trace. Failure to detect Eosine in Site 8 suggests that Big Creek does not contribute any flow to this spring, and that Firescald Creek is the primary source of water for Site 8. This

78

implies that the actual confluence of Firescald Creek and Big Creek is at Site 8 and not at the apparent confluence (just west of Site 10).

An ancillary result of dye tracer tests was the detection of high levels of background fluorescence in the wavelength of organic acids (humic and fulvic acids) in the study area. Every sample contained this evidence of high concentrations of dissolved organic matter (DOM), which plays a ubiquitous and significant role in biogeochemical and ecological processes (Birdwell and Engel 2010).

5.4.3 Geographic Information Systems and Related Case Studies

GIS was used to create a working database of Pennington caves and karst features. This digital inventory served as a valuable reference for interpreting cave morphologies in geographic context, and allowed for direct comparison between phenomena observed in the case study (SGSNA) and features indicative of similar processes occurring elsewhere. Figure 26, 27, and 28 are maps created with GIS in order to compare the hydrology and geomorphology of three different Pennington cave systems. Greeter Falls Cave system (Figure 26) was the focus of the case study and was visited frequently; Lockwood Cave (Figure 27) was visited in 2017; and Short Creek Maze Cave system (Figure 28) was analyzed solely in GIS.
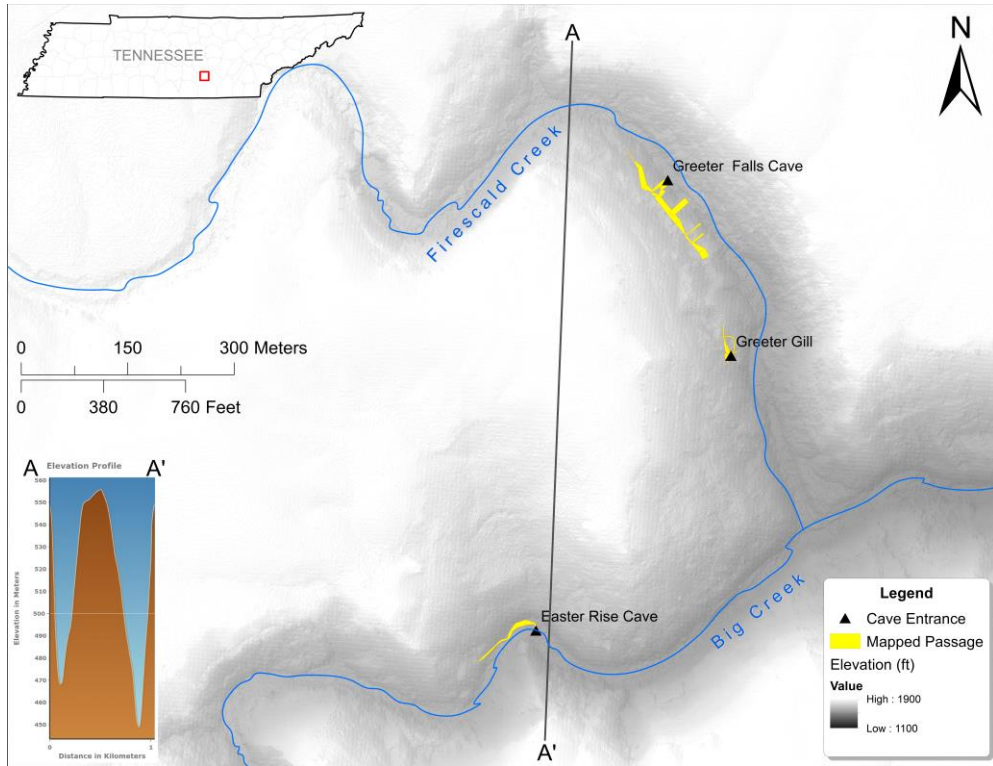
Figure 26. Greeter Falls Cave and related components of the local karst hydrologic system (cross section vertically exaggerated 22x).
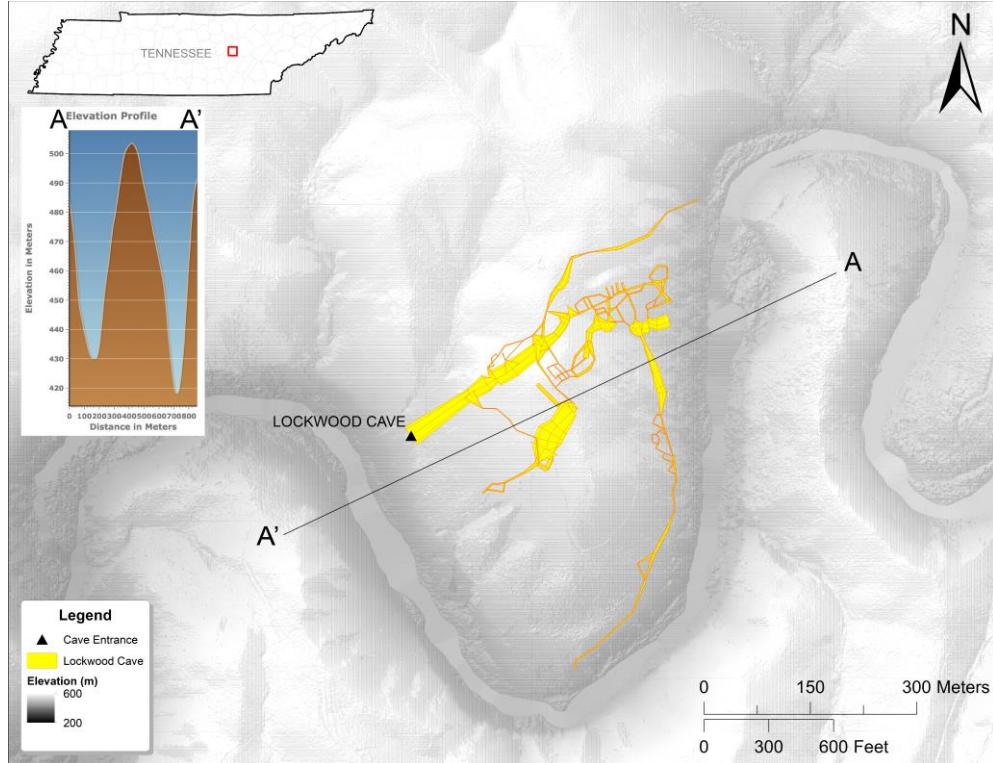
Figure 27. Lockwood Cave, a karst conduit network in the Pennington Formation which allows the Caney Fork River to undercut a major meander in the surface channel.
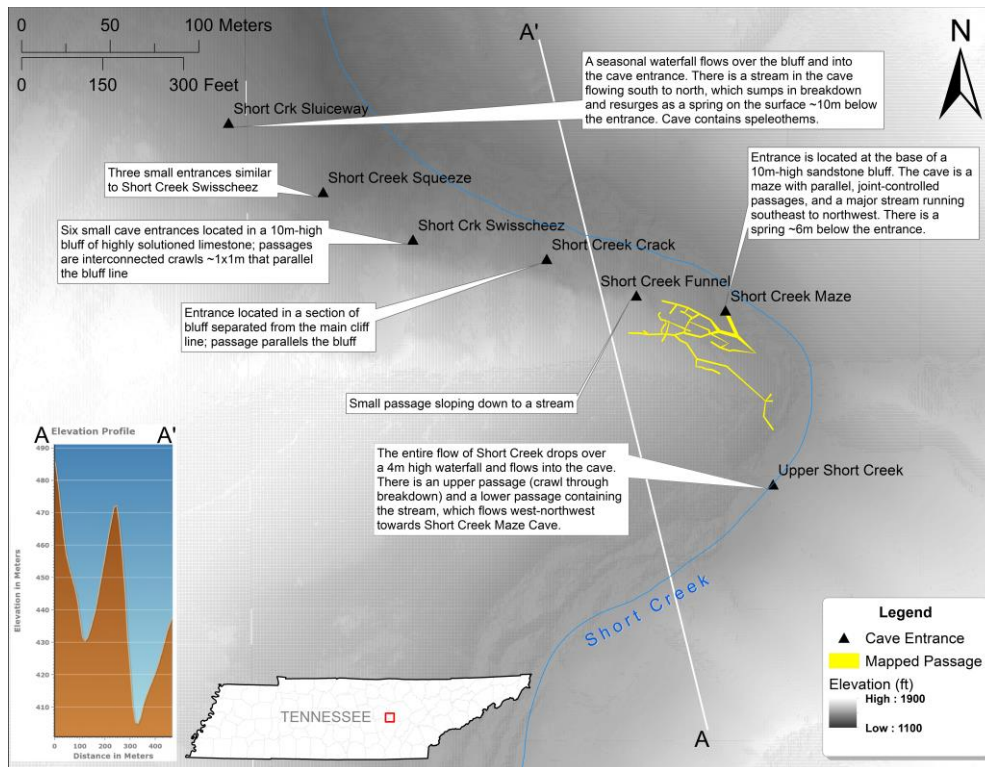
Figure 28. Short Creek Maze and related components of the local karst hydrologic system (cross section vertical exaggeration 13x).

CHAPTER 6: DISCUSSION

Karst processes occurring in the Pennington Formation are an integral part of the overall landscape development of the Cumberland Plateau. Analysis of the geology, hydrology, and cave geomorphology of the Upper Mississippian Pennington Formation has led to a better understanding of speleogenesis in this complex unit, especially where the morphology and speleogenetic characteristics of known caves (e.g. Greeter Falls Cave) can be extrapolated to less well-known caves (e.g. Short Creek Maze). Future studies should acknowledge that karst processes in the Pennington Formation, especially on the western escarpment of the plateau, are capable of producing karst features and caves that are significant in terms of local and regional hydrology and geomorphology.

6.1 Morphology and Morphometry of Pennington Caves

Georeferenced digital models of Pennington caves are useful for studying the physical and geospatial properties of caves. These data were used to interpret geologic and hydrologic controls on speleogenesis. There are several problems inherent with this approach, the most prominent being that cave surveys are limited by human size and effort and are therefore partial and subjective. Caves defined by a human modulus (Curl 1964) generally do a poor job of representing the entire network of solutional openings in a karst system, the majority of which are physically inaccessible and thus impossible to observe and survey. This method is also subject to the assumption that speleological exploration and research have progressed at the same rate throughout the study area, which is untrue but difficult to quantify. Thus, geomorphological interpretations are limited to the population of surveyed caves, which is herein assumed to be representative.

Pennington caves generally exist in thin carbonate members (1-10 m thick) and are limited in vertical extent by confining shales and clastic rocks. Commonly they are fragmented pieces of horizontal branching stream passages, with tube or canyon-like tributaries. Some small pit caves occur, especially to the south and west of the study area where limestone and dolomite beds tend to be thicker (Thomas 1972). Solutional enlargement of conjugate joints is apparent in many Pennington caves, and in confined limestones can create a maze effect by diffuse drainage and even enlargement of the joint network, enhanced by floodwater injection into the confined karst unit. The speleogenetic effects of both diffuse and direct recharge to the Pennington Formation are enhanced by the relative undersaturation (with respect to calcite/dolomite) of water draining sandstone and shale caprock.

6.2 Controls on Speleogenesis in the Pennington Formation

Karst conduit enlargement, and thus the genesis of caves, is controlled by lithologic, structural, and hydrologic factors that vary over time and space, and are interrelated in complex ways. What follows is a discussion of controls on Pennington karst development presented with respect to each of these factors.

6.2.1 Stratigraphic Controls

Patterns of cave development in the Pennington Formation, including the density and vertical distribution of caves throughout the section, reflect the general pattern of increasing clastic content to the north and east and increasing carbonate content to the south and west (Thomas 1972; Milici 1974; Milici et al. 1979; Ettensohn and Chesnut 1985). Cave entrances tend to be found at higher elevations on the western side of the Cumberland Plateau and lower elevations to the south and east (Figure 17). The entire

Cumberland Plateau province dips slightly to the southeast, which partially explains this phenomenon; however, carbonate members are not continuous throughout the unit and occur at different points in the section depending on location (Figures 19 and 20).

A factor of great importance to Pennington cave development is the highly variable nature of lithology in the Pennington Formation and the spatial inconsistencies in the presence and thickness of carbonate rocks. Milici et al.'s (1979) cross-section across the plateau (Figure 5) and Figure 19 demonstrate the changes in thickness of carbonates and gradation into clastic rock types in the northern portion of the plateau escarpment in Tennessee and Kentucky, which is supported by lithofacies interpretations presented by Ettensohn and Chesnut (1985) and others (Bergenback 1993) and comparison of geologic quadrangle maps across the plateau (Figures 19 and 20). Limestones in the upper part of the formation tend to be thicker and more well-represented to the west, grading into shale and sandstone to the east. Basal limestone and dolomite are present throughout most of the extent of the formation, but are generally thicker to the south, which accounts for the many low-elevation Pennington caves in the south of the study area (Figure 17).

The observed cave entrance elevation trends (Figure 17) allow for a rough interpolation of the geographic and stratigraphic placement of soluble rocks within the Pennington Formation. Generally speaking, Pennington cave entrances are more abundant and densely clustered in the south-central portion of the study area, which is tied to the aforementioned variations in the environment of deposition. Caves in the southern portion of the study area are formed in relatively thick limestones and in dolomite that marks the base of the Pennington Formation throughout most of its extent. Caves high in elevation on the western escarpment are formed in limestones sandwiched

by shales at the top of the formation, or in carbonate rocks in direct contact with the Pennsylvanian caprock at the disconformity.

The occurrence of true pit caves (vertical shafts formed by dissolution) in the Pennington Formation is strongly dependent on the available thickness of carbonate rocks; most "true" pits are located in the southern portion of the study area, while caves owing their vertical complexity to broken-off pieces of bluff (such as "El Abismo," a Pennington cave associated with a deep crack in the Warren Point sandstone in White County, Tennessee) exist in association with the caprock throughout the study area.

The disconformity atop the Mississippian Pennington Formation marks a period of erosion and karst landscape development prior to the deposition of Pennsylvanian aged rocks. Pennington limestone at the contact with Pennsylvanian rocks are remnants of paleotopographic highs, whereas paleotopographic lows are marked by shale and other clastic deposits in contact with Pennsylvanian rocks. In the instance that the Upper Pennington Formation contains limestone at the contact with Pennsylvanian-aged clastic rocks, there is potential for the formation of unique and interesting caves. The premier example is Lockwood Cave (White County, Tennessee). Over three miles of cave passages have been surveyed in the banks of a large meander in the Caney Fork River (Figure 27).

The main trunk passage of Lockwood Cave carries the active channel of the Caney Fork River as it undercuts the surface meander, while the upper levels of the cave consist of solutional joint mazes and an impressive collapse chamber that are now for the most part hydrologically abandoned. Yet another portion of the cave is a talus passage formed by collapse of the bluff along the surface channel of the Caney Fork. Lockwood

Cave offers a unique opportunity to view the Mississippian-Pennsylvanian disconformity

from within; in several places in the cave one can directly observe the contact between

Pennington limestone and Pennsylvanian-aged sandstones (Figure 29). Bon Air coal is

eroding out of the ceiling onto the cave floor in places (Figure 30), and the Clatter-Rock

Dome is formed as massive chunks of sandstone collapse from the ceiling. The

relationship between speleogenetic processes and the Mississippian-Pennsylvanian

disconformity certainly warrants further investigation, though it is rarely as well exposed

as in Lockwood Cave.

Figure 29. View of the Mississippian-Pennsylvanian disconformity surface (at helmet level) from within Lockwood Cave (photo by Chuck Sutherland).
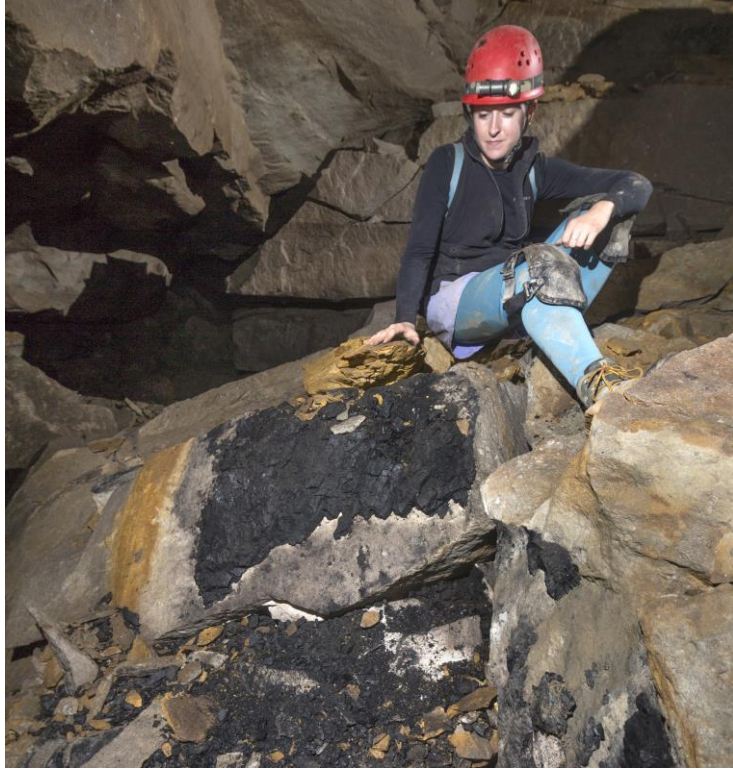
Figure 30. Pieces of Bon Air Coal eroded out of the ceiling of Lockwood Cave (photo by Chuck Sutherland).

Caves passages that develop directly beneath the caprock may also mirror the placement and orientation of conjugate joint sets in the caprock, as is the case with Coons Labyrinth Cave (Appendix A1). Its passages are mostly small tubes and canyons trending parallel to the retreating escarpment margin, with a maze of intersections and loops. The cave is hydrologically abandoned and filled with dry sediment in many places, though a small stream fed by diffuse drainage through the caprock resurges as a perennial spring at the cave entrance. The structural discontinuities leading to this pattern of cave morphology are likely related to mechanical weaknesses in the caprock, which widen into fractures as valley incision removes confining pressure on one side. A shale layer underlying the cave precludes the downward movement of water, which reinforces lateral movement of water and enlargement of the fracture network. The entrance of Coons

Labyrinth is overhung and almost completely blocked by a school bus-sized block of sandstone float (colluvium) (Figure 31), which will in time creep downhill and obscure the cave entrance. Many more small springs or seepages in the upper Pennington Formation exist that may drain a similar system of karst conduits that is disguised or rendered inaccessible by thick colluvium blanketing the escarpment.

Figure 31. Coons Labyrinth Cave entrance (just underneath the downslope side of a large sandstone boulder, on the right side of the frame).

In instances where shale in the upper Pennington Formation is at the contact with Pennsylvanian rocks (as is the case most often), underlying carbonate members of the Pennington Formation are sandwiched between impermeable confining layers. Cave passages tend to have branching or tube-like morphologies restricted in size by the thickness of the carbonate unit. Streams may be gradually losing in reaches underlain by interspersed shale and limestone, or may sink at a discrete contact. Maze caves can form

in sandwiched limestones as a result of floodwater forcing its way laterally into networks of vertical fractures. Such is the case in the Greeter Falls Cave system, where massive sandstone boulders have impounded the surfacial stream valley (Figure 23) and forced the entire flow of Firescald Creek into a confined limestone layer. Passages are laterally braided or anastomotic in nature, and form a complex distributary system of resurgent springs at the lower confining layer. The collapse of crumbly shales and impure limestones results in a sinkhole entrance (or "karst window") into the system: Greeter Gill Cave.

6.2.2 Structural Controls

Structural discontinuities are the framework for speleogenetic processes. In the Pennington Formation the most readily observable elements of structural influence are sets of near-vertical joints and fractures that guide surface runoff through the caprock and/or epikarst and into the groundwater. In the absence of major structural deformation in the form of folds or faults, stress release fractures provide the primary point of entry of water into karst conduit systems in the Pennington Formation. This is evidenced by passages that trend along-valley, or parallel to major streams (Figures 21 and 22), and statistical analysis showing no significant difference between cave and valley directional trends. This pattern is consistent with the trend observed in caves of the Mississippian Bangor and Monteagle limestones (Sasowsky and White 1994) and in Newsome Sinks, Alabama by (Varnedoe 1963; Moravec and Moore 1974).

In areas of the plateau that have undergone more intense deformation, i.e. areas with increased folding and faulting related to the Cumberland and Pine Mountain overthrusts, cave passages are likely be influenced by those deformational features.

However, no faults or folds were observed in Savage Gulf State Natural area and so their effects on Pennington cave development were not evaluated. Faults and folds that have been mapped by others (and are available as a shapefile from USGS 2016b) are included in the GIS, but no apparent relationship to known Pennington caves was observed (Appendix E).

The dip of strata on the western escarpment of the plateau is so slight as to be locally undetectable, and any effect of the regional southeastward dip on the morphology of individual Pennington caves was imperceptible. Observation of cave passages in GIS resulted in no further conclusions, since passages develop both updip and downdip from major surface streams. However, on a larger scale, dip direction affects landscape morphology and the placement of Pennington Caves. Studies of blind valleys on the Cumberland Plateau (Crawford 1992; Davis and Brook 1993) attribute the formation of blind valleys to situations where strata dip away from the plateau, rather than toward it. In Sinking Cove and Lost Cove (blind valleys in Franklin County, Tennessee), the Pennington Formation's limestone members are the first soluble unit encountered by incising streams, resulting in piracy of the surface stream (the main condition for blind valley formation) (Klimchouk et al. 2000).

6.2.3 Hydrologic Controls

Depending on localized lithology, the Pennington Formation can either confine the movement of water (as in shales that dominate the formation to the north) or conduct water rapidly through conduits (as in limestone members of increasing thickness and regularity to the south). Pennington caves are best categorized as plateau-margin caves, which interact with the modern surface and subsurface drainage as water makes a stair-

step journey down and through the plateau escarpment. Recharge to Pennington caves is both diffuse, through fractures networks and openings in the epikarst, and point source, through sinking streams. In some cases, the highly aggressive nature of runoff from the caprock causes streams to incise directly through thin limestones in the Pennington Formation with little to no karst conduit development. Where undersaturated water enters a confined limestone bed at the entrance of Greeter Falls Cave, intense dissolution results in scalloping on the walls and ceiling of the cave (Figure 23).

Because recharge is primarily allogenic, the geochemical gradient in Pennington karst aquifers usually favors dissolution over precipitation of calcite. The dissolutional potential of water contacting the upper Pennington limestones is immense, as drainage from the caprock is highly undersaturated with respect to calcite (Davis and Brook 1993). Speleothems were not common in hydrologically active Pennington caves observed in this study, except in cases where recharge was slow or diffuse, as in drips through thin fractures.

Many Pennington caves fed by diffuse allogenic recharge (e.g. Coon's Labyrinth Cave and Buckets of Blood Cave in Franklin County, Tennessee) have streams that converge to a single discharge point or spring. However, distributary flow paths are also common, especially in caves where a flood-prone point source of recharge is channeled laterally into soluble layers sandwiched between impermeable rocks. "Flood mazes" such as Greeter Falls Cave and Short Creek Maze Cave have many points of outlet, which may change depending on the amount of water passing through the system. Seasonal variations in stage, and the general flashiness of the Cumberland Plateau hydrologic system, cause the behavior of Pennington karst aquifers to differ according to the amount

91

of flow present (White 2009). The series of intermittent springs draining the Greeter Falls Cave system are a good example of this; under dry conditions they are mostly inactive, and in the rainy season maintain steady flow.

Dye tracing results from SGSNA shed light on the complex behavior of anastomotic and distributary flow routes through karst conduits in upper Pennington Formation carbonates. Based on surveyed cave passages and hydrologic tracer tests of springs in the Greeter Falls system, there is likely a maze-like conduit network within the western bank of Firescald Creek. The sink at Greeter Falls Cave entrance is the primary source of recharge to this system, which behaves differently depending on stage. At high stage, Firescald Creek resurges at a multitude of ephemeral springs and seeps that are inactive at low stage. Site 8, a spring that continued to be active during low stage, is the resurgence of an underground flow path from Firescald Creek to Big Creek. The spring is the surface depiction of stream piracy through a karst conduit network in the Pennington Formation; this is likely to occur elsewhere (and occurs in the form of meander cutoffs in many places). For example, a similar system appears to exist in the Pennington Formation at Short Creek (White County, Tennessee). Based on cave narratives and visualization of data in GIS, a maze-like system of conduits facilitates a preferred hydrologic gradient, distributing the flow of Short Creek from a single sink to multiple outlets (Figure 28). Lockwood Cave (Figure 27) is another cave formed in preferred-gradient karst conduits in the Pennington Formation in White County, Tennessee.

6.3 Suggestions for Future Work

This preliminary investigation of speleogenesis in the Pennington Formation sheds light on countless avenues for further research, a few of which are presented here.

92

First, there is a need to extend the study area outward to areas not considered in this study, namely, the northern Cumberland Plateau in Kentucky, the Sequatchie Valley, the eastern Cumberland Plateau, and the Valley and Ridge. The changing lithology of the Pennington Formation and effects of structural deformation related to the Cumberland overthrust and Pine Mountain overthrust on Pennington cave development in these areas is of particular interest. When considering such a large region, the effects of major base level drainages (i.e. the Cumberland River and Tennessee River) should not be overlooked. There is a great deal of work yet to be done in defining watershed boundaries with proper consideration for underground flow routes.

There is a need for more research into the relationships between karst processes in the Pennington Formation and the geomorphology and hydrology of features in units above and below the Pennington Formation. Joints in the caprock have a well-understood effect on speleogenesis, but there is work to be done in understanding how faults and folds in the Pennsylvanian strata might influence Pennington cave development. Seemingly anomalous closed depressions in the caprock, visible on 1:24,000-scale topographic maps near the edge of the western plateau escarpment, are likely related to structural anomalies interacting with karst processes in the Pennington Formation. The Mississippian-Pennsylvanian disconformity, which truncates the top of the Pennington, may also have an effect on cave development and deserves further attention. Caves in the underlying Bangor limestone sometimes have an obvious relationship to the hydrology of Pennington karst features, like the relatively common case of a Pennington cave spring flowing overland for a short distance before disappearing into a Bangor pit. This relationship is pertinent to the dynamics of the entire Mississippian aquifer system.

6.4 Summary and Conclusions

A regional analysis of 660 Pennington Formation (TCS 2017; ACS 2018) cave descriptions from state cave survey databases and 60 digital Pennington cave models resulted in quantitative and qualitative descriptions of the nature of caves in the Pennington Formation. Morphometric indices derived from cave survey data allowed the geometry and dimensionality of caves in the Pennington Formation to be quantified, then visually compared using GIS. The elevation of cave entrances was used to indicate stratigraphic placement of soluble rocks in the Pennington Formation. Statistical analysis of cave rose diagrams and valley trends helped elucidate structural influences on cave development. Cave survey, cartography, and fluorescent dye tracer testing in Savage Gulf State Natural Area provided a case study upon which to test conclusions from the regional study.

When lithology, stratigraphy, structure, and hydrology are favorable, there is the potential for intense karstification and speleogenesis in the Pennington Formation. The stratigraphy of the western Cumberland Plateau is particularly favorable for Pennington cave development due to the presence of multiple unnamed carbonate members interspersed with shale in the Pennington Formation. Geochemical conditions are especially favorable for speleogenesis in the upper Pennington Formation since drainage from the caprock is highly solutionally aggressive. Structural disturbance from valley stress release creates the framework for conduit development, meaning passages generally trend in the direction of major streams. Long and complex cave systems like Lockwood Cave tend to be the exception, with the majority of Pennington caves consisting of small, horizontal branch- or tube-like passages. Network mazes are

common in Pennington caves as a result of thin, confined limestone beds that are subject to dissolution by diffuse flow through vertical fractures and lateral floodwater injection into the fracture network.

Countless adaptations of Crawford's original Cumberland Plateau escarpment cross-sectional diagram (Crawford 1978; Figure 8) have taken for granted the classification of the Mississippian-aged Pennington Formation as member of the impervious caprock sequence, and many of the premier works on karst caves of the Cumberland Plateau make no mention of the potential for speleogenesis in this unit. And yet, state cave databases in Tennessee and Alabama (where most of the karst geologic investigations on the Plateau have occurred) have hundreds of Pennington caves on record, a testament to the karstic nature of this mixed clastic-carbonate sequence.

The distribution and nature of Pennington caves on the Cumberland Plateau is dependent on the lithologic characteristics of the formation, which are related to the sedimentary conditions in the basin during the time of deposition. Generally speaking, continental clastic deposits dominate the Pennington Formation in the north of the study area, grading into estuarine and shallow marine coastal-tidal deposits to the south. So, Crawford's classification holds true in the northern portions of the plateau where the Pennington Formation is made up almost entirely of impermeable shales and mudrocks, but does not accurately represent the Pennington Formation in the central and southern portions of the plateau where soluble limestone and dolomite are interspersed throughout.

Therefore, a revised Cumberland Plateau karst developmental model is proposed, which addresses the presence of karst conduits and caves in carbonate members of the Upper Mississippian Pennington Formation (Figure 32). Figure 32 indicates two levels of

karst cave development; this is based roughly on the stratigraphy of the western plateau escarpment near SGSNA and should not be assumed true in other parts of the plateau due to the inherent variation in the lithology of the Pennington Formation (as shown in Figures 19 and 20).

Savage Gulf State Natural Area and the entire Cumberland Plateau escarpment hosts critical reserves of biological diversity, the development of which is founded upon a diverse assemblage of sedimentary rocks with differential rates of weathering, providing a wide range of soil and habitat types. Of these habitats, caves are perhaps the most sensitive, unique, and poorly understood environments of all, housing rare and endemic species of concern to conservationists and land managers. Understanding the geologic diversity and the influences and limitations on cave development in the Pennington Formation is fundamental if these features and their inhabitants are to be preserved.
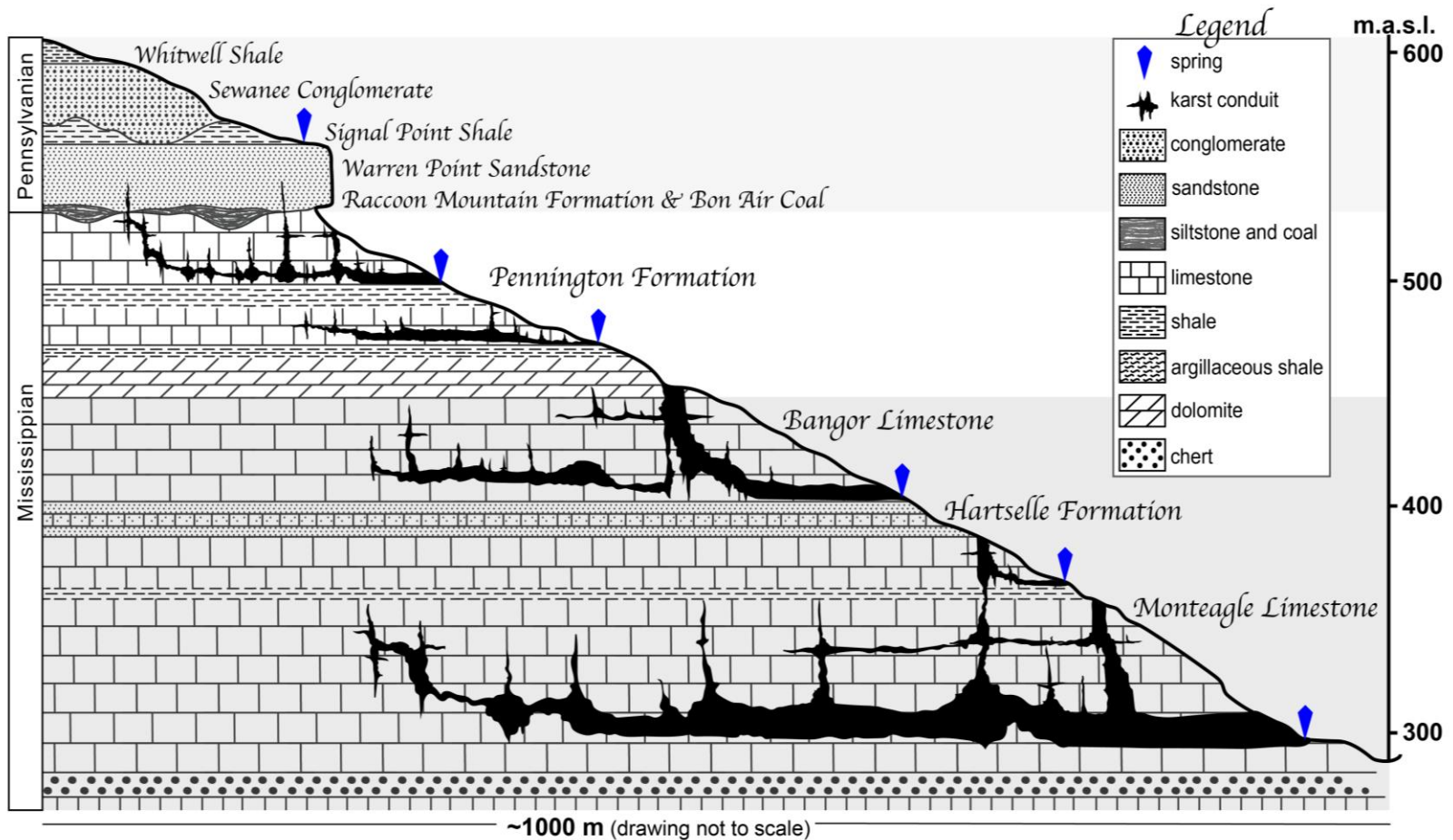
Figure 32. A revised karst geologic model of the Cumberland Plateau escarpment (vertically exaggerated) recognizing the potential for karst conduit development in limestone members of the Upper Mississippian Pennington Formation.

LITERATURE CITED

Alabama Cave Survey, 2018. https://www.alabamacavesurvey.org. Accessed October 2016.

Anthony, D.M. and Granger, D.E., 2004. A Late Tertiary Origin for Multilevel Caves Along the Western Escarpment of the Cumberland Plateau, Tennessee and Kentucky, Established by Cosmogenic ^{26}Al and ^{10}Be. *Journal of Cave and Karst Studies* 66(2), 46-55.

Anthony, D.M. and Granger, D.E., 2006. Five million years of Appalachian landscape evolution preserved in cave sediments. *Geological Society of America Special Papers* 404, 39-50.

Barr Jr, T.C., 1967. Observations on the ecology of caves. *American Naturalist*, 475-491.

Bergenback, R.E., 1993. Lower Pennsylvanian-Upper Mississippian deposystems, Monteagle Mountain, Tennessee. *Journal of the Tennessee Academy of Science* 68(3), 94-98.

Blakey, R.C. and Wong, T.E., 2003. Carboniferous–Permian paleogeography of the assembly of Pangaea. *Proceedings of the XVth International Congress on Carboniferous and Permian Stratigraphy*. 443-456.

Brahana, J.V., and Bradley, M.W., 1986. Preliminary delineation and description of the regional aquifers of Tennessee – the Highland Rim Aquifer system. *Water Resources Investigations* 82-4054, 1-38.

Brucker, R.W., Hess, J.W. and White, W.B., 1972. Role of vertical shafts in the movement of ground water in carbonate aquifers. *Ground Water* 10(6), 5-13.

Cave Research Foundation Personnel Manual, 2010.

Christman, M.C. and Culver, D.C., 2001. The relationship between cave biodiversity and available habitat. *Journal of Biogeography* 28(3), 367-380.

Clements, R.K. and Wofford, B.E., 1991. The vascular flora of Wolf Cove, Franklin County, Tennessee. *Castanea* 268-286.

Crawford Hydrology Laboratory, 2016a. Karst Groundwater Investigation Research Procedures. 1-16.

Crawford Hydrology Laboratory, 2016b. Step-by-Step Field Procedures and Recommendations. 1-16.

Crawford, N.C., 1978. Subterranean stream invasion, conduit cavern development, and slope retreat: a surface-subsurface erosion model for areas of carbonate rock overlain by less soluble and less permeable caprock. Dissertation, Clark University, Worcester, Massachusetts.

Crawford, N.C., 1992. The Karst Hydrogeology of the Cumberland Plateau Escarpment of Tennessee. *Tennessee Department of Environment and Conservation: Report of Investigations* No. 44, Part III.

Culver, D.C. and Pipan, T., 2009. *The Biology of Caves and Other Subterranean Habitats*. Oxford University Press, USA.

Curl, R.L., 1986. Fractal dimensions and geometries of caves. *Mathematical Geology* 18(8) 765-783.

Dale, V.H., Lannom, K.O., Tharp, M.L., Hodges, D.G. and Fogel, J., 2009. Effects of climate change, land-use change, and invasive species on the ecology of the Cumberland forests. *Canadian Journal of Forest Research* 39(2), 467-480.

Dasher, G.R., 1999. *On Station: A Complete Handbook for Surveying and Mapping Caves*. National Speleological Society: Huntsville, AL.

Davis, J.D. and Brook, G.A., 1993. Geomorphology and hydrology of upper Sinking Cove, Cumberland Plateau, Tennessee. *Earth Surface Processes and Landforms* 18, 339-362.

DeSelm, H.R. and Sherman, M.D., 1982. Species diversity and site position at Savage Gulf, Cumberland Plateau, Tennessee. Proceedings of the fourth central hardwood conference. University of Kentucky, Lexington, 356-366.

Dicken, C.L., Nicholson, S.W., Horton, J.D., Foose, M.P. and Mueller, J.A., 2005. Preliminary integrated geologic map databases for the United States: Alabama, Florida, Georgia, Mississippi, North Carolina, and South Carolina (No. 2005-1323).

Driese, S.G., Capelle, D.G., Glumac, B., Srinivasan, K., Stefaniak, A. and Stapor, F.W., 1994. Pre-Pennsylvanian paleokarst at the top of the upper Pennington Formation, central Tennessee. *Geological Society of America, Abstracts with Programs* 26(4).

Driese, S.G., Caudill, M.R., Srinivasan, K., 1998. Late Mississippian to Early Pennsylvanian paleokarst in east-central Tennessee: field, petrographic, and stable isotope evidence. *Southeastern Geology* 37(4), 189-204.

Dogwiler, T. and Wicks, C.M., 2004. Sediment entrainment and transport in fluviokarst systems. *Journal of Hydrology* 295(1), 163-172.

Duncan, J.R., and Lockwood, J.L, 2001. Spatial homogenization of the aquatic fauna of Tennessee: extinction and invasion following land use change and habitat alteration. In *Biotic homogenization*, 245-257.

Evans, J.P., Oldfield, C.A., Priestley, M.P., Gottfried, Y.M., Estes, L.D., Sidik, A. and Ramseur, G.S., 2016. The Vascular Flora of the University of the South, Sewanee, Tennessee. *Castanea* 81(3), 206-236.

Ettensohn, F.R., and Chesnut, D.R., 1985. Depositional Environments and Stratigraphy of the Pennington Formation (Upper Visean-Namurian A), East-Central and Eastern Kentucky, U.S.A. *Tenth International Congress of Carboniferous Stratigraphy and Geology, Madrid, Spain* 269-283.

Farrant, A.R. and Smart, P.L., 2011. Role of sediment in speleogenesis; sedimentation and paragenesis. *Geomorphology 134*(1), 79-93.

Field, M.S. and Nash, S.G., 1997. Risk assessment methodology for karst aquifers: (1) Estimating karst conduit-flow parameters. *Environmental Monitoring and Assessment* 47(1) 1-21.

Filipponi, M., Jeannin, P.Y., and Tacher, L., 2009. Evidence of inception horizons in karst conduit networks. *Geomorphology* 106(1), 86-99.

Fish, L., 2018. Compass Cave Survey and Mapping Software. [online] Fountainware.com. Available at: http://www.fountainware.com/compass/ [Accessed 10 Oct. 2016].

Ford, D.C., 1999. Perspectives in Karst Hydrogeology and Cavern Genesis. *Karst Waters Institute Special Publications* 5, 17-29.

Ford, D.C., 2006. Karst Geomorphology, caves, and cave deposits: A review of North American contributions during the past half century. *Geological Society of America Special Paper* 404.

Ford, D.C. and Ewers, R.O., 1978. The development of limestone cave systems in the dimensions of length and depth. *Canadian Journal of Earth Sciences* 15(11), 1783-1798.

Ford, D.C., Palmer, A.N., and White, W.B., 1988. Landform development; karst. *The Geological Society of America*.

Ford, D.C. and Williams, P.D., 2007. *Karst Hydrogeology and Geomorphology*. John Wiley & Sons.

(Gallay et al. 2016) Geomorphometric analysis of cave ceiling channels mapped with 3-D terrestrial laser scanning. *Hydrology & Earth System Sciences* 20(5).

Goodchild, M.F. and Mark, D.M., 1987. The fractal nature of geographic phenomena. *Annals of the Association of American Geographers* 77(2), 265-278.

Groves, C.G. and Howard, A.D., 1994. Minimum hydrochemical conditions allowing limestone cave development. *Water Resources Research* 30(3), 607-615.

Groves, C.G. and Meiman, J., 2005. Weathering, geomorphic work, and karst landscape evolution in the Cave City groundwater basin, Mammoth Cave, Kentucky. *Geomorphology* 67(1), 115-126.

Gunn, J., 2004. Fluviokarst. *Encyclopedia of Caves and Karst Science*. Taylor and Francis, London, UK.

Hack, J.T., 1966. Interpretation of Cumberland Escarpment and Highland Rim, South-Central Tennessee and Northeast Alamaba. *United States Geological Survey Professional Paper* 524-C.

Hammer, R.D., O'Brien, R.G. and Lewis, R.J., 1987. Temporal and spatial soil variability on three forested landtypes on the mid-Cumberland Plateau. *Soil Science Society of America Journal* 51(5), 1320-1326.

Hardeman, W.D., Miller, R.A., and Swingle, G.D., 1966. Geologic map of Tennessee [east central sheet]. *Tennessee Division of Geology*.

Harmon, R.S., Schwarcz, H.P., and Ford, D.C., 1978. Stable isotope geochemistry of speleothems and cave waters from the Flint Ridge-Mammoth Cave system, Kentucky: Implications for terrestrial climate change during the period 230,000 to 100,000 years BP. *The Journal of Geology* 86(3), 373-384.

Hart, J.L., Clark, S.L., Torreano, S.J. and Buchanan, M.L., 2012. Composition, structure, and dendroecology of an old-growth Quercus forest on the tablelands of the Cumberland Plateau, USA. *Forest Ecology and Management* 266, 11-24.

Hintze, J.L., 2007. Chapter 230: Circular Data Analysis in NCSS User's Guide II. NCSS, Kaysville, UT.

Humbert, S.E., 2001. Subaerial Paleokarst in the Upper Pennington Formation (Upper Mississippian) Limestones at Leatherwood Ford, Big South Fork, Tennessee. Master's Thesis, University of Tennessee, Knoxville.

Jacobson, R.L. and Langmuir, D., 1974. Controls on the quality variations of some carbonate spring waters. *Journal of Hydrology* 23(3), 247-265.

Jacoby, B.S., Peterson, E.W., Kostelnick, J.C. and Dogwiler, T., 2013. Approaching cave level identification with GIS: A case study of Carter Caves. *ISRN Geology* 2013(160397), 1-7.

Kambesis, P.N., 2014. Influence of coastal properties on speleogenesis and landforms in the Caribbean Region. Dissertation, Mississippi State University, Mississippi State, Mississippi.

Kambesis, P.N., Larson, E.B. and Mylroie, J.E., 2015. Morphometric analysis of cave patterns using fractal indices. *Geological Society of America Special Papers* 516, 1-20.

Kastning, E.H., 1999. The surface-subsurface interface and the influence of geologic structure in karst. *Karst Waters Institute Special Publications* 5, 43-47.

Kaufmann, G. and Braun, J., 1999. Karst aquifer evolution in fractured rocks. *Water Resources Research* 35(11), 3223-3238.

Kirchberg, J., Cecala, K.K., Price, S.J., White, E.M. and Haskell, D.G., 2016. Evaluating the impacts of small impoundments on stream salamanders. *Aquatic Conservation: Marine and Freshwater Ecosystems*. DOI: 10.1002/aqc.2664

Klimchouk, A.B., 2003. Cave morphometry. *Encyclopedia of Cave and Karst Science*. Fitzroy Dearborn: New York.

Klimchouk, A. Ford, D.C., Palmer, A.N., Dreybrodt, W., 2000. *Speleogenesis. Evolution of Karst Aquifers.* National Speleological Society: Huntsville, AL.

Klimchouk, A.B., Ford, D.C., Palmer, A.N., Dreybrodt, W., Miicke, B., Volker, R., Wadevirz, S., Slabe, T., Tarhule-Lips, R., Ford, D.C. and Zupan Hajna, N., 2004. Morphometry of caves. *Journal of Geology* 6(2), 675-811.

Knoll, M.A., Potter, D.B. and Van De Ven, C., 2015. Geology, hydrology, and water use history atop the Cumberland Plateau in the Sewanee and Tracy City, Tennessee, area. *Geological Society of America Field Guides* 39, 197-218.

Kruckeberg, A.R., 1986. An Essay: The Stimulus of Unusual Geologies for Plant Speciation. *Systematic Botany* 11(3), 455-463.

LaFleur, R.G., 1999. Geomorphic aspects of groundwater flow. Hydrogeology Journal 7(1), 78-93.

LaMoreaux, P.E., Powell, W.J. and LeGrand, H.E., 1997. Environmental and legal aspects of karst areas. Environmental Geology 29(1-2), 23-36.

Lauritzen, S.E., Abbott, J., Arnesen, R., Crossley, G., Grepperud, D., Ive, A. and Johnson, S., 1985. Morphology and hydraulics of an active phreatic conduit. *Cave Science* 12, 139-146.

Levenson, Y. and Emmanuel, S., 2017. Repulsion between calcite crytals and grain detachment during water-rock interaction. *Geochemical Perspectives Letters* 3, 133-141. May, V.J., 1983. Hydrology of Area 21, Eastern Coal Province, Tennessee, Alabama and Georgia. *United States Geological Survey* (No. 82-679).

McGrath, D.A., Evans, J.P., Smith, C.K., Haskell, D.G., Pelkey, N.W., Gottfried, R.R., Brockett, C.D., Lane, M.D. and Williams, E.D., 2004. Mapping land-use change and monitoring the impacts of hardwood-to-pine conversion on the Southern Cumberland Plateau in Tennessee. *Earth Interactions* 8(9), 1-24.

Milici, R.C., 1970. The Allegheny structural front in Tennessee and its regional tectonic implications. American Journal of Science 268(2), 127-141.

Milici, R.C., 1974. Stratigraphy and depositional environments of Upper Mississippian and Lower Pennsylvanian rocks in the southern Cumberland Plateau of Tennessee. *Geological Society of America Special Paper* 148, 115-133.

Milici, R.C., Briggs, G., Knox, L.M., Sitterly, P.D., and Statler, A.T., 1979. The Mississippian and Pennsylvanian (Carboniferous) systems in the United States – Tennessee. *United States Geological Survey Professional Paper* 1110-G, 1-38.

Moravec, G.F. and Moore, J.D., 1974. Hydrologic evaluation and application of ERTS data. *INVESTIGATION USING DATA IN ALABAMA FROM ERTS-A–FINAL REPORT*: 3(12), 404-439.

Moser, P.H. and Ricci, D., 1974. A comparison of sinkhole, cave, joint and lineament orientation. *INVESTIGATION USING DATA IN ALABAMA FROM ERTS-A–FINAL REPORT*: 3(12),179-122.

Muir, J., 1916. *A Thousand Mile Walk to the Gulf*, Chapter 2: Crossing the Cumberland Mountains. Houghton Mifflin Company: New York.

Mull, D. S., Liebermann, T. D., Smoot, J. L. and Woosley, L. H.: 1988. Application of Dye-Tracing Techniques for Determining Solute Transport Characteristics of Ground Water in Karst Terranes. *U.S. Environmental Protection Agency* (EPA 904/6-88-001).

Nicholson, S.W., Dicken, C.L., Horton, J.D., Labay K.A., Foose, M.P., and Mueller, J.A., 2005. Tennessee geologic map data. *USGS Open-File Report* 2005(1324).

Nicholson, S.W.D., Horton, C.L., Labay, J.D., Foose, K.A., Mueller, M.P. and Julia, A.L., 2005. Preliminary integrated geologic map databases for the United States: Kentucky, Ohio, Tennessee, and West Virginia.

Ngmdb.usgs.gov, 2018. National Geologic Map Database. [online] Available at: https://ngmdb.usgs.gov/ngmdb/ngmdb_home.html [Accessed 10 Aug. 2017].

Palmer, A.N., 1990. Groundwater processes in karst terranes. *Geological Society of America Special Paper* 252(8), 177-209.

Palmer, A.N., 1991. Origin and morphology of limestone caves. *Geological Society of America Bulletin* 103(1), 1-21.

Palmer, A.N., 2001. Dynamics of cave development by allogenic water. *Acta carsologica* 30(2), 14-32.

Palmer, A.N., 2007a. *Cave Geology*. Cave Books: Dayton, OH.

Palmer, A.N., 2007b. Variation in rates of karst processes. *Acta Carsologica* 36(1), 15-24.

Palmer, A.N., 2011. Distinction between epigenic and hypogenic maze caves. *Geomorphology* 134(1), 9-22.

Pardo-Iguzquiza, E., Durán-Valsero, J.J. and Rodríguez-Galiano, V., 2011. Morphometric analysis of three-dimensional networks of karst conduits. *Geomorphology* 132(1), 17-28.

Peterson, M.N.A., 1962. The mineralogy and petrology of upper Mississippian carbonate rocks of the Cumberland Plateau in Tennessee. *The Journal of Geology* 70(1), 1-31.

Piccini, L., 2011. Recent developments on morphometric analysis of karst caves. *Acta Carsologica* 40(1), 43-52.

Powell, R.L., 1969. Base level, lithologic and climatic controls of karst groundwater zones in South-central Indiana. *Proceedings of the Indiana Academy of Science* 79(1), 281-291.

Redovniković, L., Stančić, B. and Cetl, V., 2016, January. Comparison of Different Methods of Underground Survey. *GNSS and Indoor Navigation* 465-472.

Rodgers, J., 1953. Geologic Map of East Tennessee With Explanatory Text. *State of Tennessee Department of Environment and Conservation Division of Geology* Bulletin 58, Part II.

Sasowsky, I.D., 1992. Evolution of the Appalachian Highlands: East Fork Obey River, Fentress County, Tennessee. Dissertation, Pennsylvania State University, State College, Pennsylvania.

Sasowsky, I.D., 1999. Structural Effects on carbonate aquifers. *Karst Waters Institute Special Publication* 5, 38-42.

Sasowsky, I.D. and White, W.B., 1994. The role of stress release fracturing in the development of cavernous porosity in carbonate aquifers. *Water Resources Research* 30(12), 3523-3530.

Sasowsky, I.D., White, W.B. and Schmidt, V.A., 1995. Determination of stream-incision rate in the Appalachian plateaus by using cave-sediment magnetostratigraphy. *Geology* 23(5), 415-418.

Scanlon, B.R. and Thrailkill, J., 1987. Chemical similarities among physically distinct spring types in a karst terrain. *Journal of Hydrology* 89(3), 259-279.

Shaver, S.A., Eble, C.F., Hower, J.C. and Saussy, F.L., 2006. Petrography, palynology, and paleoecology of the Lower Pennsylvanian Bon Air coal, Franklin County, Cumberland Plateau, southeast Tennessee. International Journal of Coal Geology 67(1), 17-46.

Shuster, E.T. and White, W.B., 1971. Seasonal fluctuations in the chemistry of limestone springs: A possible means for characterizing carbonate aquifers. *Journal of Hydrology* 14(2), 93-128.

Siemers, J. and Dreybrodt, W., 1998. Early development of karst aquifers on percolation networks of fractures in limestone. *Water resources research* 34(3), 409-419.

Simms, M.J., 2004. Tortoises and hares: Dissolution, erosion and isostasy in landscape evolution. *Earth Surface Processes and Landforms* 29(4), 477-494.

Simpson, L.C. and Florea, L.J., 2009. The Cumberland Plateau of Eastern Kentucky. *Caves and Karst of America* 70-79.

Smart, C. and Campbell, C.W., 2003. A Speleogenetic Model for the Cumberland Plateau of Northeastern Alabama. *Sinkholes and the Engineering and Environmental Impacts of Karst* 683-691.

Szabo, M. W., Osborne, E. W., Copeland, C. W. Jr., Neathery; T. L., 1988, Geologic Map of Alabama, Geological Survey of Alabama Special Map 220, scale 1:250,000.

Taylor, C.J. and Greene, E.A., 2008. Hydrogeologic characterization and methods used in the investigation of karst hydrology. *USGS Techniques and Methods* 4-D2, 75-107.

Taylor, C.J. and Nelson, H.L., 2008. A compilation of provisional karst geospatial data for the Interior Low Plateaus physiographic region, central United States. US Geological Survey, Reston, VA.

Tennessee Cave Survey, 2017. Digital database. Accessed October 2017.

Tennessee Department of Environment and Conservation (TDEC), 2003. Collins River Watershed (05130107) of the Cumberland River Basin Watershed Water Quality Management Plan. *Division of Water Pollution Control, Watershed Management Section.*

Thomas, W.A., 1972. Mississippian stratigraphy of Alabama. *Geological Survey of Alabama* Monograph 12.

U.S. Geological Survey, 2016a. National Water Information System data. Available on the World Wide Web (USGS Water Data for the Nation), accessed [October 10, 2016] at URL [http://waterdata.usgs.gov/nwis/].

U.S. Geological Survey, 2016b. Tennessee Geologic Map data. Available on the World Wide Web (USGS Mineral Resources Online Spatial Data), accessed [October 10, 2016] at URL [https://mrdata.usgs.gov/catalog/cite-view.php?cite=671].

Van Wagoner, J.C., Posamentier, H.W., Mitchum, R.M.J., Vail, P.R., Sarg, J.F., Loutit, T.S., and Hardenbol, J., 1988. An overview of the fundamentals of sequence stratigraphy and key definitions. Society of Economic Paleontologists and Mineralogists *Special Publication No. 42*, 39-45.

Varnedoe, W.W. Jr., 1963. Cross Piracy Drainage Development in the Newsome Sinks Area of Alabama. *National Speleological Society Bulletin* 25(2), 83-87.

Veni, G., 1999. A geomorphological strategy for conducting environmental impact assessments in karst areas. *Geomorphology* 31(1), 151-180.

Veni, G., 2013. A framework for assessing the role of karst conduit morphology, hydrology, and evolution in the transport and storage of carbon and assossiated sediments. *Acta Carsologica* 42(2-3), 203-211.

Vesper, D.J., and White, W.B., 2004. Storm pulse chemographs of saturation index and carbon dioxide pressure: implications for shifting recharge sources during storm events in the karst aquifer at Fort Campbell, Kentucky/Tennessee, USA. *Hydrogeology Journal*, 12(2), 135-143.

White, E.L. and White, W.B., 1983. Karst landforms and drainage basin evolution in the Obey River basin, north-central Tennessee, USA. *Journal of Hydrology* 61(1), 69-82.

White, W.B., 1969. Conceptual models for carbonate aquifers. *Ground Water* 7(3), 15-21.

White, W.B., 1988. Geomorphology and Hydrology of Karst Terrains. Oxford University Press: New York, NY.

White, W.B., 2007a. A brief history of karst hydrogeology: contributions of the NSS. *Journal of Cave and Karst Studies* 69(1), 13-26.

White, W.B., 2007b. Evolution and age relations of karst landscapes. *Acta Carsologica* 36(1).

White, W.B., 2009. The evolution of Appalachian fluviokarst: competition between stream erosion, cave development, surface denudation, and tectonic uplift. *Journal of Cave and Karst Studies* 71(3), 159-167.

White, W., 2015. Chemistry and karst. *Acta Carsologica* 44(3), 349-362.

Wicks, C.M. and Groves, C.G., 1993. Acidic mine drainage in carbonate terrains: geochemical processes and rates of calcite dissolution. *Journal of Hydrology* (146), 13-27.

Williams, P.W., 2008. The role of the epikarst in karst and cave hydrogeology: a review. *International Journal of Speleology* 37(1), 1-10.

Wilson, C.W. and Stearns, R.G., 1958. Structure of the Cumberland Plateau, Tennessee. *Geological Society of America Bulletin* 69(10), 283-1296.

Wofford, B.E., Patrick, T.S., Phillippe, L.R. and Webb, D.H., 1979. The vascular flora of Savage Gulf, Tennessee. SIDA, *Contributions to Botany* 8(2), 135-151.

Worthington, S.R., 2004. Hydraulic and geological factors influencing conduit flow depth. *Cave and Karst Science* 31(3), 123-134.

Worthington, S.R., 2009. Diagnostic hydrogeologic characteristics of a karst aquifer (Kentucky, USA). *Hydrogeology Journal* 17(7), 1665-1678.

Worthington, S.R.H. and Ford, D.C., 2009. Self-organized permeability in carbonate aquifers. *Ground Water* 47(3), 326-336.

Zar, J.H., 1984. *Biostatistical Analysis*. Prentice Hall: Englewood Cliffs, NJ.

A1. COONS LABYRINTH CAVE MAP

GREETER GILL CAVE

GD323
GRUNDY COUNTY, TENNESSEE

HORIZONTAL LENGTH: 429 ft (131 m)
VERTICAL EXTENT: 30 ft (9 m)

Low, anastomotic passages
(too tight to enter)

Wet sand and
pools of water

Grade 5 survey conducted October 1, 2017 by:
Hali Steinmann
Ryan Gardner
Cartography by Hali Steinmann (NSS 65702)

E2

E1

LEGEND

small breakdown		ledge	
large breakdown		ceiling ledge	
bedrock		③ ceiling height (ft)	
sand/small gravel		speleothems	
silt/clay		soda straws	
slope		tree roots	

10   50   100ft

EASTER RISE CAVE

GD320
GRUNDY COUNTY, TENNESSEE

HORIZONTAL LENGTH: 378 ft (115 m)
VERTICAL EXTENT: 20 ft (6 m)

LEGEND
E entrance
dripline
breakdown
bedrock
sand/small gravel
silt/clay
slope
ceiling ledge

CROSS SECTIONS

Grade 5 survey conducted September 3, 2017 by:
Hali Steinmann
Caleb Koostra
Josh Blanchette

Cave is formed in the Upper Mississippian Pennington Formation in an incised meander of Big Creek. Dye traces conducted in 2017 confirmed that the cave stream is recharged by losing reaches of Big Creek. The cave is owned by the State of Tennessee.

Cartography by Hali Steinmann (NSS 65702).

TENNESSEE
State Parks

Fall Creek Saltpeter Cave

GD277

Grundy County, Tennessee

Grade 5 Survey
22 October 2016
Hali Steinmann, Marty Abercrombie, and Lee White
DistoX, Suunto Compass, Clinometer, and tape
Drafted by: Hali Steinmann (NSS 65702)

LENGTH: 152.3 m (500 ft)
VERTICAL EXTENT: 5.5 m (18 ft)

CROSS SECTIONS

LEGEND

	small breakdown		ledge
	large breakdown		ceiling ledge
	bedrock	③	ceiling height (ft)
	sand/small gravel		speleothems
	silt/clay		soda straws
	slope		tree roots

Entrance 1

Entrance 2

PROFILE VIEW

113

JEZABEL CAVE

GD278
GRUNDY COUNTY, TENNESSEE

HORIZONTAL LENGTH: 176 ft (54 m)
VERTICAL EXTENT: 18 ft (5.5 m)

Grade 5 (Suunto and DistoX) survey conducted September 3, 2017 by:
Hali Steinmann, John McMacken, and Homero Rivas

10   50 ft

Jezabel Cave is formed in the Upper Mississippian Pennington Formation and is located on the north bank of the Collins River in Savage Gulf State Natural Area. The cave is owned by the state of Tennessee and was first documented by James Smith in 1999. Water that sinks at the cave entrance resurges as a spring 50 feet downhill of the entrance and 10 feet above the Collins River.

L E G E N D

breakdown	dripline	③ ceiling height (ft)
sand/gravel	water	vegetal debris
silt/clay	ledge	--- ceiling ledge
slope		

PLAN VIEW
Entrance

CROSS SECTIONS
(to scale)

PROFILE VIEW

Pennington Formation

20 ft

10

TENNESSEE State Parks

Cartography by Hali Steinmann (NSS 65702)

B. MODELED CAVE MORPHOMETRY

State	County	Name	Elev_m	SurvLen_m	PlanLen_m	VertExt_m	SurfaceLen_m	SurfaceWid_m	FloorArea_m2	CaveField_m2	CaveBlock_m	ArealCov	Vol_m3	SpecificVol	PassNetDens	Vert_Index	Hor_Index	Valley_trend°	Cave_trend°	Cave_trend2°	Type
AL	MD	Abbey Squeeze, The	478.5	21.6	19.0	4.6	9.4	5.4	37.7	50.8	232.1	0.74	100.5	5.3	0.43	0.21	0.88	125	115	35	B
AL	JK	Above Upper Kennamer	365.8	71.0	37.5	6.1	33.3	60.0	611.4	1998.0	12179.8	0.31	1200.9	32.0	0.04	0.09	0.53	175	175	115	B
TN	FR	Alabama Run Cave	365.8	425.9	416.5	16.2	121.3	113.9	2009.7	13816.1	223190.3	0.15	3669.2	8.8	0.03	0.04	0.08	10	15	175	B
TN	GD	Bear Hole	420.6	3676.2	3561.9	12.2	256.5	118.6	4444.3	30420.9	370891.6	0.15	4444.3	1.2	0.12	0.00	0.97	95	95	85	M
AL	MD	Ben's Den	414.5	60.3	51.5	2.1	16.7	19.2	91.2	320.6	684.1	0.28	103.6	2.0	0.19	0.04	0.85	32	35	115	M
AL	MG	Black Walnut Cave	329.2	111.2	78.0	26.2	48.3	30.4	605.1	1468.3	38488.8	0.41	1445.8	18.5	0.08	0.24	0.70	160	168	55	B
TN	OV	Briar Hill Cave	438.9	243.8	221.3	9.1	104.5	68.9	731.4	7200.1	65837.3	0.10	1697.8	7.7	0.03	0.04	0.91	140	75	175	B
AL	MD	Broken Bluff Cave	469.4	62.5	42.7	10.7	40.0	7.2	88.7	288.0	3072.4	0.31	342.8	8.0	0.22	0.17	0.68	40	85	5	B
TN	FR	Buckets of Blood Cave	484.6	311.5	304.8	7.3	79.6	83.6	525.4	6654.6	48679.4	0.08	398.3	1.3	0.05	0.02	0.98	60	25	115	M
TN	FR	Cave Springs Pit	457.2	105.2	90.7	20.1	27.7	37.1	505.5	1027.7	20673.4	0.49	1845.9	20.4	0.10	0.19	0.86	160	10	115	P
AL	MG	Chapel Cave	225.6	783.3	527.1	18.3	131.7	66.9	1144.8	8810.7	161130.6	0.13	2803.1	5.3	0.09	0.02	0.67	140	105	132	M
TN	FR	Coons Labyrinth Cave	542.5	736.4	731.5	3.4	98.1	136.3	1566.9	13371.0	44830.4	0.12	1604.7	2.2	0.06	0.00	0.99	5	135	12	M
AL	MG	Corral Cave	243.8	30.2	24.1	9.1	13.3	20.4	73.5	271.3	2481.0	0.27	135.2	5.6	0.11	0.30	0.80	15	20	70	B
TN	WH	Crafty Commie Cave	487.7	488.9	466.3	7.6	54.0	29.0	883.5	1566.0	11932.9	0.56	2585.9	5.5	0.31	0.02	0.95	100	75	155	M
AL	MG	Cricket Cave	231.6	42.6	33.8	9.1	21.1	26.0	66.2	548.6	5016.4	0.12	98.8	2.9	0.08	0.21	0.79	155	175	115	B
TN	FR	Devils Pit	512.1	14.3	12.2	12.2	7.6	7.9	41.3	60.0	732.0	0.69	236.8	19.4	0.24	0.85	0.85	50	125	175	P
AL	MG	Doghouse Cave	231.6	280.4	274.3	9.1	77.9	111.5	754.1	8685.9	79423.4	0.09	2577.4	9.4	0.03	0.03	0.98	160	155	68	B
TN	GD	Easter Rise Cave	454.2	115.2	106.7	6.1	85.5	53.4	719.8	4565.7	27832.5	0.16	890.1	8.3	0.03	0.05	0.93	75	45	75	B
TN	GD	Fall Creek Saltpeter Cave	426.7	152.3	149.4	5.5	46.1	63.9	491.9	2945.8	16201.8	0.17	599.5	4.0	0.05	0.04	0.98	150	145	125	B
AL	MG	Fish Hook Pit	335.3	34.7	28.6	15.2	9.3	20.8	86.4	193.4	2948.0	0.45	370.4	13.0	0.18	0.44	0.82	150	40	40	P
AL	JK	Frazier Cave	432.8	66.1	61.0	4.9	10.3	48.7	169.8	501.6	2446.3	0.34	309.7	5.1	0.13	0.07	0.92	5	175	35	B
AL	MD	George Cave	303.9	61.0	37.6	39.9	26.8	16.7	69.3	447.6	17870.5	0.15	411.3	10.9	0.14	0.66	0.62	140	55	55	P
TN	FR	Grapevine Cave	502.9	591.0	585.2	10.7	159.7	196.6	1803.5	31397.0	334943.4	0.06	4134.0	7.1	0.02	0.02	0.99	25	15	65	B
TN	FR	Green View Slit	451.1	20.7	14.8	12.2	2.7	13.6	30.5	36.7	447.7	0.83	137.3	9.3	0.56	0.59	0.71	25	5	165	B
TN	GD	Greeter Falls Cave	463.3	320.1	318.5	7.6	108.9	151.8	1715.2	16531.0	125966.4	0.10	3222.0	10.1	0.02	0.02	1.00	155	145	45	M
TN	GD	Greeter Gill Cave	463.3	130.7	128.1	9.1	22.5	54.2	352.2	1219.5	11151.1	0.29	707.5	5.5	0.11	0.07	0.98	155	175	5	B
AL	MD	Gregg's Misery Cave	408.4	289.0	259.1	0.9	160.9	198.5	928.7	31938.7	29204.7	0.03	385.8	1.5	0.01	0.00	0.90	20	30	85	B
AL	MG	Gum Cave	268.2	25.9	24.4	9.1	8.0	16.3	116.7	130.4	1192.4	0.89	389.4	15.9	0.20	0.35	0.94	175	5	5	B
AL	MD	High Top Cave	502.9	125.0	124.0	9.1	26.9	103.1	774.0	2773.4	25359.9	0.28	3145.1	25.4	0.05	0.07	0.99	60	45	155	B
AL	JK	Humongous Maze Cave	396.2	669.8	622.1	15.2	81.2	147.3	1383.3	11960.8	182282.0	0.12	1731.5	2.8	0.06	0.02	0.93	45	175	40	M
AL	MG	I Cave	249.9	15.8	15.2	12.2	10.5	5.9	31.7	62.0	755.3	0.51	288.7	18.9	0.26	0.77	0.96	165	108	5	B
AL	MG	James Brown Well	268.2	43.0	21.1	39.6	14.2	18.4	30.4	261.3	10353.0	0.12	489.4	23.2	0.16	0.92	0.49	105	105	155	P
TN	GD	Jezabel Cave	426.7	54.0	53.3	3.0	8.4	46.5	283.1	390.6	1190.5	0.72	697.9	13.1	0.14	0.06	0.99	150	25	35	B
AL	MD	Kroeger's Hole	420.6	22.9	19.8	24.1	15.0	8.6	56.2	129.0	3106.2	0.44	267.8	13.5	0.18	1.05	0.87	170	95	25	P
TN	WH	Lockwood Cave	451.1	5110.0	3576.4	47.5	404.7	664.9	22960.2	269085.0	12794670.3	0.09	68160.2	19.1	0.02	0.01	0.70	70	45	145	B
TN	WH	Lost Labyrinth Cave	484.6	961.6	942.6	5.8	106.4	184.8	2990.0	19662.7	113870.7	0.15	5996.2	6.4	0.05	0.01	0.98	60	145	25	M
AL	MG	Louise Cave	274.3	53.3	53.0	4.6	14.4	27.5	114.5	396.0	1810.5	0.29	249.4	4.7	0.13	0.09	0.99	100	80	135	B
AL	MD	Michael's Cave	359.7	202.1	164.6	2.4	74.4	76.8	316.4	5713.9	13932.8	0.06	433.4	2.6	0.04	0.01	0.81	45	145	115	B
AL	JK	Pack Rat Cave	487.7	18.7	18.3	9.1	7.7	12.0	35.5	92.4	844.9	0.38	28.0	1.5	0.20	0.49	0.98	10	5	95	B
AL	MD	Pavlick's Pit	353.6	15.2	10.3	15.2	2.5	6.0	8.2	15.0	228.6	0.55	62.6	6.1	1.02	1.00	0.67	135	175	35	P
AL	JK	Pennington Cave	359.7	30.2	25.9	0.5	13.1	14.6	41.2	191.3	87.4	0.22	37.9	1.5	0.16	0.02	0.86	35	5	100	B
TN	GD	Pinnacle Rock Cave	442.0	109.5	108.4	4.6	28.0	52.4	420.4	1467.2	6708.0	0.29	880.6	8.1	0.07	0.04	0.99	80	145	175	B
TN	OV	Quarles Cave	390.1	63.7	49.1	13.1	29.7	15.6	179.7	463.3	6072.5	0.39	405.5	8.3	0.14	0.21	0.77	115	112	22	B
AL	MD	Rabbit Hole	413.0	22.9	5.7	21.6	4.0	5.7	21.2	22.8	493.4	0.93	28.5	5.0	1.01	0.94	0.25	90	178	178	P
AL	MD	Road Pit	374.0	40.8	30.5	40.8	7.7	27.9	115.2	214.8	8774.3	0.54	1602.1	52.6	0.19	1.00	0.75	25	5	25	P
AL	MD	Rock Shelter Cave	378.0	26.5	25.9	1.5	12.6	15.2	108.3	191.5	291.9	0.57	88.0	3.4	0.14	0.06	0.98	40	45	45	B
TN	MN	Sams Cave	396.2	3075.7	1017.7	15.2	110.4	324.4	2758.6	35813.8	545801.7	0.08	8135.5	8.0	0.09	0.00	0.33	140	45	135	M
TN	WH	Short Creek Maze Cave	426.7	381.7	320.6	6.1	81.9	72.9	453.0	5970.5	36396.2	0.08	484.0	1.5	0.06	0.02	0.84	110	115	95	M
AL	MD	Slimy Disappointment	451.1	9.0	7.6	8.2	7.1	3.0	40.2	21.3	175.3	1.89	190.6	25.0	0.42	0.92	0.85	155	125	75	B
TN	GD	Small Bluff Cave	384.0	21.6	20.4	2.4	16.6	10.9	41.1	180.9	441.2	0.23	39.3	1.9	0.12	0.11	0.94	65	65	65	B
AL	MG	Snail Cave	243.8	165.2	156.5	10.7	81.6	35.6	303.1	2905.0	30990.1	0.10	563.5	3.6	0.06	0.06	0.95	55	65	5	B
AL	MD	Soapstone Hollow C.	432.8	340.2	189.1	55.5	87.2	48.4	375.3	4220.5	234125.2	0.09	1417.0	7.5	0.08	0.16	0.56	150	105	15	B
AL	MG	Stillhouse Cave	350.5	58.9	57.4	15.2	15.7	21.3	141.4	334.4	5096.4	0.42	314.4	5.5	0.18	0.26	0.97	140	15	55	B
AL	MG	T Cave	243.8	30.5	29.6	9.1	22.6	9.0	59.2	203.4	1859.9	0.29	118.4	4.0	0.15	0.30	0.97	165	5	110	B
AL	MG	Turner Cave	268.2	57.0	47.9	0.0	4.9	46.9	114.0	229.8	0.0	0.25	108.1	2.3	0.25	0.00	0.84	170	175	5	B
AL	MD	Turtle Pit	411.5	34.1	14.0	27.4	10.9	3.1	32.8	33.8	926.9	0.97	310.6	22.2	1.01	0.80	0.41	95	95	95	P
TN	VB	Wagon Wheel Cave	487.7	836.4	735.2	8.8	583.7	83.8	2457.2	48914.1	432361.2	0.05	5398.6	7.3	0.02	0.01	0.88	25	115	90	B
TN	PU	Welch-Bowling Cave	515.1	5381.9	4859.1	25.3	764.2	1097.8	4928.9	838938.8	21223808.3	0.01	6923.0	1.4	0.01	0.00	0.90	140	155	135	B
TN	MN	White Cricket Cave	393.2	767.8	762.0	12.2	92.9	437.7	4206.6	40662.3	495755.1	0.10	1067.5	1.4	0.02	0.02	0.99	10	5	65	B
TN	OV	Wolf Branch Cave	438.9	50.3	44.5	2.7	19.8	29.8	134.1	590.0	1618.6	0.23	245.6	5.5	0.09	0.05	0.88	140	5	95	B

Abbey Squeeze

Black Walnut Cave

Chapel Cave

Above Upper Kennamer

Briar Hill Cave

Coons Labyrinth Cave

Alamaba Run Cave

Broken Bluff Cave

Corral Cave

Bear Hole

Buckets of Blood Cave

Crafty Commie Cave

Ben's Den

Cave Springs Pit

Cricket Cave

116
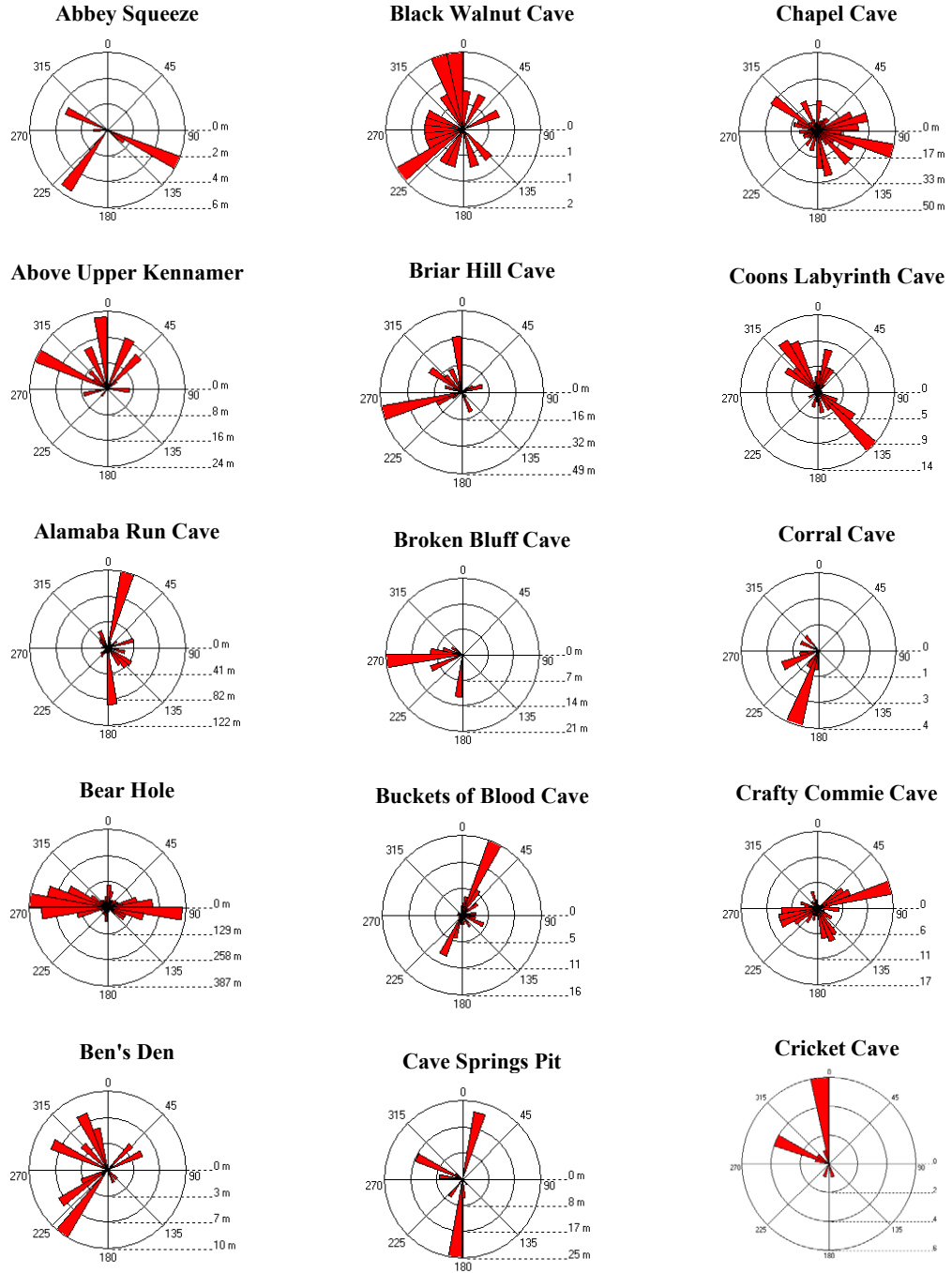
Devils Pit
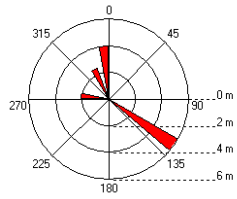
Frazier Cave
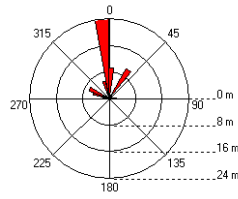
Greeter Gill Cave
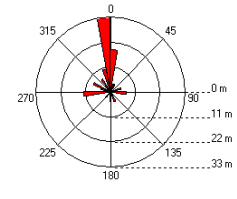
Doghouse Cave
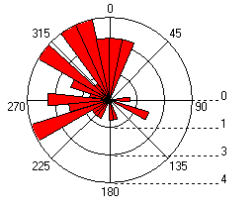
George Cave
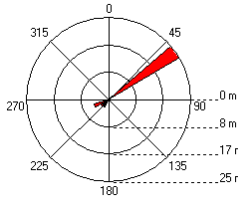
Greggs Misery Cave
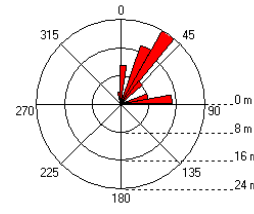
Easter Rise Cave
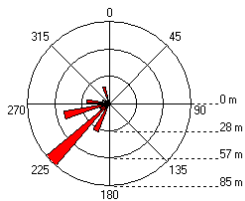
Grapevine Cave
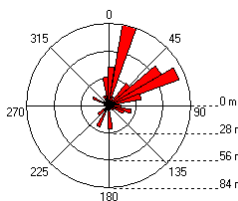
Gum Cave
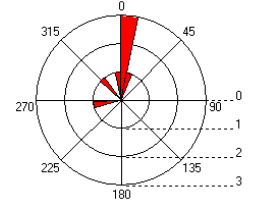
Fall Creek Saltpeter Cave
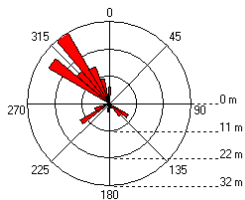
Green View Slit
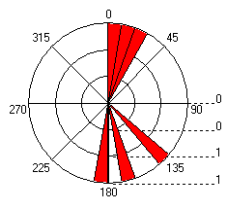
High Top Cave
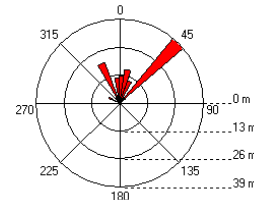
Fish Hook Pit
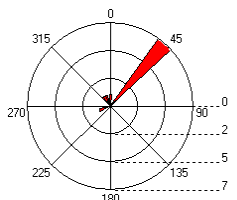
Greeter Falls Cave
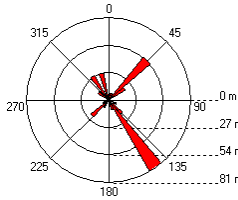
Humongous Maze Cave
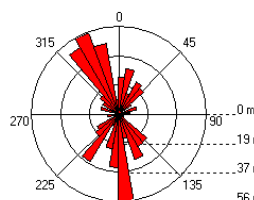
I Cave
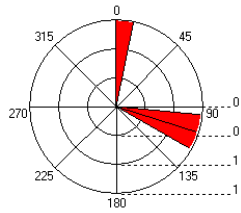
Lost Labyrinth Cave
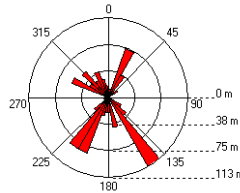
Pennington Cave
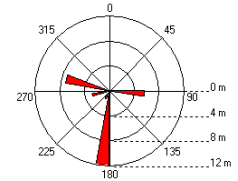
James Brown Well
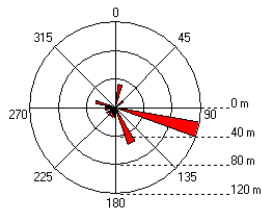
Louise Cave
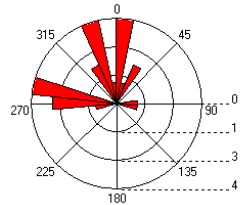
Pinnacle Rock Cave
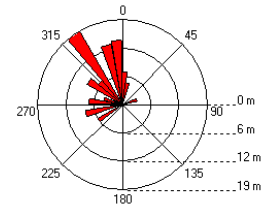
Jezabel Cave
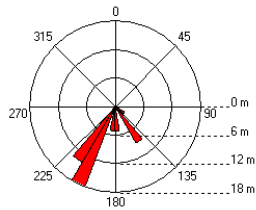
Michaels Cave
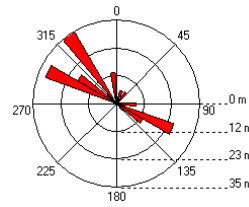
Quarles Cave
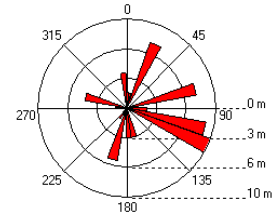
Kroegers Hole
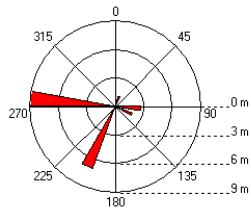
Pack Rat Cave
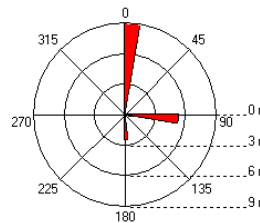
Rabbit Hole
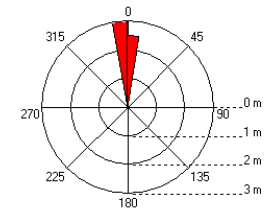
Lockwood Cave
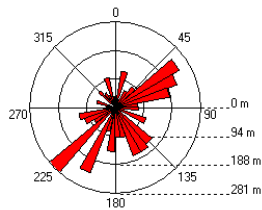
Pavlicks Pit

Road Pit

118
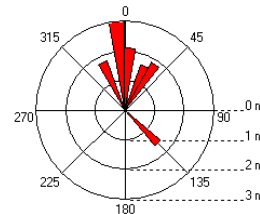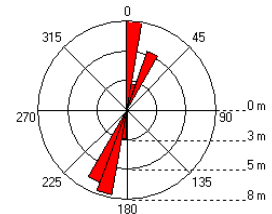
Rock Shelter Cave
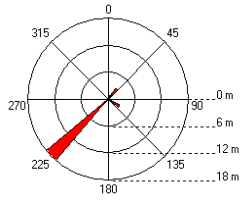
Snail Cave
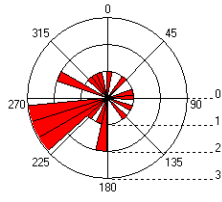
Turtle Pit
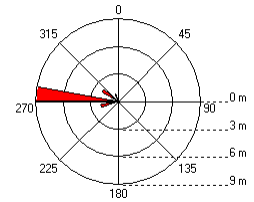
Sams Cave
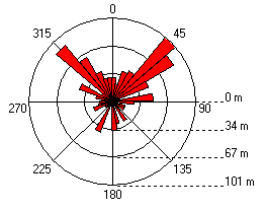
Soapstone Hollow Cave
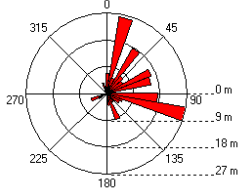
Wagon Wheel Cave
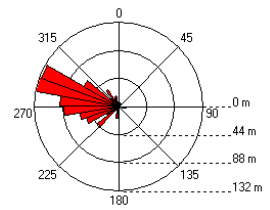
Short Creek Maze Cave
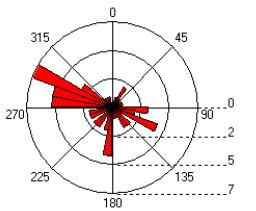
Stillhouse Cave
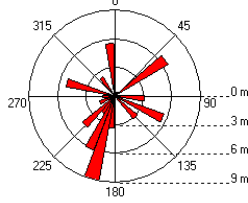
Welch-Bowling Cave
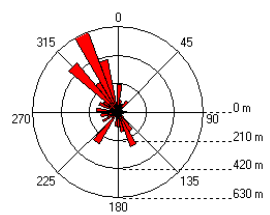
Slimy Disappointment
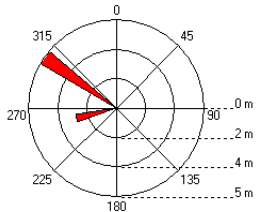
T Cave
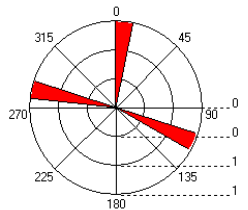
White Cricket Cave
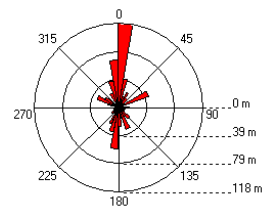
Small Bluff Cave
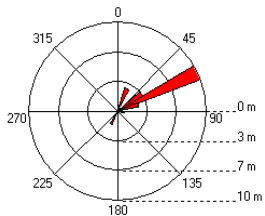
Turner Cave
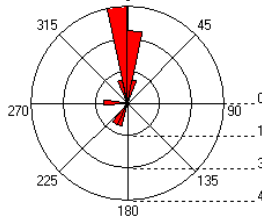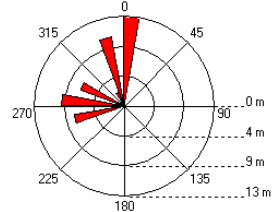
Wolf Branch Cave

State	County	Name	Valley_trend°	Cave_trend°	Cave_trend2°	Sin(ValAz)	Cos(ValAz)	Sin(CavAz)	Cos(CavAz)	Sin(CavAz2)	Cos(CavAz2)
AL	MD	Abbey Squeeze, The	125	115	35	0.81915	-0.57358	0.90631	-0.42262	0.57358	0.81915
AL	JK	Above Upper Kennamer	175	175	115	0.08716	-0.99619	0.08716	-0.99619	0.90631	-0.42262
TN	FR	Alabama Run Cave	10	15	175	0.17365	0.98481	0.25882	0.96593	0.08716	-0.99619
TN	GD	Bear Hole	95	95	85	0.99619	-0.08716	0.99619	-0.08716	0.99619	0.08716
AL	MD	Ben's Den	32	35	115	0.52992	0.84805	0.57358	0.81915	0.90631	-0.42262
AL	MG	Black Walnut Cave	160	168	55	0.34202	-0.93969	0.20791	-0.97815	0.81915	0.57358
TN	OV	Briar Hill Cave	140	75	175	0.64279	-0.76604	0.96593	0.25882	0.08716	-0.99619
AL	MD	Broken Bluff Cave	40	85	5	0.64279	0.76604	0.99619	0.08716	0.08716	0.99619
TN	FR	Buckets of Blood Cave	60	25	115	0.86603	0.50000	0.42262	0.90631	0.90631	-0.42262
TN	FR	Cave Springs Pit	160	10	115	0.34202	-0.93969	0.17365	0.98481	0.90631	-0.42262
AL	MG	Chapel Cave	140	105	132	0.64279	-0.76604	0.96593	-0.25882	0.74314	-0.66913
TN	FR	Coons Labyrinth Cave	5	135	12	0.08716	0.99619	0.70711	-0.70711	0.20791	0.97815
AL	MG	Corral Cave	15	20	70	0.25882	0.96593	0.34202	0.93969	0.93969	0.34202
TN	WH	Crafty Commie Cave	100	75	155	0.98481	-0.17365	0.96593	0.25882	0.42262	-0.90631
AL	MG	Cricket Cave	155	175	115	0.42262	-0.90631	0.08716	-0.99619	0.90631	-0.42262
TN	FR	Devils Pit	50	125	175	0.76604	0.64279	0.81915	-0.57358	0.08716	-0.99619
AL	MG	Doghouse Cave	160	155	68	0.34202	-0.93969	0.42262	-0.90631	0.92718	0.37461
TN	GD	Easter Rise Cave	75	45	75	0.96593	0.25882	0.70711	0.70711	0.96593	0.25882
TN	GD	Fall Creek Saltpeter Cave	150	145	125	0.50000	-0.86603	0.57358	-0.81915	0.81915	-0.57358
AL	MG	Fish Hook Pit	150	40	40	0.50000	-0.86603	0.64279	0.76604	0.64279	0.76604
AL	JK	Frazier Cave	5	175	35	0.08716	0.99619	0.08716	-0.99619	0.57358	0.81915
AL	MD	George Cave	140	55	55	0.64279	-0.76604	0.81915	0.57358	0.81915	0.57358
TN	FR	Grapevine Cave	25	15	65	0.42262	0.90631	0.25882	0.96593	0.90631	0.42262
TN	FR	Green View Slit	25	5	165	0.42262	0.90631	0.08716	0.99619	0.25882	-0.96593
TN	GD	Greeter Falls Cave	155	145	45	0.42262	-0.90631	0.57358	-0.81915	0.70711	0.70711
TN	GD	Greeter Gill Cave	155	175	5	0.42262	-0.90631	0.08716	-0.99619	0.08716	0.99619
AL	MD	Gregg's Misery Cave	20	30	85	0.34202	0.93969	0.50000	0.86603	0.99619	0.08716
AL	MG	Gum Cave	175	5	5	0.08716	-0.99619	0.08716	0.99619	0.08716	0.99619
AL	MD	High Top Cave	60	45	155	0.86603	0.50000	0.70711	0.70711	0.42262	-0.90631
AL	JK	Humongous Maze Cave	45	175	40	0.70711	0.70711	0.08716	-0.99619	0.64279	0.76604
AL	MG	I Cave	165	108	5	0.25882	-0.96593	0.95106	-0.30902	0.08716	0.99619
AL	MG	James Brown Well	105	105	155	0.96593	-0.25882	0.96593	-0.25882	0.42262	-0.90631
TN	GD	Jezabel Cave	150	25	35	0.50000	-0.86603	0.42262	0.90631	0.57358	0.81915
AL	MD	Kroeger's Hole	170	95	25	0.17365	-0.98481	0.99619	-0.08716	0.42262	0.90631
TN	WH	Lockwood Cave	70	45	145	0.93969	0.34202	0.70711	0.70711	0.57358	-0.81915
TN	WH	Lost Labyrinth Cave	60	145	25	0.86603	0.50000	0.57358	-0.81915	0.42262	0.90631
AL	MG	Louise Cave	100	80	135	0.98481	-0.17365	0.98481	0.17365	0.70711	-0.70711
AL	MD	Michael's Cave	45	145	115	0.70711	0.70711	0.57358	-0.81915	0.90631	-0.42262
AL	JK	Pack Rat Cave	10	5	95	0.17365	0.98481	0.08716	0.99619	0.99619	-0.08716
AL	MD	Pavlick's Pit	135	175	35	0.70711	-0.70711	0.08716	-0.99619	0.57358	0.81915
AL	JK	Pennington Cave	35	5	100	0.57358	0.81915	0.08716	0.99619	0.98481	-0.17365
TN	GD	Pinnacle Rock Cave	80	145	175	0.98481	0.17365	0.57358	-0.81915	0.08716	-0.99619
TN	OV	Quarles Cave	115	112	22	0.90631	-0.42262	0.92718	-0.37461	0.37461	0.92718
AL	MD	Rabbit Hole	90	178	178	1.00000	0.00000	0.03490	-0.99939	0.03490	-0.99939
AL	MD	Road Pit	25	5	25	0.42262	0.90631	0.08716	0.99619	0.42262	0.90631
AL	MD	Rock Shelter Cave	40	45	45	0.64279	0.76604	0.70711	0.70711	0.70711	0.70711
TN	MN	Sams Cave	140	45	135	0.64279	-0.76604	0.70711	0.70711	0.70711	-0.70711
TN	WH	Short Creek Maze Cave	110	115	95	0.93969	-0.34202	0.90631	-0.42262	0.99619	-0.08716
AL	MD	Slimy Disappointment	155	125	75	0.42262	-0.90631	0.81915	-0.57358	0.96593	0.25882
TN	GD	Small Bluff Cave	65	65	65	0.90631	0.42262	0.90631	0.42262	0.90631	0.42262
AL	MG	Snail Cave	55	65	5	0.81915	0.57358	0.90631	0.42262	0.08716	0.99619
AL	MD	Soapstone Hollow C.	150	105	15	0.50000	-0.86603	0.96593	-0.25882	0.25882	0.96593
AL	MG	Stillhouse Cave	140	15	55	0.64279	-0.76604	0.25882	0.96593	0.81915	0.57358
AL	MG	T Cave	165	5	110	0.25882	-0.96593	0.08716	0.99619	0.93969	-0.34202
AL	MG	Turner Cave	170	175	5	0.17365	-0.98481	0.08716	-0.99619	0.08716	0.99619
AL	MD	Turtle Pit	95	95	95	0.99619	-0.08716	0.99619	-0.08716	0.99619	-0.08716
TN	VB	Wagon Wheel Cave	25	115	90	0.42262	0.90631	0.90631	-0.42262	1.00000	0.00000
TN	PU	Welch-Bowling Cave	140	155	135	0.64279	-0.76604	0.42262	-0.90631	0.70711	-0.70711
TN	MN	White Cricket Cave	10	5	65	0.17365	0.98481	0.08716	0.99619	0.90631	0.42262
TN	OV	Wolf Branch Cave	140	5	95	0.64279	-0.76604	0.08716	0.99619	0.99619	-0.08716

|		sum(Val)	34.32534	-4.98569	sum(Cav)	32.02608	3.08552	sum(Cav)	37.10823	5.93522

Y	0.57208903	0.32728586
X	-0.0830949	0.00690476
r	**0.57809223**	
sina	0.98961551	
cosa	-0.1437398	
Ɵ r	-81.735688	

Y	0.53376806	0.28490835
X	0.05142537	0.00264457
r	**0.53623961**	
sina	0.99539097	
cosa	0.09589999	
Ɵ r	84.4968782	

Y	0.61847057	0.38250584
X	0.09892035	0.00978523
r	**0.62633144**	
sina	0.98744933	
cosa	0.1579361	
Ɵ r	80.9128796	

mean angle	98.265		mean angle	84.496		mean angle	80.912

Rayleigh z	20.051437		Rayleigh z	17.253175		Rayleigh z	23.537465

D2. STRUCTURAL STATISTICAL ANALYSIS: WATSON'S U^2 STATISTIC

i	Val_trend_n1	i/n1	j	Cav_trend_n2	j/n2	dk	dk2
1	5	0.01667	1	5	0.01667	0.00000	0.00000
2	5	0.03333	2	5	0.03333	0.00000	0.00000
2	5	0.03333	3	5	0.05000	-0.01667	0.00028
2		0.03333	4	5	0.06667	-0.03333	0.00111
2		0.03333	5	5	0.08333	-0.05000	0.00250
2		0.03333	6	5	0.10000	-0.06667	0.00444
2		0.03333	7	5	0.11667	-0.08333	0.00694
2		0.03333	8	5	0.13333	-0.10000	0.01000
3	10	0.05000	9	10	0.15000	-0.10000	0.01000
4	10	0.06667	9		0.15000	-0.08333	0.00694
5	10	0.08333	9		0.15000	-0.06667	0.00444
6	15	0.10000	10	15	0.16667	-0.06667	0.00444
6		0.10000	11	15	0.18333	-0.08333	0.00694
6		0.10000	12	15	0.20000	-0.10000	0.01000
7	20	0.11667	13	20	0.21667	-0.10000	0.01000
8	25	0.13333	14	25	0.23333	-0.10000	0.01000
9	25	0.15000	15	25	0.25000	-0.10000	0.01000
10	25	0.16667	15		0.25000	-0.08333	0.00694
11	25	0.18333	15		0.25000	-0.06667	0.00444
11		0.18333	16	30	0.26667	-0.08333	0.00694
12	32	0.20000	16		0.26667	-0.06667	0.00444
13	35	0.21667	17	35	0.28333	-0.06667	0.00444
14	40	0.23333	18	40	0.30000	-0.06667	0.00444
15	40	0.25000	18		0.30000	-0.05000	0.00250
16	45	0.26667	19	45	0.31667	-0.05000	0.00250
17	45	0.28333	20	45	0.33333	-0.05000	0.00250
17		0.28333	21	45	0.35000	-0.06667	0.00444
17		0.28333	22	45	0.36667	-0.08333	0.00694
17		0.28333	23	45	0.38333	-0.10000	0.01000
18	50	0.30000	23		0.38333	-0.08333	0.00694
19	55	0.31667	24	55	0.40000	-0.08333	0.00694
20	60	0.33333	24		0.40000	-0.06667	0.00444
21	60	0.35000	24		0.40000	-0.05000	0.00250
22	60	0.36667	24		0.40000	-0.03333	0.00111
23	65	0.38333	25	65	0.41667	-0.03333	0.00111
23		0.38333	26	65	0.43333	-0.05000	0.00250
24	70	0.40000	26		0.43333	-0.03333	0.00111
25	75	0.41667	27	75	0.45000	-0.03333	0.00111
25		0.41667	28	75	0.46667	-0.05000	0.00250
26	80	0.43333	29	80	0.48333	-0.05000	0.00250
26		0.43333	30	85	0.50000	-0.06667	0.00444
27	90	0.45000	30		0.50000	-0.05000	0.00250
28	95	0.46667	31	95	0.51667	-0.05000	0.00250
29	95	0.48333	32	95	0.53333	-0.05000	0.00250
29		0.48333	33	95	0.55000	-0.06667	0.00444
30	100	0.50000	33		0.55000	-0.05000	0.00250
31	100	0.51667	33		0.55000	-0.03333	0.00111
32	105	0.53333	34	105	0.56667	-0.03333	0.00111
32		0.53333	35	105	0.58333	-0.05000	0.00250
32		0.53333	36	105	0.60000	-0.06667	0.00444
32		0.53333	37	108	0.61667	-0.08333	0.00694
33	110	0.55000	37		0.61667	-0.06667	0.00444
33		0.55000	38	112	0.63333	-0.08333	0.00694
34	115	0.56667	39	115	0.65000	-0.08333	0.00694
34		0.56667	40	115	0.66667	-0.10000	0.01000
34		0.56667	41	115	0.68333	-0.11667	0.01361
35	125	0.58333	42	125	0.70000	-0.11667	0.01361
35		0.58333	43	125	0.71667	-0.13333	0.01778
36	135	0.60000	44	135	0.73333	-0.13333	0.01778
37	140	0.61667	44		0.73333	-0.11667	0.01361
38	140	0.63333	44		0.73333	-0.10000	0.01000
39	140	0.65000	44		0.73333	-0.08333	0.00694
40	140	0.66667	44		0.73333	-0.06667	0.00444
41	140	0.68333	44		0.73333	-0.05000	0.00250
42	140	0.70000	44		0.73333	-0.03333	0.00111
43	140	0.71667	44		0.73333	-0.01667	0.00028
43		0.71667	45	145	0.75000	-0.03333	0.00111
43		0.71667	46	145	0.76667	-0.05000	0.00250
43		0.71667	47	145	0.78333	-0.06667	0.00444
43		0.71667	48	145	0.80000	-0.08333	0.00694
43		0.71667	49	145	0.81667	-0.10000	0.01000
44	150	0.73333	49		0.81667	-0.08333	0.00694
45	150	0.75000	49		0.81667	-0.06667	0.00444
46	150	0.76667	49		0.81667	-0.05000	0.00250
47	150	0.78333	49		0.81667	-0.03333	0.00111
48	155	0.80000	50	155	0.83333	-0.03333	0.00111
49	155	0.81667	51	155	0.85000	-0.03333	0.00111
50	155	0.83333	51		0.85000	-0.01667	0.00028
51	155	0.85000	51		0.85000	0.00000	0.00000
52	160	0.86667	51		0.85000	0.01667	0.00028
53	160	0.88333	51		0.85000	0.03333	0.00111
54	160	0.90000	51		0.85000	0.05000	0.00250
55	165	0.91667	51		0.85000	0.06667	0.00444
56	165	0.93333	51		0.85000	0.08333	0.00694
56		0.93333	52	168	0.86667	0.06667	0.00444
57	170	0.95000	52		0.86667	0.08333	0.00694
58	170	0.96667	52		0.86667	0.10000	0.01000
59	175	0.98333	53	175	0.88333	0.10000	0.01000
60	175	1.00000	54	175	0.90000	0.10000	0.01000
60		1.00000	55	175	0.91667	0.08333	0.00694
60		1.00000	56	175	0.93333	0.06667	0.00444
60		1.00000	57	175	0.95000	0.05000	0.00250
60		1.00000	58	175	0.96667	0.03333	0.00111
60		1.00000	59	175	0.98333	0.01667	0.00028
60		1.00000	60	178	1.00000	0.00000	0.00000
					SUM	-4.15000	0.47083

Watsons U2	0.0818
U2critical	0.185

E. MAPPED STRUCTURAL FEATURES AND PENNINGTON CAVE ENTRANCE LOCATIONS (NO DATA SHOWN FOR GEORGIA)
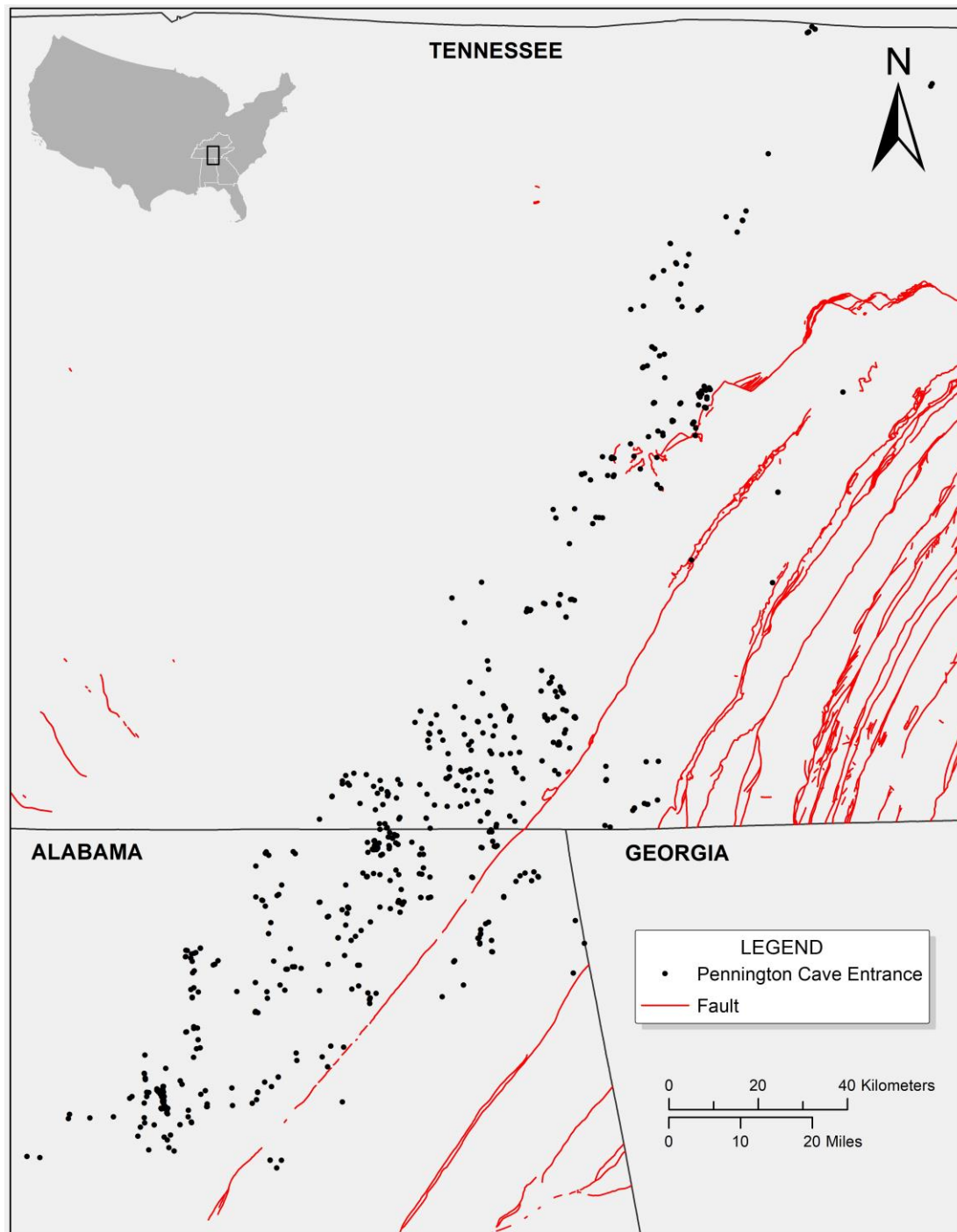
F. FLUORESCENT DYE ANALYSIS

CRAWFORD HYDROLOGY LAB

Hydrogeologists, Geologists, Environmental Scientists
*Karst Groundwater Investigations * Fluorescent Dye Analysis*

LABORATORY REPORT SHEET
FLUORIMETRIC ANALYSIS RESULTS

Big Creek Dye Trace: Round 1

Analysis requested by:

Hali Steinmann

		EOSINE	SULPHORHODAMINE B
		Color Index:	Color Index:
		Acid Red 87	Acid Red 52
		Dye Receptor:	Dye Receptor:
		Activated Charcoal	Activated Charcoal
		Analysis by:	Analysis by:
		Spectrofluorophotometer	Spectrofluorophotometer

	EOSINE	SULPHORHODAMINE B
	PQL in Eluent: 0.005 ppb	PQL in Eluent: 0.005 ppb
	PQL in Water: 0.010 ppb	PQL in Water: 0.010 ppb
	λ in Eluent: 541.3 nm	λ in Eluent: 579.7 nm
	λ in Water: 535.3 nm	λ in Water: 583.4 nm

Lab ID	Event	Date Collected	Feature Name	TIME	PeakFit	EOSINE Results	EOSINE Conc in ppb	EOSINE Peak Center (nm)	SULPH Results	SULPH Conc in ppb	SULPH Peak Center (nm)	Comments
ELUENT-1			QA-ELUENT			ND			ND			
EL-EO-1			QA-EOSINE			+	0.005		ND			0.005 ppb
EL-EO-1A			QA-EOSINE			+	0.100		ND			0.100 ppb
EL-SRB-1			QA-SULPHORHODAMINE B			ND			+	0.005		0.005 ppb
EL-SRB-1A			QA-SULPHORHODAMINE B			ND			+	0.093		0.100 ppb
EH-EO-1			QA-EOSINE			+	100.000		ND			100 ppb
EH-SRB-1			QA-SULPHORHODAMINE B			ND			+	100.000		100 ppb
EL-001-0	BR	07/15/17	Greeter Gill Cave			ND			ND			
	01	07/29/17				ND			+++	7.279	579.2	
	02	08/13/17										
	03	09/03/17										
EL-002-0	BR	07/15/17	Spring 2			ND			ND			
	01	07/29/17				ND			ND			
	02	08/13/17										
	03	09/03/17										
EL-003-0	BR	07/15/17	Spring 3			ND			ND			
	01	07/29/17										
	02	08/13/17				ND			ND			
	03	09/03/17										
EL-004-0	BR	07/15/17	Spring 4			ND			ND			
	01	07/29/17				ND			ND			
	02	08/13/17				ND			ND			
	03	09/03/17										
EL-005-0	BR	07/15/17	Spring 5			ND			ND			
	01	07/29/17				ND			ND			
	02	08/13/17				ND			ND			
	03	09/03/17										
EL-006-0	BR	07/15/17	Spring 6			ND			ND			
	01	07/29/17				ND			ND			
	02	08/13/17					0.057	NPI	ND			
	03	09/03/17										
EL-007-0	BR	07/15/17	Spring 7			ND			ND			
	01	07/29/17				ND			ND			
	02	08/13/17				ND			ND			
	03	09/03/17										
EL-008-0	BR	07/15/17	Spring 8			ND			ND			
	01	07/29/17				ND			ND			
	02	08/13/17					0.205	NPI	++	1.990	577.0	
	03	09/03/17										
EL-009-0	BR	07/15/17	Easter Rise Cave			ND			ND			
	01	07/29/17				+++	14.997	542.2	ND			
	02	08/13/17				+	0.944	536.8	ND			
	03	09/03/17										
EL-010-0	BR	07/15/17	Confluence			ND			ND			
	01	07/29/17				ND			ND			
	02	08/13/17					0.373	NPI		0.135	NPI	
	03	09/03/17										
EL-011-0	BR	07/21/17	Grundy Big Spring			ND			ND			
	01	08/13/17										
	02	09/03/17										
EL-012-0	BR	07/21/17	Cemetery on Collins River			IB	0.069	NPI	ND			
	01	08/13/17				ND			ND			
	02	09/03/17										
ELUENT-2			QA-ELUENT			ND			ND			ELUENT
EL-EO-2			QA-EOSINE			+	0.004		ND			0.005 ppb
EL-EO-2A			QA-EOSINE			+	0.099		ND			0.100 ppb
EL-SRB-2			QA-SULPHORHODAMINE B			ND			+	0.004		0.005 ppb
EL-SRB-2A			QA-SULPHORHODAMINE B			ND			+			0.100 ppb
EH-EO-2			QA-EOSINE			+	96.361		ND			10ppb
EH-SRB-2			QA-SULPHORHODAMINE B			ND			+	92.854		100ppb

Analyzed by:	Hali Steinmann	on	8/18/17
Entered by:	Hali Steinmann	on	9/6/17
Comments:			

IB = Initial Background
B = Background (<10 times background or lowest detection limit)
POR = Peak Out of Range (>5nm, <10nm from dye peak center)
ND = No Detection
NPI = No Peak Indicated
EL - Eluent Low- High Sensitivity Scan
EH - Eluent High- Low Sensitivity Scan

+ = Positive (10 times background or lowest detection limit)
++ = Very positive (100 times background or lowest detection limit)
+++ = Extremely positive (1000 times background or lowest detection limit)
?+ = Questionable Positive, needs two hits in a row to equal +
Q = Lab Duplicate
QA = Quality Assurance/Quality Contol Laboratory Dye Standards
PeakFit Utilized (Statistical Analysis Peakfitting Software)

ND Below Quantitation Limit
B Background
NS No Sample

+ Positive
++ Very Positive
+++ Extremely Positive

Created 7/1/18
©2001 Dr. Nicholas Crawford

CRAWFORD HYDROLOGY LAB *

*   *Hydrogeologists, Geologists, Environmental Scientists*
*   *Karst Groundwater Investigations * Fluorescent Dye Analysis*

LABORATORY REPORT SHEET
FLUORIMETRIC ANALYSIS RESULTS

Big Creek Dye Trace: Round 2

Analysis requested by:

Hali Steinmann

			FLUORESCEIN	EOSINE	RHODAMINE WT	SULPHORHODAMINE B
			Color Index:	Color Index:	Color Index:	Color Index:
			Acid Yellow 73	Acid Red 87	Acid Red 388	Acid Red 52
			Dye Receptor:	Dye Receptor:	Dye Receptor:	Dye Receptor:
			Activated Charcoal	Activated Charcoal	Activated Charcoal	Activated Charcoal
			Analysis by:	Analysis by:	Analysis by:	Analysis by:
			Spectrofluorophotometer	Spectrofluorophotometer	Spectrofluorophotometer	Spectrofluorophotometer

			FLUORESCEIN		EOSINE		RHODAMINE WT		SULPHORHODAMINE B		
			PQL in Eluent: 0.005 ppb		PQL in Eluent: 0.005 ppb		PQL in Eluent: 0.010 ppb		PQL in Eluent: 0.005 ppb		
			PQL in Water: 0.010 ppb		PQL in Water: 0.010 ppb		PQL in Water: 0.010 ppb		PQL in Water: 0.010 ppb		
			λ in Eluent: 517.4 nm		λ in Eluent: 541.3 nm		λ in Eluent: 568.9 nm		λ in Eluent: 570.7 nm		
			λ in Water: 511.1 nm		λ in Water: 535.3 nm		λ in Water: 577.1 nm		λ in Water: 583.4 nm		

Lab ID	Event	Date Collected	Feature Name	TIME	Peak#	Results	Conc in ppb	Peak Center (nm)	Results	Conc in ppb	Peak Center (nm)	Results	Conc in ppb	Peak Center (nm)	Results	Conc in ppb	Peak Center (nm)	Comments
ELUENT-1			QA-ELUENT			ND			ND			ND			ND			
EL-FL-1			QA-FLUORESCEIN			+	0.005		ND			ND			ND			0.005 ppb
EL-FL-1A			QA-FLUORESCEIN			+	0.097		ND			ND			ND			0.100 ppb
EL-EO-1			QA-EOSINE			ND			+	0.005		ND			ND			0.005 ppb
EL-EO-1A			QA-EOSINE			ND			+	0.102		ND			ND			0.100 ppb
EL-RWT-1			QA-RHODAMINE WT			ND			ND			+	0.014		ND			0.010 ppb
EL-RWT-1A			QA-RHODAMINE WT			ND			ND			+	0.111		ND			0.100 ppb
EL-SRB-1			QA-SULPHORHODAMINE B			ND			ND			ND			+	0.003		0.005 ppb
EL-SRB-1A			QA-SULPHORHODAMINE B			ND			ND			ND			+	0.089		0.100 ppb
EH-FL-1			QA-FLUORESCEIN			+	97.242		ND			ND			ND			100 ppb
EH-EO-1			QA-EOSINE			ND			+	95.581		ND			ND			100 ppb
EH-RWT-1			QA-RHODAMINE WT			ND			ND			+	91.543		ND			100 ppb
EH-SRB-1			QA-SULPHORHODAMINE B			ND			ND			ND			+	96.196		100 ppb
EL-001-0	IB	11/19/17	001 - Greeter Gill Cave															RECEPTOR MISSING
	01	11/22/17				ND			ND			?	107.437	NPI	+++	195.908	579.6	
	02	11/26/17				?	0.007	NPI	ND			ND			+	0.43	574.6	SRB- POR
EL-002-0	IB	11/19/17	002 - Spring 2			IB	0.012	NPI	ND			IB	0.048	NPI	ND			
	01	11/22/17																SITE NOT MONITORED (DRY)
	02	11/26/17																SITE NOT MONITORED (DRY)
EL-003-0	IB	11/19/17	003 - Spring 3			IB	0.018	NPI	ND			ND			ND			
	01	11/22/17				ND			ND			?	116.157	NPI	+++	224.588	579.8	
	02	11/26/17				ND			ND			?	0.367	NPI	++	0.89	577.4	
EL-004-0	IB	11/19/17	004 - Spring 4															RECEPTOR MISSING
	01	11/22/17				ND			ND			?	116.153	NPI	+++	228.914	579.8	
	02	11/26/17				?	0.003	NPI	ND			?	0.211	NPI	++	0.659	577	
EL-005-0	IB	11/19/17	005 - Spring 5			IB	0.025	NPI	ND			ND			ND			
	01	11/22/17				ND			ND			?	114.08	NPI	+++	231.667	579.8	
	02	11/26/17				?	0.015	NPI	ND			?	0.195	NPI	++	0.767	576.4	
EL-006-0	IB	11/19/17	006 - Spring 6															RECEPTOR MISSING
	01	11/22/17				ND			ND			?	116.751	NPI	+++	234.407	579.8	
	02	11/26/17				?	0.014	NPI	ND			?	0.368	NPI	++	1.011	577.4	
EL-007-0	IB	11/19/17	007 - Spring 7			IB	0.034	NPI	ND			ND			ND			
	01	11/22/17				ND			ND			?	115.996	NPI	+++	241.146	579.8	
	02	11/26/17				?	0.012	NPI	ND			?	0.322	NPI	++	0.963	577.6	
EL-008-0	IB	11/19/17	008 - Spring 8			IB	0.045	NPI	ND			ND			ND			
	01	11/22/17				ND			ND			?	103.741	NPI	+++	187.574	579.6	
	02	11/26/17				?	0.012	NPI	ND			?	0.263	NPI	++	0.745	576.6	
EL-009-0	IB	11/19/17	009 - Easter Rise Cave			ND			IB	0.018	NPI	ND			ND			
	01	11/22/17				ND			+++	194.725	542.2	ND			ND			
	02	11/26/17				ND			+++	13.922	542.2	ND			ND			
EL-010-0	IB	11/19/17	010 - Confluence (Big Creek)			IB	0.021	NPI	IB	0.009	NPI	ND			ND			
	01	11/22/17				ND			+++	202.247	542.4	ND			+++	110.257	579.4	
	02	11/26/17				ND			++	0.726	539.6	ND			++	0.199	NPI	
EL-100-0	IB	11/19/17	100 - Grundy Big Spring															DID NOT TAKE BACKGROUND SAMPLES
	01	11/22/17				++	1.524	518.6	+++	34.491	542.2	+++	37.339	573.6	+++	27.345	NPI	
	02	12/03/17				+++	12.514	517.6	ND			+++	42.138	571	+++	10.639	NPI	
EL-101-0	IB	11/19/17	101 - Collins River Rise															DID NOT TAKE BACKGROUND SAMPLES
	01	11/22/17				++	3.375	518.2	+++	23.364	542.2	+++	30.181	573.6	+++	22.171	NPI	
	02	12/03/17				+++	9.563	517.4	ND			+++	32.462	571.2	+++	7.937	NPI	
ELUENT-2			QA-ELUENT									ND			ND			ELUENT
EL-FL-2			QA-FLUORESCEIN			+	0.005		ND			ND			ND			0.005 ppb
EL-FL-2A			QA-FLUORESCEIN			+	0.097		ND			ND			ND			0.100 ppb
EL-EO-2			QA-EOSINE			ND			+	0.005		ND			ND			0.005 ppb
EL-EO-2A			QA-EOSINE			ND			+	0.102		ND			ND			0.100 ppb
EL-RWT-2			QA-RHODAMINE WT			ND			ND			+	0.018		ND			0.010 ppb
EL-RWT-2A			QA-RHODAMINE WT			ND			ND			+	0.121		ND			0.100 ppb
EL-SRB-2			QA-SULPHORHODAMINE B			ND			ND			ND			+	0.003		0.005 ppb
EL-SRB-2A			QA-SULPHORHODAMINE B			ND			ND			ND			+	0.083		0.100 ppb
EH-FL-2			QA-FLUORESCEIN			+	96.163		ND			ND			ND			100 ppb
EH-EO-2			QA-EOSINE			ND			+	96.423		ND			ND			100 ppb
EH-RWT-2			QA-RHODAMINE WT			ND			ND			+	91.621		ND			100 ppb
EH-SRB-2			QA-SULPHORHODAMINE B			ND			ND			ND			+	96.495		100 ppb

ND	Below Quantitation Limit	+	Positive
B	Background	++	Very Positive
NS	No Sample	+++	Extremely Positive

Created 7/1/18
©2001 Dr. Nicholas Crawford

124